RE-TR-68-11

AD

UB 2508-E-1

RADAR CLUTTER RESEARCH (U)

FINAL REPORT

S.N. Andre, M.E. Bechtel and D.A. Foster

July 1968

Sponsored by:
U.S. ARMY MISSILE COMMAND
CONTRACT NO. DAAH01-67-C-2516
RESEARCH AND DEVELOPMENT DIRECTORATE
ADVANCED SENSORS LABORATORY

Prepared by:
CORNELL AERONAUTICAL LABORATORY, INC.
OF CORNELL UNIVERSITY, BUFFALO, N.Y. 14221

CORNELL AERONAUTICAL LABORATORY, INC.
BUFFALO, NEW YORK 14221

RADAR CLUTTER RESEARCH (U)

FINAL REPORT

JULY 1968

CORNELL AERONAUTICAL LABORATORY
REPORT NO. UB 2508-E-1
CONTRACT NO. DAAH01-67-C-2516

ABSTRACT

The objective of this program was to prepare a clutter research plan for Army air defense weapons that encompasses the anticipated methods of employment of these weapons, as well as the problems associated with the introduction of new radar technology in these systems. Specifically, the investigations included studies of the physics of electromagnetic scattering from rough surfaces, a definition of clutter problems as related to innovations in radar technology such as electronic beam steering, signal processing and design, computer technology, study of clutter models and simulation techniques, and a study of clutter effects in a radar defense complex.

Probability density functions, correlation functions and doppler spectra of clutter signals are derived for the configuration in which only a few major scatterers are present. Results are presented for both coherent and noncoherent detection.

Methods of simulating clutter, using both analog and digital approaches, are described. Emphasis is placed on advanced forms of simulators such as would be required for evaluation of future multi-dimensional radar systems rather than on additive filtered noise for the simulation of clutter. The simulation techniques are based on two suggested generic forms of clutter models, called open-loop and closed-loop. Because of the greater flexibility of closed-loop simulation, this is presented in greater detail.

Techniques for performing radar clutter measurements are described and some of the significant problems, related primarily to terrain and cultural observables, are discussed. Clutter problems as related to radar systems and innovations in radar technology, such as electronically steered phase arrays, are also described.

The program plan for future clutter research incorporates the findings of the supporting studies performed on this program. The program plan identifies the major areas of development and research required to perform a meaningful program of clutter measurements. It is stressed that: 1) the electromagnetic

observables should be measured in such a way that correlation is maintained among the measured parameters and 2) that environmental descriptors are of importance equal to that of the radar sensor data and must be derived and associated with it.

FOREWORD

This report was prepared by the Electronics Research and the Avionics Departments of Cornell Aeronautical Laboratory on Contract DAAH01-67-C-2516. The studies were administered by the Advanced Sensors Laboratory, Research and Development Directorate of the U.S. Army Missile Command, Redstone Arsenal, Huntsville, Alabama. Mr. Maurice Belrose and Mrs. Caroline Broten were the project monitors.

The authors acknowledge Messrs. B. Riley Tripp and Robert E. Kell and Dr. Frank M. Pelton for the invaluable assistance and suggestions they provided during the program and in the preparation of this report.

TABLE OF CONTENTS

TABLE OF CONTENTS (Cont.)

TABLE OF CONTENTS (Cont.)

TABLE OF CONTENTS (Cont.)

LIST OF ILLUSTRATIONS

LIST OF ILLUSTRATIONS (Cont.)

LIST OF TABLES

Section 1
INTRODUCTION AND SUMMARY

1.1 INTRODUCTION

The objective of this program was to prepare a clutter research plan for Army air defense weapons that encompasses the anticipated methods of employment of present weapons, as well as the problems associated with the introduction of new radar technology in these systems. Emphasis was placed on terrain clutter; other sources of clutter such as sea and precipitation were not treated explicitly.

This task was approached by identifying several specific topics which are logical elements of a clutter research program and then by examining each topic in turn in its relation to the others. The topics selected for this purpose are: 1) physics of electromagnetic scattering from rough surfaces, 2) definition of clutter problems as related to innovations in radar technology such as electronic steering, signal processing and design, 3) computer technology, 4) clutter models and simulation techniques, 5) clutter effects in a radar defense complex. Each one is discussed in the corresponding section of the report and their interrelation to form a well integrated clutter research program plan is described in Section 10.

Clutter has been defined as a conglomeration of unwanted echoes.[1] From a phenomonological view, a more accurate and fundamental description would be the presence of unwanted scatterers or collections of scatterers within the system environment. It is true that these unwanted scatterers produce unwanted echoes. However, since observed echoes are strong functions of both illumination and observation systems, basic phenomena cannot be described in such terms. For example, observed echoes (clutter) are a function of the resolution of illumination and observation systems. The overall environment has not changed, just the observation technique. This change in emphasis removes the particular radar system from consideration and views the

clutter problem only in terms of the basic phenomena of scattering. This point is of utmost importance when simulation of a number of radar types is required because changes in radar observables for an environment in which the scatterers (and their time variations) are defined can be traced directly to changes in radar system parameters. Moreover, use of a suitably defined scattering model permits evaluation of clutter effects on such diverse systems as CW Doppler (for personnel intrusion detection) and missile semiactive homing systems. The former, of course, requires a definition of scatterer motion and cross section (amplitude and phase), while the latter requires, in addition, definition of target-scatterer interactions.

In general, effects of clutter can be broken into three broad categories. The first is the monostatic return from clutter itself where clutter radar cross section is sufficiently high to obscure the true target return. The second is modification of radar system parameters by clutter-radar interaction, and the third is modification of true target return by target-clutter interaction. Examples of each are readily available. For the first, we have the difficulty of discerning a low-altitude, low-radar-cross-section vehicle in terrain clutter, particularly with a low-resolution radar. For the second, we have the modification of antenna lobe structure and boresight of a ground-based radar operating close to grazing incidence which can increase the apparent target scintillation, or under conditions of local terrain masking can interrupt the line of sight between the radar and target. For the third, we have the difficulty of differentiating between a target and its image with the antenna beam close to terrain. (Usually the Doppler frequency difference or range resolution is insufficient for effective discrimination.)

These observed clutter effects are functions of radar system parameters as well as the electromagnetic environment, and generally depend on system resolution, both in range and angle and on range/angle scan rates. In fact, it is precisely this dependence on system parameters which limits the usefulness of much of the experimental clutter data obtained in the past. While much data exist which are valid for particular systems employed to make the measurements, they cannot be extrapolated to predict the performance of systems with different capabilities.

Another factor of major importance, which has all too often been neglected, is an adequate description of the environment in which a set of clutter measurements has been made. Data on environmental variables, such as terrain cover and masking, is of equal importance with electromagnetic variables for the interpretation and understanding of clutter. The major problem in selecting environmental descriptors is that a set sufficient to categorize terrain with respect to clutter has not been defined. This factor stresses the need for care in the design and conduct of a clutter measurements program. The emphasis during such a program should be primarily on gathering, analyzing and interpreting data to more fully understand the basic nature of the interactions involved. Clutter data per se, is of limited value and should not be the sole end product of a measurements program.

1.2 SUMMARY

In the analytic description of phenomena, simplified models are generally used to represent the interactions occurring in nature. After postulating a model, presumably on the basis of reasonable assumptions, the analyst can draw conclusions concerning the outcome of a process given a set of stimuli. This same process occurs with respect to clutter. Clutter, however, involves an extremely complicated set of processes and no simple model will suffice to represent it. One simplified model has assumed Gaussian statistics. It is known from the Central Limit Theorem in probability theory that the sum of a number of random functions, satisfying reasonable constraints, will tend to a Gaussian random process in the limit of an infinite number of functions. This theorem, when applied to clutter, has been used by analysts to formulate a model of clutter as a Gaussian random process for which only the variance, mean and spectrum is required in order to specify the process. Results over the past years from clutter measurements, which have been based primarily on this model, can hardly be called definitive.

In Section 2 of this report the manner in which clutter affects the division of radar functions in an air defense complex is described. The important case of surface-to-air missile systems and the role that clutter

plays in their effectiveness in defending against low-altitude, high-speed aircraft is discussed. The radar problems anticipated are used to focus initial clutter measurements, described in the program plan, to areas of key importance.

In Section 3, two generic forms of clutter models are described. In the first model, called an "open-loop" clutter model, the clutter signal is formed and added to a signal representing the target; both are coupled to the radar processor. This model, which includes the Gaussian clutter representation, requires knowledge of the dependent variations in the clutter signal due to variations in the radar system. A second generic clutter model, called a "closed-loop" model, represents the received clutter and target signals as an operation on the transmitted signal. This model is a closer representation of the actual scattering process, which occurs in the formation of clutter signals, than the open-loop model. The data on required scattering parameters, with their spatial and time dependencies, is limited because of insufficient suitable data. The program plan given in Section 10 describes a program of clutter measurements intended to provide the required data on clutter characteristics.

In Sections 4, 5 and 6, probability density functions, correlation functions and doppler spectra of clutter signals are discussed for the case in which only a few major scatterers are present. The convergence of the analytical results to the case of many scatterers is also discussed. These analytical studies, in conjunction with the closed-loop clutter model, form a basis for a clutter measurements program.

In Section 7 methods of simulating clutter are described: both analog and digital techniques are considered. Emphasis is placed on advanced forms of simulators such as would be required for evaluation of future multi-dimensional radar systems rather than on additive filtered noise simulation of clutter. Both open-loop and closed-loop simulation are discussed, although, because of its greater flexibility, closed-loop simulation is discussed in greater detail.

In Section 8, techniques for performing radar clutter measurements are described and some of the significant problems, related primarily to terrain and cultural observables, are discussed. Clutter problems related to innovations in radar technology, such as electronically steered phased arrays, are described in Section 9.

The program plan for future clutter research which incorporates the findings of the previous sections is given in Section 10. Included in the program plan are the major areas of development and research required to perform a meaningful program of clutter measurements. It is stressed that: 1) the electromagnetic observables should be measured in such a way that correlation is maintained among the measured parameters and 2) environmental descriptors are of importance equal to that of the radar sensor data and must be associated with it.

Section 2
CLUTTER PROBLEMS IN RADAR AIR DEFENSE SYSTEMS

Clutter will affect the division of radar functions in an air defense complex in a manner dependent on the characteristics of the clutter and on the particular function (detection or tracking). One of the major air defense systems in use today is the surface-to-air missile system (SAM) and the role that clutter plays in affecting air defense systems effectiveness is illustrated in the following discussion of the problem SAM systems encounter in defending against low-altitude, high-speed aircraft attacks. The program plan given in Section 10 covers many facets of the clutter problem. Because the problem is such a large one, the establishment of realistic bounds is required to focus data acquisition, at least initially, in the critical areas of air defense. This section also provides a discussion of these critical areas. Available data strongly indicate that Line-Of-Sight (LOS) coverage limitations (caused by terrain and/or vegetative masking) are primary factors in determining the effectiveness of a ground based (or truck mounted) SAM system against low altitude high speed aircraft targets in most environments.* Appropriate guidance technology and hardware are well advanced and potential threats to future SAM systems can be expected to have a very good capability to exploit the characteristics of the environment by proper planning and execution of low altitude high speed missions. Future tactical aircraft threats should be anticipated with capabilities for flying in close proximity to the ground (minimum clearance of 200 ft or so) at speeds appropriate for the environment. For any particular site, the interactions between anticipated offensive and defensive weapons system capabilities, the tactics employed, and their effects on target availability and clutter existence should be evaluated. Such a study should include defense site quality as a function of sensor elevation above ground level deployment density, and their effect on expected overall

*For this discussion, the optical LOS can be assumed. The effect of ridge diffraction and multipath to provide an increase in the effective LOS is probably small although this premise is subject to experimental verification.

defense system effectiveness. Knowledge of these factors would greatly assist in quantifying the problems to be solved by low altitude air defense systems.

On a qualitative basis, consideration of the interactions discussed above indicate that for SAM systems deployed in relatively flat to rolling terrain, both target availability and clutter existence (as a function of range from the site) will be greatly different depending on whether or not the SAM sensor is ground based (vehicle mounted) or elevated above objects contributing to the local masking (such as small terrain variations, trees, buildings etc.).

The effects of local masking may cause significantly decreased LOS ranges to both target and clutter sources. It is expected that non-elevated sensors deployed in temperate zones would often be subject to initial LOS to target at ranges of 1-3 n.mi. As potential clutter sources are masked beyond the range of the object causing the local mask, the target should be available for detection in a clutter-free state in many situations. Because of the short LOS ranges involved, such SAM systems would be required to have very short reaction times (approximately 6-8 seconds) to be effective.

SAM systems employing a sensor elevated above the local mask, on the other hand, are presented with significantly different situations when deployed in the same environment. Target LOS ranges on the order of 10-15 miles would be common and clutter might exist over a significant portion of the target path. While the target might be available for detection in a clutter free situation, both clutter and multipath effects could be expected to be important for a large portion of the target track. From the SAM sensor design standpoint, the clutter problem is more difficult for the elevated sensor because of the longer ranges required. The availability of the target at long ranges does, however, greatly increase the allowable SAM reaction time.

Experience has shown that accurate determination of LOS to target for ground based defenses requires optical measurements (or their equivalent from stereo pair photos) of the objects causing local masking.[2] It is expected that target LOS determined from topographical map data would be adequate for cases where the sensor was elevated well above the local mask.

Accurate determination of LOS to clutter sources is predictable only when significant mask angles are involved (valleys, etc.). It is recommended that field survey's using a helicopter borne clutter mapping radar (PPI) be used in evaluating the LOS to clutter sources for elevated sensors.

It is assumed that maps of radar LOS as a function of target altitude above the local terrain can be obtained. These maps will govern the maximum allowable interval between successive searches in various directions for defense against radially entering targets. That is, regions where small LOS ranges to target exist will be searched frequently in order to obtain detection within the SAM reaction time.

Provision of adequate interval of LOS exposure by reducing vegetation masking effects does not, alone, necessarily allow the defensive system to be effective because its radar may not be able to acquire and track the low-altitude target which is in close proximity to the terrain. The terrain produces clutter which typically affects the radar system detection capability. In general, the radar cross section of an attacking tactical aircraft may be on the order of 10 to 20 dBsm with potential reduced radar cross sections of future aircraft being lower than 0 dBsm. On the other hand, the radar cross section of terrain and cultural features per square meter of surface area may vary from -30 dB to perhaps +30 dB, with -15 dB being a typically encountered average value. For practical SAM radar systems, the area of the pulse packet on the terrain results in a backscattered radar signal from the terrain which is typically very large compared to the return from the target (assuming the terrain in the vicinity of the target is not masked), especially for long-range detection of low-altitude tactical aircraft attacking radially over "choppy" terrain. Using a clutter LOS map, those areas where terrain is masked can be determined and detection of visible targets in these regions will be relatively easy due to the reduced amplitude of the clutter. A clutter signal will be present even if the terrain in the same range gate as the target is masked, because of unmasked terrain in the antenna sidelobes or in a part of the main lobe. The clutter amplitude will, however, be significantly reduced if clutter in the main lobe is masked. The target visibility will be governed by the target altitude as described by the radar LOS maps previously discussed. Thus, search of an area where clutter is masked will provide high detectability

of targets having radar LOS. The availability of LOS to target must be evaluated, however, in terms of an assessment of minimum altitudes which can be achieved by potential threats.

To provide the required target detection (and tracking) capability in regions where the terrain is not masked, it is necessary to make use of other characteristics in addition to the amplitude of the radar return signal. As the target typically has a relatively high radial velocity (if it is a threat to the SAM system), the Doppler shift of the return from the target is typically used to provide an additional "dimension" which aids in the separation of the target from clutter. Experience has shown, however, that in many environments, the Doppler separation, azimuth beamwidth and range resolution capability are not sufficient to permit effective detection of low-altitude targets at long ranges. This situation requires (1) that the reaction times of the overall defense system be reduced so that shorter ranges of detection are permitted without impairing SAM system effectiveness, (2) that the size of the radar resolution cell be reduced, or (3) that additional characteristics of the radar return be employed which improve separation of the target return from the clutter signals. Any characteristic of the target return which is significantly different from the clutter return alone, whether on an instantaneous or a statistical basis, whether natural or induced, potentially offers a means for improving the capability of future radar systems to detect targets in clutter. These additional characteristics include such things as frequency sensitivity, phase coherence, fluctuation and scintillation rates, target size, polarization, angle-of-arrival variations and knowledge of the masking and clutter characteristics at a particular site. A much improved knowledge of the characteristics of both clutter and target-clutter interaction effects is needed to permit efficient design and use of multidimensional radar sensing for the development of more effective SAM systems and to assess their performance capabilities. These data are needed for all environments in which the SAM system will be required to operate. A program plan for experimentally obtaining the required clutter data and methods for data reduction/correlation and use in simulation is given in Section 10.

For the short and long range conditions mentioned above, the clutter signal amplitude will probably cover a 60 dB dynamic range. During a clutter measurements program, as described in Section 10, it would be desirable to use a sensor radar providing clutter cross sections which approach typical target radar cross sections (1 m^2). A synthetic aperture system with an effective resolution of 1 milliradian and a pulse length of 20 nanoseconds will, for much of the terrain, provide effective clutter cross section approaching 1 m^2 (assuming a nominal 20 dB terrain reflectivity). Variation in the transmitted pulse length by a factor of 100-500 (through the use of pulse compression techniques) should provide a good representative distribution of effective clutter cross sections and associated target-to-clutter ratios.

The potential existence of multiple transmission paths to a low-altitude target (or any target at low elevation angles) can impair the target detection range by causing fading of the target return and widening of the apparent Doppler spectrum of the target. In addition, multipath can also seriously degrade the accuracy of target tracking radars whenever the target is separated from the clutter by less than an antenna beamwidth (which is the typical case for low-altitude targets). In particular, the multipath signals, when added vectorially to the direct radar returns, cause variations in the apparent angle of arrival, and, depending on the particular situation, the apparent angle of arrival may appear to come from angular regions outside the angular extent of the target and the clutter for a significant percentage of the time.[3] These errors, together with signal fluctuations and fading, greatly complicate the tracking of low-altitude targets. It should be noted that the multipath returns from low-angle targets typically exist near the Doppler-shifted frequency of the target and, therefore, the multipath effects cannot be rejected on the basis of Doppler separation alone. It is expected that the use of additional characteristics such as previously described will be required to allow the desired improvements in tracking of targets in clutter. Study of multipath effects is included in the program plan of Section 10.

A similar situation prevails for low-level missile systems. Here an illuminator is used to reflect energy from the incoming target. The missile "sees" this energy, and tracking circuits within the missile force

it into collison course with the target. However, for low flying vehicles, the illuminator also illuminates ground clutter so that the resultant illumination pattern is modulated as a function of target position. Simultaneously, the signal reflected from the target also illuminates ground clutter, forming a diffuse "image." The combination of both multipath perturbations place a lower bound on system effectiveness, preventing system deployment against targets penetrating below a given altitude. However, lack of detailed information on clutter multipath prevents an accurate assessment of the lower bound, short of actual firings.

The foregoing discussion has briefly indicated the complexity of the SAM system design problem and the importance of target and clutter characteristics knowledge in arriving at a suitable SAM design. Although the masking problem could often be solved by elevating the site above the local mask (especially in nearly flat terrains), clutter effects would still restrict the effectiveness of the SAM systems in many environments.

Section 3
CLUTTER MODELS

A clutter model, for the purposes of the discussion below, is a methodology to determine the clutter and clutter/target interactions in a radar system. The form of a clutter model can, in part, suggest methods and techniques for clutter simulation and in some cases a model and a simulation technique have become synonymous. The representation of clutter return as a narrow-band Gaussian process and use of an additive, filtered Johnson noise source for clutter simulation purposes are usually referred to interchangeably. This representation can lead to erroneous results because the clutter may be only partially simulated. For example, the spectrum of a noise source can be adjusted so that the simulated clutter has the appropriate correlation interval as a function of range (time delay) on a single radar scan but then the correlation between clutter at the same range but on successive radar scans may be incorrect (see Section 7.2 for a further discussion). The model itself may be incorrect; i.e., the signal from a Gaussian process is unbounded, whereas the clutter signal amplitude is necessarily bounded and thus not Gaussian. In the following section the major applications of clutter models and two suggested generic forms of clutter models are described.

3.1 CLUTTER MODEL APPLICATIONS

It is useful to consider potential applications of a clutter model in order to evaluate the degree of complexity required in the model and in potential simulation techniques.

3.1.1 Average Performance

In the past, the most frequent use of clutter models has been to determine average radar performance criteria, such as the probabilities of false alarm and detection and RMS track angle error, for various types of

terrain and radar system parameters. Most of the past clutter measurements were directed to this application and data were obtained on average clutter backscatter cross section, probability distributions, and clutter spectra for various types of terrain and radar system configurations.

3.1.2 Engagement System

In an engagement system application of a clutter model, the time history of system performance must be evaluated in a dynamic situation in which the target/clutter radar information is a system input on which future action is to be based. An example of this type of application is a missile-borne radar seeker for which it may be desirable to determine system performance for general classes of terrain or in some cases for a very specific site.

The requirements on the clutter model imposed by an engagement system application are generally more severe than those imposed by an average performance evaluation. For example, in an engagement system one may be interested in the peak clutter amplitude in studies of loss of angle or range track. The peak clutter amplitude, achieved during only a small portion of the total period of concern, can vary considerably without significantly affecting the average clutter amplitude or average system performance.

3.1.3 Comparative Evaluation of Radar Systems

It may be necessary to critically compare radar performance for various systems having different design configurations (frequency band, pulse shape, antenna patterns and polarization, data processing) in a prescribed clutter and target environment. In this case it is necessary for the clutter model to have sufficient flexibility that physical differences in illuminator and/or observer radar parameters can be represented to good accuracy by corresponding changes in the characteristics of the clutter and target signals. Included in this application is the use of the model for radar system design

wherein the performance capabilities of specific radar techniques, such as electronic beam scanning, MTI, Doppler filtering, etc., could be optimized on paper or in laboratory simulations without requiring recourse to field experiments.

3.2 GENERIC CLUTTER MODELS

In this section are considered the basic forms a radar-clutter model might take. Classes of models are presented rather than final, detailed models; factors that must be considered in a sophisticated clutter model are described here and discussed in greater detail in Section 7. It is assumed that only a relatively refined clutter representation is of interest; very little attention is therefore paid to the use of additive band-limited noise to represent a complete clutter signal, even though such simulation is adequate for some applications.

It seems reasonable to consider two general classes of models; any model must lie in one of these classes or else must contain a combination of elements belonging to both classes. These classes are henceforth called "open-loop" models and "closed-loop" models.

3.2.1 Open-Loop Model

In Figure 3-1 is shown the basic form of an open-loop clutter model. Here a Clutter-Signal Generator produces a signal with characteristics similar to the one received from the clutter for the specific radar being evaluated. Similarly, the Target-Signal Generator produces a signal with characteristics similar to that received from the target (note that, although only clutter

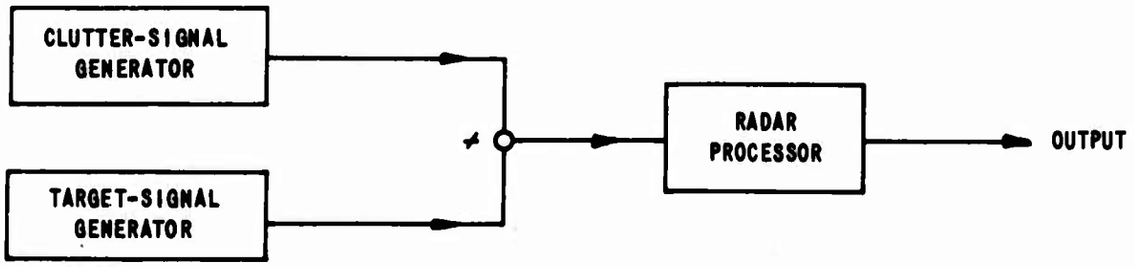

Figure 3-1 OPEN-LOOP CLUTTER MODEL

models are considered, the technique for incorporating the target signal characteristics cannot be ignored). These two signals are then added and the sum fed to the radar processor and the desired measures of performance are computed.

3.2.2 Closed-Loop Model

In Figure 3-2 is shown the basic form of a closed-loop clutter model. Here a signal corresponding to that transmitted by the radar is processed to obtain signals having characteristics of the clutter and target signals. Provision is made for the mutual interaction of target and clutter to modify both signals, as shown by the coupling between clutter and target-signal formation processes. The resulting signals are added and fed to the radar processor. The indirect-generation method is therefore more nearly like the actual radar situation (in which the original signal is modified by reflection from the target and clutter scatterers) than is the direct-generation method.

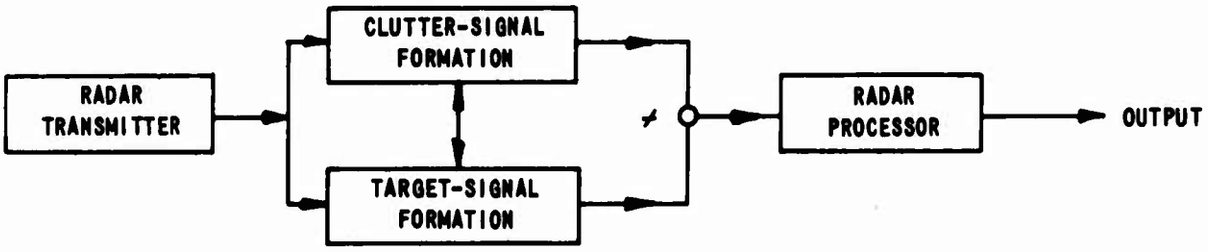

Figure 3-2 CLOSED-LOOP CLUTTER MODEL

With the open-loop model the characteristics of the clutter signal, such as probability density functions, spectrum, polarization characteristics and correlation functions among radar observables, must be known as a function of the radar parameters and terrain type. Most of the previous work in the clutter field has resulted in use of some form of "open-loop" model for radar system analysis. For example, it is conventional to assume a Gaussian probability distribution for the clutter with average power given by the integral of the terrain reflectivity, two-way antenna pattern and pulse-shape product over the terrain surface. The clutter correlation function as seen by the radar is determined from the internal "motion" clutter spectrum, typically assumed to

have a Gaussian shape, and from the effects of antenna pattern and platform motion, range gate movement, and various system instabilities.

In the closed-loop clutter model, the scattering processes which result in the clutter return are emphasized. Most clutter analyses usually begin with some form of closed-loop model. By assuming the terrain satisfies a set of restrictions regarding spatial stationarity (in a statistical sense), roughness scale, and roughness curvature, one obtains a tractable analytical problem. Terrain of concern in radar systems, however, does not satisfy the required set of assumptions at (for example, roughness must usually be assumed either very large or very small with respect to wavelength) typical radar frequencies. Thus, phenomena such as depolarization, local masking, and multiple scattering cannot, at the present time, be included analytically. This does not mean that use of the closed-loop model will completely represent the physical processes mentioned above, but rather that consideration of clutter as a scattering process in a closed-loop model can serve as a guideline for the planning and data interpretation of future clutter measurements programs.

Section 4
PROBABILITY DENSITY FUNCTIONS FOR A SMALL NUMBER OF SCATTERERS

4.1 GENERAL

If ground clutter is to be realistically represented, it is necessary that the clutter signal have statistical properties closely related to, if not identical with, those of the signal that would be received from the radar system. Perfect similarity is not likely to be necessary, particularly in view of the wide range of clutter types that can exist. Two of the characteristics that must be represented with reasonable accuracy are the power level and amplitude distribution. The clutter correlation function also must be determined in some cases, especially if the radar to be evaluated uses integration or clutter cancellation techniques to achieve MTI. Spectral characteristics will also be important if a coherent radar is to be considered.

In this section, probability density functions of the in-phase, and also quadrature phase, components of the clutter signal and of the envelope of the clutter signal are considered with emphasis on the configuration involving a small number of scatterers. For phase-coherent detection, one is interested in the probability density function of the in-phase and quadrature signals, whereas for envelope detection, the envelope probability density function is required. The few-scatterer configuration is significant because the statistics of the clutter signal will vary widely when only a few scatterers are dominant. It is important in experimental investigations, such as those described in the program plan of Section 10, to determine whether this effect is likely to be significant.

The most common clutter representation is based on application of the Central Limit Theorem to show that the in-phase and quadrature components of the clutter signal are approximately independent Gaussian random functions and that the envelope of the clutter signal will therefore be approximately Rayleigh distributed. This assumption is valid for many cases of interest.

For example, scattering from most meteorological targets (raindrops, snowflakes) or from a relatively uniform rough surface will produce a signal envelope having a Rayleigh amplitude distribution.

However, many forms of terrain and man-made clutter will not satisfy the requirements for application of the Center Limit Theorem. Whether they do depends on the radar resolution-cell size. As the radar resolution increases (size of resolution cell decreases) it is expected that the clutter signal will deviate to a larger degree from a Rayleigh amplitude distribution because of the reduced number of effective scatterers. Two of the requirements that must be met, for application of the Central Limit Theorem are[4]: 1) there must be many scatterers contributing to the clutter signal, and 2) the mean-square value of the field from any one of these scatterers must be much less than the sum of the mean-square values of the fields from all of the scatterers. Although these facts are well known, there seems to be little information available relative to how many scatterers are required or how much smaller than the total mean-square value any individual mean-square value must be. Asymptotic expressions indicate that for more than five equal amplitude scatterers the Gaussian and Rayleigh statistics are reasonably accurate. However, the total failure of the asymptotic expression when there are two equal scatterers raises questions concerning its accuracy for five to ten scatterers. For this reason, the probability densities for in-phase and quadrature components, as well as those for the envelope, of the clutter signal received from a two-scatterer model and from a four-scatterer model have been computed for several specific values of relative scatterer amplitude. These probability densities are compared with those computed from various commonly used approximations (depending on the situation) to determine how accurate the approximations are when there are a small number of scatterers.

In all of the work reported here it is assumed that the relative phase of the signal received from each scatterer is uniformly distributed over 2π radians and that the relative phases of the scatterers are statistically

independent. This assumption is valid if the placement of scatterers within the resolution cell of the radar is assumed random and the random process giving rise to the scattered signal is considered as the ensemble of possible scatterer placements. For a given set of scatterers in a resolution cell the assumption will also be satisfied if the relative phase among scatterers is independent and changes (due to scatterer movement, internal scatterer variations or changes of radar frequency) with a variance much larger than radians.

It is possible that this assumption will not be satisfied if the clutter at a given radar frequency from only a single resolution cell is considered and if the relative scatterer movements are small relative to a wavelength. Probability density functions can be derived for this case if there are many scatterers present. This configuration can be included in the closed-loop clutter model (Section 7) and its presence in experimental data may be detectable from the clutter correlation functions versus time and frequency (Section 5).

4.2 PROBABILITY DENSITY FUNCTIONS

The clutter signal received from N scatterers can be written

$$S = Re^{i\theta} = \sum_{j=1}^{N} A_j e^{i\phi_j} \tag{4-1}$$

where the A_j and ϕ_j are the relative amplitude and phase of the signal from the j^{th} scatterer and R is the envelope. The sum signal S can now be expressed in terms of an in-phase, x, and quadrature component, y, given by

$$x = Re(S) = R\cos\theta = \sum_{j=1}^{N} A_j \cos\phi_j \tag{4-2}$$

$$y = Im(S) = R\sin\theta = \sum_{j=1}^{N} A_j \sin\phi_j \tag{4-3}$$

For many radar and clutter situations, ϕ_j can be assumed to be uniformly distributed as previously discussed. The A_j can be considered to be fixed constants (as they are here) or to be random variables having identical distributions (as they are in Reference 5). In Appendix A, the probability density functions for the in-phase and quadrature signals ($p(x)$ and $p(y)$) and for the envelope, $p(R)$, are determined by numerical integration. These probability functions are exact to within the numerical approximations used in performing the computations. The probability density $p(x)$ appropriate for phase coherent detection analysis is compared in Appendix A to two frequently used approximations to $p(x)$ for the cases of two ($N=2$) and four ($N=4$) independent scatterers and for several specific values of relative scatterer amplitude. The approximate functions are the Gaussian density function $p_G(x)$ and an asymptotic[5] expansion $p_{GA}(x)$ which, as $N \to \infty$, converges to a Gaussian function.

The calculated envelope probability density, $p(R)$, is also compared in Appendix A to the Rayleigh density, $p_R(R)$, to an asymptotic expansion $p_{RA}(R)$ which converges to a Rayleigh density[5] for large N, and to the Nakagami[6] m-distribution function $p_N(R)$. Graphs of these probability functions and the analytical expressions used can be found in Appendix A.

4.3 DISCUSSION OF RESULTS

Computations of probability densities for in-phase (or quadrature) components and for amplitudes of two or four randomly phased scatterers have been made and the results are presented in Appendix A. For the in-phase (or quadrature) component the probability density, $p(x)$, is non-Gaussian for two vectors regardless of their relative amplitudes. This is also true for four scatterers of unequal amplitudes. For four scatterers of equal, or nearly equal, amplitudes the probability density is very nearly Gaussian. The asymptotic formulation for the Central Limit Theorem, as given in Equation A-10 of Appendix A, is not much more accurate than the unmodified Gaussian probability density function for four scatterers. This fact makes questionable the generally used assumption that the Center Limit Theorem is very nearly valid for five or more random variables.

Computations of the probability density of the envelope, $p(R)$, indicates that the Rayleigh approximation is fairly good for four equal scatterers but becomes poor if the scatterers are unequal in amplitude. Again the asymptotic formulation does not seem particularly good. The Nakagami m-distribution is a very good one when there is one strongly dominant scatterer with three much smaller ones, and it appears to be a better approximation for all of the four-scatterer cases considered here. For two scatterers, neither the Rayleigh nor the Nakagami m-distribution is very good, but the latter is the more nearly accurate, especially when one scatterer is much larger than the other.

For six equal scatterers, results by Greenwood and Durand[7] have been used to indicate that all of the approximations are reasonably valid, $p_{RA}(R)$ being more accurate than $p_R(R)$, which in turn is more accurate than $p_N(R)$.

From the trends found for the cases considered in this investigation, some conclusions regarding the envelope probability density function, $p(R)$, can be drawn:

1. For two scatterers, as would be expected, $p(R)$ is not well represented by Rayleigh or Nakagami m-distribution functions; probably the latter is a better approximation.
2. For four scatterers, $p(R)$ is quite well represented by the Nakagami m-distribution for a wide range of scatterer amplitudes, whereas the Rayleigh distribution is a reasonable approximation only when the scatterers are equal, or very nearly equal, in amplitude.

The configuration of a relatively few significant scatterers in the radar resolution cell has been emphasized because this case seems likely to arise for some types of terrain with the higher resolution being used today and because this configuration and its effects on clutter measurements and data interpretation has been largely ignored in previous measurements. The many

scatterer case is justified for certain types of terrain and examples of both the many-scatterer[8] and few-scatterer[9] cases can be found in clutter measurements data. High resolution C-band measurements (0.1 μ sec) in conjunction with site surveys performed in England[10] indicated major scatterers (cross section $\approx 100\ m^2$) were man-made metal structures occurring with a density of $20/mi^2$. The maximum cross section measured with lower resolution (4 μ sec pulse) was approximately $100\ m^2$ with a 50 percentile of $10\ m^2$. For this particular example the few major scatterer configuration would probably predominate in determining the clutter characteristics for a large portion of the measured data.

Because of the large effect the occurrence of the few major scatterer case has on clutter probability density functions and correlation functions (discussed in Section 5) and the implications with respect to clutter simulation it is important to be able to isolate, identify and determine the scattering characteristics of major scatterers during the performance of clutter measurements. The use of a high resolution coherent radar is probably necessary.

Section 5
CLUTTER CORRELATION FUNCTIONS

5.1 GENERAL

Correlation functions are of interest in the analytical and experimental investigation of clutter and its effects on radar systems because they are a means of describing the dependence of one random variable on another. In the design of radar systems, correlation functions frequently are introduced when performance criteria, such as clutter cancellation in an MTI system, are evaluated using an average mean square analysis.[11] In the analysis of clutter measurement data, dependencies of one parameter on another, such as between the orthogonal polarization components of the clutter signal, can be determined by evaluating their correlation functions. In clutter simulation it is necessary to ensure the correct form of dependence (correlation) among the simulated clutter parameters for accurate evaluation of radar systems, especially when clutter rejection techniques such as MTI, Doppler, or polarization ratio cancellation are employed. Thus correlation functions play a major role in all aspects of the clutter problem.

The discussion in this section is directed to the correlation function relating signal intensity to time delay, frequency variation and resolution cell movement. Signal intensity is only one of the clutter observables (see Section 8) and, for radar system evaluation, one is interested in a much broader class of correlation functions. Parameters such as the correlation between polarization components of the clutter signal, between amplitude and phase and between angle of arrival at different spatial locations are important characteristics of clutter. Many of these clutter characteristics are presently not subject to analytical determination and a clutter measurements program as described in Section 10, embodying an approach as outlined in Section 8 is required.

In this section the correlation function for the signal intensity (squared envelope) of the clutter signal is derived for an arbitrary number of scatterers in the resolution cell of the radar. The probability density function of the clutter-signal amplitude was discussed in Section 4. This information is basic to any statistical characterization of the clutter signal: any simulator to be used for radar evaluation should be capable of matching reasonably well the amplitude characteristics of the clutter signal. Unspecified as yet, however, and not considered in the previous section, is the rate at which the clutter signal changes with time due to motion of the scatterers, and the change in the clutter signal if either the frequency of the radar or the observed region (set of scatterers) is changed. If a radar employs some form of clutter cancellation technique, such as MTI, then the performance of the radar system will vary depending on the amount that the clutter signals are correlated pulse-to-pulse, scan-to-scan, or intrapulse. Consequently, if the radar is to be evaluated using a simulator, the simulator must produce a clutter signal having appropriate time, frequency, and spatial correlation (although in a specific case only some of these properties might be important).

5.2 INTENSITY CORRELATION FUNCTION

Analyses of correlation properties of signals arising from large numbers of scatterers have been made by numerous authors; some of these analyses will be referred to subsequently. In this section are considered the correlation properties of clutter signals obtained from smaller numbers of scatterers, specifically for cases for which the in-phase and quadrature components of the received signal are not Gaussian (i.e., when the conditions of the Central Limit Theorem are not satisfied by the random process). The relationships between these results and the results obtained in the many-scatterer cases are examined as well.

It is shown in Appendix B that the correlation function for signal intensity (squared envelope) can, in general, be expressed as the product of three correlation functions, one for frequency shift, one for time (scatterer motion effect), and one for displacement of the radar resolution cell. It

is not possible at the present time to verify experimentally the complete factorization of the clutter correlation function as described above. The results of this section are therefore intended to demonstrate the method of factorization of the correlation function, with delineation of the assumptions made regarding the characteristics of the scatterers, for the case of an arbitrary number of scatterers in the radar resolution cell. Discussion of measurements techniques applicable to determine the correlation function are given in the program plan, Section 10, and the effects of clutter correlation in simulator design are discussed in Section 7.

The correlation function of signal intensity (envelope squared) is dependent on time (because of scatterer movements), on frequency of the observing radar, and on position of the radar resolution cell (which governs the particular set of scatterers which are observed). Assume that two clutter measurements are performed at times t_1 and t_2 at frequencies of ω_1 and ω_2 respectively. For the measurement performed at t_1 a set of scatterers N_1, governed by the size and position of the range and angle resolution cell of the radar at t_1, is observed. At t_2 the set of scatterers observed is N_2 which may include all, some or none of the N_1 set of scatterers depending on the position of the radar resolution cell at t_2 (and, possibly, scatterer movement between t_1 and t_2). The intensities measured at times t_1 and t_2 are defined as I_1, and I_2. For any specific case of scatterer configuration it is possible to determine I_1 and I_2 and evaluate the variations between them as caused by time, frequency, and resolution cell changes. This result, however, is so specific that it would be of relatively limited application in radar system analysis or design. Another approach is to determine the average manner in which I_1 and I_2 are related. One of the averages frequently used[4] to study the dependence among variables is the correlation function, G, which is defined as:

$$G(t_1, t_2, \omega_1, \omega_2, N_1, N_2) = \frac{\langle I_1 I_2 \rangle - \langle I_1 \rangle \langle I_2 \rangle}{\sigma_1 \sigma_2} \qquad (5\text{-}1)$$

where $\langle\ \rangle$ denotes an average over all statistical parameters and $\sigma_{1,2}$ is the variance defined as

$$\sigma_{1,2} = \sqrt{\langle (I_{1,2} - \langle I_{1,2} \rangle)^2 \rangle} \qquad (5\text{-}2)$$

If I_1 and I_2 are uncorrelated, $G = 0$, whereas if they are highly correlated, $G \approx 1$. Experimentally, the averages are approximated by forming the mean of results of a large number of independent measurements[4]. It will be assumed that the clutter signal is stationary, which of course must be verified for any set of clutter data.[12] Variations of clutter signal statistical characteristics with time can be caused by such factors as rainfall or snowfall, atmospheric effects (ducting) and season. These effects must be identified in the evaluation of clutter data by meteorological observations (see Section 8) and by estimates of stationarity from the clutter data itself.[12] Assuming stationarity, the correlation function can be shown to be dependent only on the time delay, $\tau = t_2 - t_1$, between the measurements rather than on the actual times, t_1 and t_2. The effects of changes in the environment (hourly - daily - seasonal) on radar performance are small over the radar signal processing times (of the order of seconds). If clutter characteristics change with time due to the effects mentioned above, the efficacy of various clutter rejection techniques will also vary and this is most readily evaluated by treating clutter as quasi-stationary; that is, evaluate system performance assuming stationarity for the variety of clutter characteristics which can occur. It is extremely important in a clutter measurements program, as discussed in Section 10, to correlate meteorological conditions/data with electromagnetic observable data to determine the range of clutter conditions, their frequency of occurrence and causal effects.

In Appendix B, the correlation function of Equation 5-1 is derived and shown to be factorable into the form:

$$G(\tau, \omega_1, \omega_2, N_1, N_2) = G(N)\, G(\tau)\, G(\Delta\omega) \qquad (5\text{-}3)$$

where $G(N)$ is the correlation function which expresses the effect of radar scanning (if N_1 and N_2 are identical, $G(N) = 1$). Further discussion of $G(N)$ is given later in this section. $G(\tau)$ is the correlation function which gives the effect of receiving pulses a time τ apart and $G(\Delta\omega)$ describes the effect of changing frequency by $\Delta\omega$, where $\Delta\omega = \omega_2 - \omega_1$. Note that stationarity has been assumed in the derivation of Equation 5-3. Further assumptions made in the derivation are:

1. effects of multiple scattering and local masking are small (only single bounce scattering is included)
2. amplitude and phase of the individual scatterers is independent of frequency
3. relative scatterer locations are statistically independent and the scatterers are randomly distributed over a region large with respect to wavelength
4. net scatter movement over the period will not remove the scatterer from the radar resolution cell
5. scatterer velocities are statistically independent.

Specific expressions for $G(\tau)$ and $G(\Delta\omega)$ are given for uniformly distributed scatterer locations in Appendix B, Equation B-21 or B-22 for uniform or Gaussian velocity distributions, respectively. Multiple scattering and local masking makes the amplitude of the scatterers dependent on their relative locations. This can occur, for example, if one scatterer masks the radar illumination of another or if the scattered signal (bistatic) from one scatterer to a second has approximately the same amplitude as the direct radar illumination of the second scatterer. If the scatterers are relatively far apart with respect to their size, these effects may be small. For cases such as trees in a dense forest, local masking and multiple scattering are significant and only the tree tops may contribute as significant scatterers. Multipath scattering, for example, due to the terrain between the radar and resolution cell, was also not included in the analysis (see Section 7.6).

Variations of the amplitude and phase of the scattering obstacles in a radar resolution cell with changes in frequency are caused by mutual phase cancellation effects among the scattering centers (assuming a composite scatterer), changes of material characteristics (ϵ,σ) with frequency and size dependent effects (Rayleigh/optical scattering regions and resonance). Certainly all of the above factors are important in evaluating relative radar performance at two different frequency bands. For frequency variations of, say 10 percent, only phase cancellation effects within a composite scatterer and resonance effects would be of importance in causing frequency dependence in the individual scatterers.

The assumption that the scatterers are distributed over a region large with respect to wavelength is consistent with the resolution cell size of most radars. The correlation function of Equation 5-3 is the result obtained when scatterer positions can be considered independent for successive measurements of $\mathcal{I}_1$ and $\mathcal{I}_2$. If only a single set of scatterers is considered and the relative scatterer locations are constrained to small movements about some mean location, the complete factorization as shown in Equation 5-3 will not apply. The correlation function for this case can be derived by extension of the analysis given in Appendix B.

The fourth assumption, that scatterers will not move outside of the resolution cell within the time τ, is usually satisfied because major terrain scatterers are constrained to relatively small displacements about some mean position.

The assumption of statistically independent scatterer velocities is reasonable considering the variations in wind conditions, which are the major source of scatterer movement, over a typical resolution cell.

It should be noted that the closed-loop clutter simulator discussed in Section 7 is not constrained by the assumptions described above and also made in the derivation of Equation 5-3. Thus, the sensitivity of the clutter characteristics and correlation functions could be evaluated. Because open-loop simulation, discussed in Appendix E, is not as closely related to basic

scattering characteristics as closed-loop simulation, it is difficult to ascertain whether open-loop simulation is constrained by the assumptions 1 through 5 without further study of their effects on clutter signal characteristics.

5.3 DISCUSSION OF RESULTS

Numerous references are available in which correlation functions have been derived for the frequency-shift, moving-scatterer, and moving-gate situations. In most, if not all, of these references, the many-scatterer assumption is made. In this section, some of these earlier results are considered and compared with those obtained here.

First, consider the effects of a frequency shift; assume that the observed region remains the same and that scatterer velocity is zero. Goldstein[13] derives an expression for the mean-square difference in signal power when there is a change in frequency $\Delta\nu$. His result contains a misprint: in his equation 134, the exponential 2 should be inside, not outside, the square bracket. Although his $(\rho_2 - \rho_1)^2$ is not the same as the correlation function we found in the preceding section, the similarity in significance and functional form can be seen. McGinn and Pike (Reference 12, p. 60) claim that Goldstein's result is seriously in error. This contention does not appear to be justified. The term arising from equality of the four subscripts has been left out, as they say, but this term is zero anyway. Failure to satisfy McGinn and Pike's electrodynamic requirement (that there be no net dc level in the pulse) should be relatively unimportant for any pulse more than a few wavelengths long or for any instantaneous signal bandwidth less than about 20 percent. Contributions arising from the net dc level are analogous to the terms dropped from Equation B-18 and used in obtaining Equation B-19 (Appendix B). McGinn and Pike say that some Monte Carlo checks indicate an error "as great as 10^5" in Goldstein's result; whether they were using the corrected form of his equation 134 is not stated, nor is the quantity equal to 10^5. On the basis of work presented here, the objection raised by McGinn and Pike thus appears invalid. Wallace[14] also derives a correlation function for frequency shifting assuming insignificant target motion during the times involved. His result, obtained for the case of many scatterers, is the same as that presented here.

Next, consider the moving-scatterer case. Fleisher[15] assumes many moving scatterers and derives a correlation function similar to that derived here. The methods of derivation differ significantly but his equation 19 reduces to our form. Fleisher also shows that the correlation function for signal intensity (which we found in the preceding section) is the square of the correlation function for envelope voltage level (ρ) if, and only if, N is large and no single scatterer dominates. These requirements are simply those for the Central Limit Theorem to apply. Therefore, the correlation function of the envelope (R) is the square root of the correlation of the intensity (I) if the envelope is Rayleigh, but as yet nothing can be said of the correlation function of R for other distributions.

Finally, consider the effect of a moving range bin; the corresponding correlation function $G(N)$ was found in Equation B-14 (Appendix B). There is no requirement that there be many scatterers present. Consider, as a special case, a situation in which there are many, homogeneously distributed, equal-amplitude scatterers in the region observed by the moving range bin. Equation B-14, for this case, reduces to:

$$G(N) \approx \frac{N_b^2}{N^2} \qquad (5\text{-}4)$$

where N is the total number of scatterers and N_b is the number of scatterers common to both measurements. This result agrees with Rogers[16] when the appropriate change of variables is made: he is concerned with envelope rather than intensity, so his correlation function is the square root of that derived here (recall Fleisher's result stated above), and he deals in relative shift of range-gate position rather than in numbers of scatterers. His result assumes range bins that are not extremely short, as does ours.

It is also of interest to consider how fast $G(N)$ approaches the value it will have for many scatterers as N increases. Suppose that all scatters have unit amplitude and that the scatterers are homogenously distributed; then, we have:

$$G(N) = \frac{N_b(N_b-1)}{N(N-1)} = \frac{\left(\frac{N_b}{N}\right)\left(\frac{N_b}{N} - \frac{1}{N}\right)}{1 - \frac{1}{N}} \qquad (5\text{-}5)$$

If we assume the scatterers to be homogeneously distributed, $\frac{N_b}{N}$ represents the fraction of the range bin that is common to the first and second measurements; it is, therefore, reasonable to fix $\frac{N_b}{N}$, which is a geometrical parameter, and to let N (and, thus, N_b) increase. In Figure 5-1 are shown some examples from which it can be seen that the limiting-case value of $\left(\frac{N_b}{N}\right)^2$ is approached relatively slowly when $\frac{N_b}{N}$ is small. It is interesting to note that when $N_b > 4$ or 5 the value of $G(N)$ is nearly equal to the $N_b = \infty$ value, at least for the range of values of $\frac{N_b}{N}$ considered here. This result is plausible from inspection of Equation 5-5.

For situations involving unequal scatterers, especially when one, or a few, of the scatterers dominate, $G(N)$ does not reduce to an easily interpreted form. The situation becomes especially hard to interpret when there are relatively few scatterers. On the basis of the analysis which led to it, it seems reasonable to expect Equation B-14 (Appendix B) to be accurate for any set of scatterers; the assumptions that were made relative to negligible terms in our derivation of $G(\tau, \Delta\omega)$ in no way affect $G(N)$. The only effect neglected in our derivation arises from scatterer motion across boundaries, which should be small for terrain clutter.

In the preceding section and the discussion above, it has been shown that the correlation functions for target motion (time correlation), frequency shift, and range-bin shift, under the set of assumptions previously described, are independent quantities that are simply multiplied together to obtain the overall correlation coefficient. It must be remembered, however, that when only a few scatterers are present, measurements are difficult to interpret, because measured quantities will in such cases tend to depart further from their mean values than when there are many scatterers (for an example of such difficulties arising in the field of radar meteorology, see References 17 and 18).

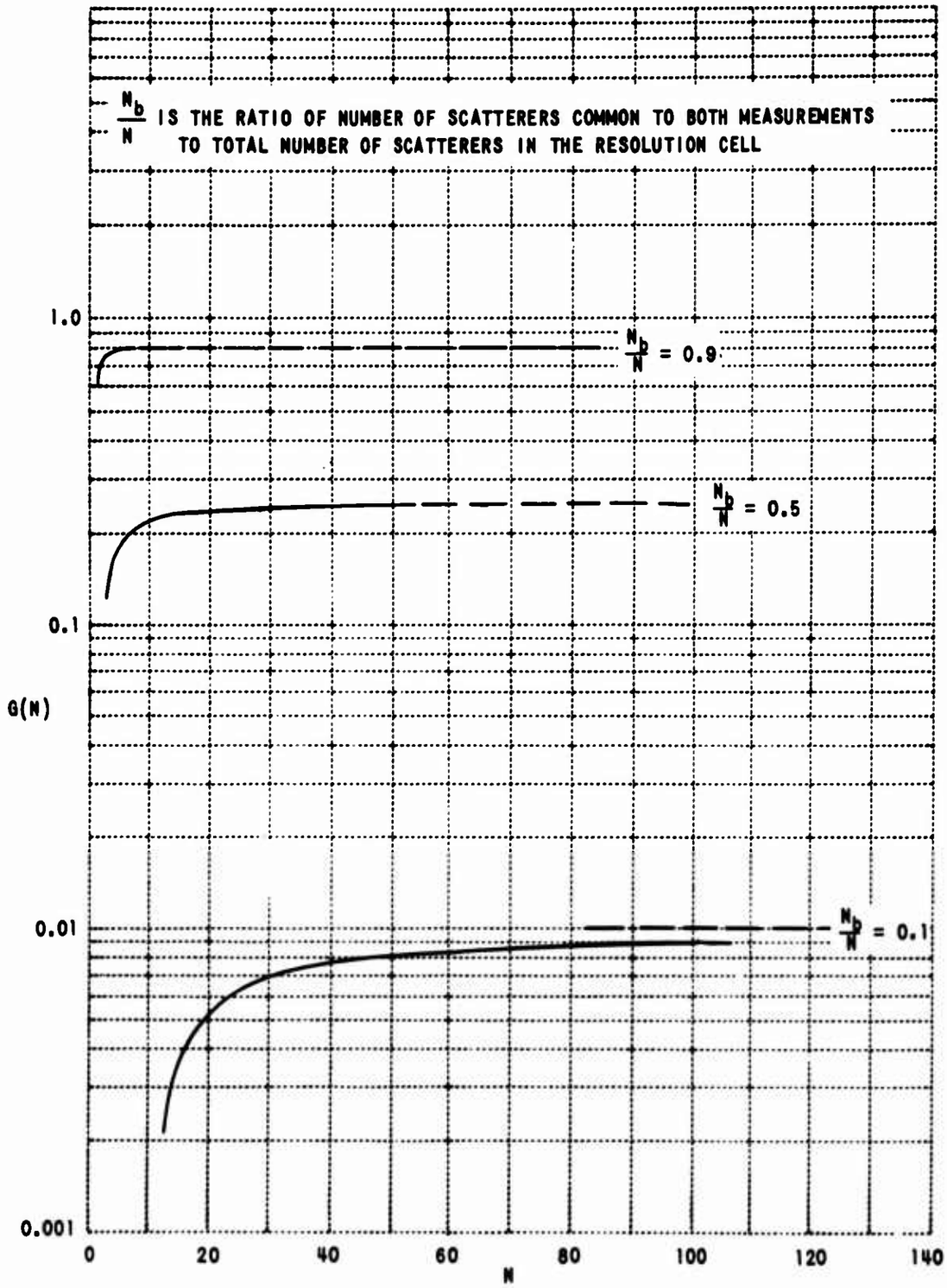

Figure 5-1 CORRELATION FUNCTION G(N) FOR RADAR RESOLUTION CELL MOVEMENT VERSUS NUMBER OF SCATTERERS (N)

Section 6
DOPPLER EFFECTS

In the two previous sections (4 and 5) the probability density functions and the correlation functions were discussed for clutter signals arising from a (not necessarily large) number of scatterers. The probability density function for the amplitude of the signal (envelope) was shown in Section 4 to deviate strongly from the Rayleigh density function when there are few scatterers, particularly when one scatterer dominates the rest. In Section 5, correlation functions relating squared signal amplitudes (i.e., the outputs of square-law detectors) were found to describe effects of frequency shift, scatterer motion, and range-gate motion. As pointed out in Section 5, the probability densities for linearly detected signal amplitudes can be converted into probability densities for square-law-detected signal amplitudes. The inverse operation for correlation functions (i.e., finding the correlation function for a linearly detected signal from that for a square-law-detected signal) is not practical, in general, except in the many-scatterer case for which the probability density function of the linearly detected signal is Rayleigh.

Results in Section 4 were obtained for both coherent and noncoherent radars, whereas Section 5 was concerned primarily with noncoherent radars, although many of the results of Section 5 apply to a coherent radar as well. If coherent (Doppler) radars are of concern, then the simulated clutter signal must have basically the same amplitude and phase spectral characteristic as the actual clutter signal would have. Effective simulation for the Doppler-radar case will be valid for a noncoherent radar, but the converse is not necessarily true.

Consider a set of N scatterers. The k^{th} scatterer is at range r_k at time $t=0$ and has a velocity component along the radar line of sight u_k (u_k positive for a velocity that increases r_k). The radar operates at a (radian)

frequency ω_0 (frequency $f_0 = \frac{\omega_0}{2\pi}$) with free-space wavelength $\lambda_0 = \frac{c}{f_0}$, C = velocity of propagation. The k^{th} scatterer has a scattering amplitude A_k that is proportional to the square root of the radar cross section of that scatterer. It is assumed that electromagnetic interaction between scatterers in the radar resolution cell is negligible; for most cases of interest, this assumption is reasonable. Multipath effects, not considered here, are however generally important and are discussed in Section 7.6. It is also assumed that u_k remains constant during a measurement. The received signal is

$$E(t) = \sum_{k=1}^{N} A_k \cos \left[2 \frac{r_k + u_k t}{c} \omega_0 - \omega_0 t \right] \qquad (6\text{-}1)$$

The following treatment is for integration over all time and embodies the assumption that the velocities u_k and amplitudes A_k are constant for all time. Practical restrictions will impose restrictions on observation time and involve velocities varying in some degree. These restrictions cause individual spectral lines to broaden. The Fourier transform of $E(t)$ is

$$G(\omega) \triangleq \int_{-\infty}^{\infty} E(t) e^{i\omega t} dt = \frac{1}{2} \sum_{k=1}^{N} A_k \left\{ \delta\left(\omega - \left(\omega_0 - \frac{4\pi u_k}{\lambda_0}\right)\right) e^{i \frac{2\omega_0 r_k}{c}} + \delta\left(\omega + \left(\omega_0 - \frac{4\pi u_k}{\lambda_0}\right)\right) e^{-i \frac{2\omega_0 r_k}{c}} \right\} \qquad (6\text{-}2)$$

This power spectrum, defined from $\omega = 0$ to $\omega = \infty$, is then

$$\left| G(\omega) \right|^2 = \sum_{k=1}^{N} A_k^2 \, \delta\left(\omega - \left(\omega_0 - \frac{4\pi u_k}{\lambda_0}\right)\right) \qquad (6\text{-}3)$$

from which, converting to conventional frequency, we obtain

$$P(f) = \sum_{k=1}^{N} A_k^2 \, \delta\left(f - \left(f_0 - \frac{2u_k}{\lambda_0}\right)\right) \qquad (6\text{-}4)$$

In deriving Equation 6-4 it is assumed that all u_k are distinct; if several scatterers have identical u_k values (i.e., $u_{k_1} = u_{k_2} = \ldots$) then A_k must be interpreted as the phasor sum of the individual scattering amplitudes

$$A_k^2 = \left| A_{k_1} e^{i\frac{2\omega_o}{c} r_{k_1}} + A_{k_2} e^{i\frac{2\omega_o}{c} r_{k_2}} + \cdots \right|^2 \qquad (6\text{-}5)$$

Note that nowhere in the derivation of Equation 6-4 was N assumed to be large; it is only necessary that N remain fixed during the time of the measurement. It is seen from Equation 6-4 that $P(f)$ has values at discrete frequencies that depend upon scatterer velocity u_k. The quantity $\frac{2u_k}{\lambda_o}$ is simply the Doppler frequency shift associated with the k^{th} scatterer. If all scatterers had the same amplitude ($A_k = A$ for all k) then $P(f)$ would have the same shape as the velocity spectrum. If the A_k are unequal, $P(f)$ is a weighted velocity spectrum.

Similar results have been obtained by Rogers (Reference 18, p. 12) for the large-N case. His result is a continuum-spectrum form analogous to our Equation 6-4.

The basic concept on which a doppler radar separates the returns from scatterers having different velocities along the line of sight is presented in the above discussion. Two limitations must be considered. First, note that in practice the power spectrum $P(f)$ is not centered on f_o but on some much lower frequency obtained from one or more heterodyning operations. A spectrum folding limitation frequently arises due to the multiple-line structure in the transmitted waveform -- the typical PRF harmonics for instance. Also, if the lower frequency is less than $\max \left| \frac{2u_k}{\lambda_o} \right|$ folding may occur and negative velocities will be confused with positive velocities. In the limit, $P(f)$ might be centered on 0 frequency (a situation that would arise if the signal were beat against a local oscillator operating at f_o) and then, for a system employing a Doppler frequency measurement, all negative velocities would be reinterpreted as positive velocities. In such systems the positive or the negative part of the velocity spectrum can be found only if the velocity spectrum is symmetrical (Reference 18, p. 16). A second limitation on measurement of scatterer velocities is the resolution

limit imposed by a finite pulse length; uncertainty in velocity measurements is of the order of $\frac{c}{(2 f_o \tau_e)}$, where τ_e is the effective length of the pulse ($\tau_e \approx T$, the pulse duration, if the pulse is approximately rectangular and multiple pulse integration is not employed) (Reference 19, p. 203). However, if a long train of coherent pulses are used, one can obtain an arbitrarily high degree of velocity resolution against "ideal" scatterers (for high $\frac{S}{N}$, velocity resolution would be independent of pulse length but dependent on total observation time).

To what extent, then, must Doppler characteristics be simulated? Certainly, if a coherent (pulse-Doppler) radar is to be evaluated using a simulated clutter signal, it is necessary that the spectral characteristics of the clutter signal match reasonably well those of the clutter being simulated. If the clutter signal were simulated by a wide-band noise source, the spectrum of the clutter signal would be determined by the bandpass characteristics of the receiver. The apparent velocity spectrum of the clutter would then be as established by the receiver characteristics independently of the actual clutter characteristics. This inadequacy is typical of a simulator that attempts to use a noise source to represent a clutter signal; further discussion of this situation is given in Section 7. Accurate simulation of the clutter-signal spectrum is of greatest importance if the radar to be evaluated uses signal temporal characteristics to discriminate between target and clutter. For example, suppose a Doppler radar employed characteristics of the phase or amplitude of the cross section versus time of aircraft or missiles to enhance detection in the presence of clutter. It would obviously be necessary in this case to use much more representative clutter signals for simulation purposes than could be generated from filtered white noise.

In the foregoing discussion it has been (inherently) assumed that the radar is stationary and that each scatterer has a (momentarily) constant velocity component along the radar line of sight. If the radar is in motion, additional Doppler shifts result. Although these effects can be described by Equation 6-4 by including radar motion in the definition of u_k (which thus

becomes the relative velocity between the radar and the k^{th} scatterer), it may at times be convenient to consider the Doppler shift as arising from two motions: first, the gross motion of the radar toward a fixed reference near the clutter-generating region, and, second, the motions of individual scatterers relative to the first reference. For ground clutter, the radar-motion effect dominates in the case of fixed scatterers (rocks, ground contour, buildings, tree trunks, etc.); the second effect arises when there is motion of scatterers relative to the ground (moving vehicles, wind-moved foliage, etc.). The radar-motion component is geometrical and can be computed, approximately, using simple trigonometry. Because (typically) ground clutter is observed over a range of elevation and azimuth angles the clutter signal is spread over a spectral width dependent on the angular width and orientation (with respect to the velocity vector) of the radar beam. Scatterer motion produces additional Doppler shifts that may be important, depending on the system. Additional spectral components can arise from antenna sidelobes that illuminate terrain at angles (and, consequently, at relative velocities) much different (usually) from those prevailing along the main lobe.

If a clutter simulation is to be used to evaluate a coherent (e.g., pulse-Doppler) radar, it is necessary that the spectral characteristics of the simulated clutter signal match those of the actual clutter signal. It is shown here (Equation 6-4) that the power spectrum of the clutter signal is a weighted form of the velocity spectrum regardless of the number of scatterers contributing to the signal provided multiple scattering effects are small. Separation of velocity into two parts, one for radar motion relative to a fixed point on the ground and one for motion of scatterers relative to the ground, may prove useful for some forms of simulation, since radar motion is thus specified independently of scatterer motion.

Section 7
CLUTTER SIMULATION

7.1 GENERAL

In the following section the simulation of clutter and clutter/target interactions for evaluation of radar systems are discussed. Clutter simulation techniques are based on some form of clutter model - that is, on a method of representing the characteristics of the clutter signal and the changes in the clutter due to changes in illuminator and/or observer radar parameters. It is assumed that only a relatively refined clutter simulation is of interest, and, thus, little attention is given to the use of additive filtered noise to represent a complete clutter signal, although some of the limitations of this approach are discussed.

The generic forms of open-loop and closed-loop clutter models as described in Section 3.2, also see Figures 3-1 and 3-2, are used to categorize simulation techniques for clutter signals. The use of additive noise to simulate clutter is an open-loop simulation; that is, the properties of the clutter signal, probability density function, average power and spectrum in this case, must be known (or assumed known) for the particular radar of interest. The clutter signal having the desired characteristics is formed and added to the target signal (see Figure 3-1) for evaluation of the radar.

7.2 BASIC CONSIDERATIONS

For either open-loop or closed-loop clutter models, two implementations as a simulator are possible: either analog or digital computation might be used (or, possibly, hybrid computation, although this technique will not be discussed explicitly here). There are, therefore, four possible simulation techniques discussed in this section: open-loop simulation, analog and digital, and closed-loop simulation, analog and digital. First, however, some basic properties of these techniques are considered.

7.2.1 Open Loop versus Closed Loop

Closed-loop simulation has significant advantages over open-loop simulation and its use for all but the simplest of simulators seems assured. The principal advantage is that a well-designed, closed-loop simulator would function for a wide variety of radar signals without internal adjustment, whereas in an open-loop simulator it would be necessary to adjust both the clutter-signal and the target signal generators for any change in radar parameters. Both techniques require about the same amount of computation, in spite of the apparent relative simplicity of the open-loop simulator, because of the need for additional computation for proper adjustment of the signal generators. This situation becomes even more serious when it is necessary to include such effects as masking and multipath.

7.2.2 Analog versus Digital

The use of analog-computation simulation is quickly found to have significant disadvantages when it is compared with digital-computation simulation. The main disadvantage is a requirement for a large number of signal generators with appropriate controls for amplitudes and phases (and, possibly, frequency as well). Frequency scaling to conventional analog-computer frequencies is not practical, except in special circumstances (such as investigation of pulse-shape distortion for a very limited number of pulses), because of the attendant increase in simulation time (thus if frequency is scaled by 10^{-6}, computation time is increased by 10^{6}). It therefore may be necessary to operate at least part of the simulator at high frequencies; although feasible, one of the conveniences of normal analog computation is lost.

Because the digital-computation, indirect-generation simulator appears to be the most flexible type, this form is discussed in the next section in some detail. Considerations involved in inclusion of polarization effects, masking effects, multipath effects, and bistatic-system effects into the closed-loop simulator are included. A discussion of closed-loop analog simulation and open-loop simulation (analog and digital) is included in Appendix E.

7.3 CLOSED-LOOP SIMULATION - DIGITAL COMPUTATION

As noted in Section 7.2, the combination of digital computation with closed-loop simulation of clutter (and target) signals offers a maximum of flexibility. Exact computation of waveform of radar signals scattered from clutter is obviously impossible. For radars and pulses of commonly used bandwidths, useful results can be obtained using straightforward approximations, provided the scatterers producing the clutter signal satisfy certain restrictions:

1. Scattering is independent (interaction among scatterers can be ignored); this approximation is reasonable, but in some cases it may not be satisfied. Inclusion of multiply scattered signals is possible in the simulation and is discussed in Section 7.3.4.
2. Scattering from a particular scatterer is not a rapidly varying function with frequency. Thus, scattering from highly resonant (within radar band) objects (e.g., dipoles) may need modified treatment, although again there is no difficulty in including such effects in the simulation if the appropriate parameters are known (see Section 7.3.5).
3. Acceleration of scatterers is small enough so that, during the time involved in a range scan, the velocity of a scatterer can be assumed constant.

Removal of these restrictions is discussed after the more simple case, in which they are satisfied, has been treated.

7.3.1 Computation of Clutter Signal Envelope

First, assume that restrictions 1 through 3 are satisfied and that the clutter signal arises from discrete scatterers in the antenna beam. For the moment, assume that the antenna does not scan and that there are N significant scatterers along the ground in the range of interest. If the transmitted radar signal is:

$$e_t(t) = e_1(t) \cos(\omega_o t) \tag{7-1}$$

where $e_1(t)$ is an envelope function that varies slowly relative to the (radian) carrier frequency ω_o, then it can be shown (Appendix C) that the signal received from the N scatterers, if they are stationary, is:

$$e_r(t) = \sum_{k=1}^{N} a_k \; e_1(t - \tau_k) \cos\left[\omega_o (t - \tau_k)\right] \tag{7-2}$$

where a_k is the amplitude of the return from the k^{th} scatterer and τ_k is the (2-way) time delay corresponding to propagation from the radar to the scatterer and back. Therefore, the appropriately scaled and time-shifted envelopes can be added together, provided the relative RF phases at the carrier frequency are taken into account. Equation 7-2 holds regardless of the bandwidth of the signal (i.e., it is not actually necessary for $e_1(t)$ to vary slowly relative to ω_o for Equation 7-2 to hold).

7.3.2 Receiver Filtering Effects

If the receiver has a bandpass characteristic that distorts the received waveform, as is commonly the case, then a modification to the above result (and that of Appendix C) is required. Provided $e_1(t)$ varies slowly enough relative to ω_o so that spectral folding is not significant,* and provided the receiver bandpass is symmetrical about ω_o, the received waveform can be found from Equation 7-2 with $e_1(t - \tau_k)$ being replaced by $e_2(t - \tau_k)$, where $e_2(t)$ is the waveform obtained when $e_1(t)$, the envelope function, is passed through the low-pass equivalent of the bandpass filter in the receiver (i.e., the filter characteristic obtained by shifting the bandpass from its center frequency in the receiver to 0). If the bandpass filter (receiver) is not symmetrical about ω_o, a more complicated analysis becomes necessary. The nonsymmetrical part of the filter response now produces a quadrature phase signal component. Two equivalent low-pass filters are also now required, one

*Spectral folding is unimportant for most radars; only in an extremely short-pulse, high-resolution radar will it be significant.

to find amplitude of the in-phase component, and the other, the amplitude of the quadrature component.[20] Although some additional computation is required, there is no fundamental difficulty introduced by an offset bandpass filter, and the basic method discussed can still be applied.

7.3.3 Doppler Effects

Another modification to Equation 7-2 is required when the scatterers are moving and thereby producing different Doppler shifts. If the k^{th} scatterer has velocity component u_k along the line of sight (positive in the direction away from the radar), and if τ_k now represents the delay associated with the k^{th} scatterer at $t = 0$, Equation 7-2 becomes:

$$e_r(t) = \sum_{k=1}^{N} a_k \, e_1\left(t - \tau_k - \frac{2u_k}{c} t\right) \cos\left[\omega_o\left(1 - \frac{2u_k}{c}\right)t - \omega_o \tau_k\right] \qquad (7\text{-}3)$$

No longer is the straightforward addition of properly phased contributions possible, because the phase shift associated with the carrier now is itself time varying (at the Doppler-frequency rate). Each of the pulses added together is thus at a different frequency (assuming distinct u_k values). The envelope is therefore time varying in a much more complicated way than when all $u_k = 0$. We can write Equation 7-3 as:

$$e_r(t) = \left\{\sum_{k=1}^{N} a_k^2 \left[e_1\left(t - \tau_k - \frac{2u_k}{c} t\right)\right]^2 + 2\sum_{k=2}^{N}\sum_{m=1}^{k-1} a_k a_m \, e_1\left(t - \tau_k - \frac{2u_k}{c} t\right) e_1\left(t - \tau_m - \frac{2u_m}{c} t\right) \cdot \right.$$
$$\left. \cdot \cos\left[\frac{2\omega_o t}{c}(u_k - u_m) + \omega_o(\tau_k - \tau_m)\right]\right\}^{1/2} \cos\left[\omega_o t + \phi\right] \qquad (7\text{-}4)$$

where $\phi(t)$ is a phase modulation, the envelope being the quantity in curly brackets (the exponent 1/2 is dropped if a square-law detector is used). For scatterers more than a pulse width apart, the interaction term drops out. If there is a large constant velocity superimposed on the u_k values (as when ground-clutter measurements are made from an airborne radar), Equation 7-4 should be modified by letting ω_o be the carrier frequency Doppler shifted by the constant velocity; u_k then are variations in the velocity relative to the

reference value used to establish ω_o. Note that even in this case computation need not be at the RF rate, since the envelope of the output, which is being computed, varies at a much lower rate, in general. Although this method is not exact, because of the ambiguity introduced by one's choice of carrier frequency in the derivation, Equation 7-4 should give useful results if some care is exercised. A more exact method would be to compute $e_r(t)$ from Equation 7-3 and use some form of (numerical) envelope detector. Possibilities include: 1) the finding of peaks of the waveform and assigning these values to the envelope and 2) the procedure of squaring $e_r(t)$ or finding its absolute value, if a linear detector is desired, and passing the result through a (numerical) low-pass filter. Such methods are more realistic but require far more computer time.

The discussion in the preceding paragraph applies to an incoherent radar that envelope detects the received signal. A Doppler radar uses filters to separate components of different frequencies, and, hence, the portions of the signal received from scatterers having different velocities (Section 6). If $e_f(t)$ varies much more slowly than ω_o, one can, to a first order, assign those scatterers for which $\omega_o\left(1-\frac{2u_k}{c}\right)$ lies in a particular Doppler-filter bandwidth to that channel of the receiver. Each channel will then have a signal formed by a subset of the N scatterers. If the signals in the Doppler channels are then detected incoherently, the above methods can be applied separately in each channel. If $e_f(t)$ is short (contains few cycles of ω_o) there is a broadening of the spectrum associated with each u_k value that must be taken into account; this broadening is a cause of the Doppler ambiguity, an uncertainty in velocity measurement of the order of $\frac{c}{2f_o\tau_e}$, where $f_o = \frac{\omega_o}{2\pi}$ and τ_e, the effective pulse length, is of the order of the pulse duration if the pulse is approximately rectangular (Reference 19, p. 203). Inclusion of these effects in the clutter simulation could take at least two, and probably more, forms. First, one could compute the RF waveform and use numerical filtering to sort out which signals appear in which channel. This method is accurate for any spectral characteristics but involves a large number of computations. Alternatively, analytical expressions for the amount of spectral spreading could be developed and used to modify the first-order approximation in which no spreading was assumed. Of greatest significance here is the fact that the

form of simulation may have to be changed, depending on the form of processing involved; the alternative would be to produce the complete waveform, which would be usable in any processor, but which would be expensive in computer time. It is clear that further work, as described in the program plan, is required before an optimum technique can be recommended for simulation of clutter for a coherent (pulse-Doppler) radar.

7.3.4 Multiple Scattering

The discussion so far has been based on the assumption that restrictions 1 through 3 at the beginning of this section are satisfied. Let us consider the effect of relaxing these restrictions. Restriction 1 can be violated in at least two ways. If interaction of scatterers is a simple, multiple-bounce effect whereby the wave striking one scatterer is diffracted to another and thence back to the radar, a straightforward extension of the methods discussed above is possible. It is only necessary to introduce a fictitious scatterer in addition to each member of an interaction pair; this fictitious scatterer has a delay corresponding to the total propagation path and an amplitude that depends on the appropriate bistatic cross sections of the intersecting scatterers and the range between them. The difficulty in implementing this computation lies with the assignment of parameters, not in the computation itself. If, on the other hand, the scatterers are close enough that they are electromagnetically coupled, no simple model will suffice. It is probable that, in this case, the interacting pair could best be treated as a single scatterer with (possibly) a rapidly varying frequency response. This situation then would correspond to a violation of restriction 2.

7.3.5 Scatterer Frequency Dependence

If a scatterer has a scattering amplitude that varies rapidly with frequency, in violation of restriction 2, the system response can be found by assuming the frequency-response characteristic of the scatterer to be combined with the filtering characteristic of the receiver.* The resulting (generally)

*It is necessary, of course, that a suitable scattering description of the scatterer be available.

nonsymmetrical filter can then be treated using in-phase and quadrature equivalent low-pass filters as discussed above. For each such scatterer, then, two distorted pulse envelopes are fou. i, one being an envelope for an in-phase carrier, and the other, an envelope for a quadrature carrier. The resultant envelope of the received signal can be computed as before.

7.3.6 Scatterer Acceleration

Failure to satisfy restriction 3 in a noncoherent radar causes little difficulty if the RF waveform is to be computed and detected. If Equation 7-4 is to be used, variable u_k can be included straightforwardly with (probably) little, if any, error. Restriction 3 is important if a coherent (pulse-Doppler) radar is involved, because the change in velocities will cause smearing of the Doppler spectrum. The feasibility of including variable u_k in the computation depends upon the type of computation being made, which in turn depends, as noted above, upon the use to be made of the simulation. If the time-varying RF waveform is computed from Equation 7-3, u_k can be made a variable with little additional effort. If analytical expressions for spectral spreading are used to modify the first-order approximation, additional modification to compensate for spectral spreading resulting from nonconstant velocities must be made. Thus, to some extent at least, the restrictions can be relaxed at the expense of added computations.

7.3.7 Range Gate

We have thus seen that, if some reasonable restrictions are met, relatively straightforward computation will yield a simulated clutter signal, $e_r(t)$, as a function of time, provided suitable values can be found for the a_k and τ_k parameters. If the receiver is range gated, $e_r(t)$ can be simply multiplied by a time function corresponding to the range gate; in its simplest form, the range gate accepts values of $e_r(t)$ for t within specific limits and makes $e_r(t)$ zero for times not within these limits (rectangular range gate). If there are several τ_k values in each range-resolution cell, the (simulated)

received clutter signal will have reasonable time, frequency, and spatial (in the range direction) correlation functions (Section 5), so long as appropriate parameters are assigned the variables. If some scatterers are far enough to the side of the radar line of sight, they may be less strongly illuminated because of the antenna pattern. This effect can easily be accounted for by a modification of a_k for each scatterer to compensate for the antenna gain in its direction. Note that a_k must also contain an r_k^{-4} (or, analogously, τ_k^{-4}) factor to correct for the range to the scatterer; this correction is unimportant if a relatively narrow range interval far from the radar is of interest but becomes very important if many ranges, both near and far away, are included in the investigation.

7.3.8 Antenna Scanning

Next, suppose the radar antenna scans in azimuth. As it scans, new scatterers enter the beam and old ones leave it (at a fixed range). One straightforward simulation procedure is to assign angular locations to scatterers over the range to be covered by the (azimuth) scanning antenna and to use factors related to the antenna gain to modify the scattering coefficient of each scatterer, depending on its angular location. To provide a reasonable approximation to the actual spatial correlation properties of the signal during azimuth scan, several scatterers must occur per beamwidth in each range-resolution length. If the antenna is to scan over wide angles, a much larger number of scatterers must therefore be assigned than was the case for a non-scanning antenna. Computer-storage problems may arise because of the large number of scatterers whose amplitudes and phases must be stored.

Note that regardless of the manner of representing the transmitted and received radar signals (i.e., whether just envelopes or the entire RF waveform are computed), the same representation of the scatterers suffices: a reflection coefficient and location must be stored for each scatterer. The only change in scatterer information required by changes in radar type is in the frequency dependence; if the simulation is to be used for radars operating at different frequencies, the stored reflection coefficients must then be

functions of frequency. Another modification might be desirable in the computation: if the radar had a large resolution cell, one might use fewer scattering elements (with correspondingly increased amplitudes) than he would for a radar having a small resolution cell. Again, it is clear that this consideration affects the computational procedure used but not the clutter information needed, since enough scatterer parameters must be included to produce realistic correlation behavior with the highest resolution radar to be investigated.

7.4 SIMULATION OF POLARIZATION CHARACTERISTICS OF RADAR CLUTTER

Thus far the polarization properties of the clutter signal have been ignored. If a radar using one particular polarization were always to be simulated, the foregoing would be an adequate clutter model. However, many current and proposed radars use multiple or variable polarizations, and for such radars the simple clutter model, wherein a single reflection coefficient (possibly a function of frequency) permits computation of that portion of the received signal arising at one scatterer, is not sufficient.

If polarization properties of radar scatterers (whether target or clutter sources) are to be included in a scattering model, the reflection coefficient for each scatterer must be expressed as a matrix rather than as a single number (Reference 19, pp. 560-566; Reference 21, Appendix E). Three amplitudes and two relative phases (in addition to another phase associated with γ_k) are required to describe the backscattering from a target or clutter scatterer (the eight elements of the matrix, four amplitudes and four phases, are reduced because of reciprocity considerations and the removal of one phase angle that can be associated with an effective range to the scatterer). Computer storage requirements are therefore greatly increased over those for simulation when clutter polarization is neglected.

Computation of waveform envelopes, or of complete RF waveforms, is only slightly complicated (although computation time may be significantly increased) by the requirement that polarization information be included. Two

transmitted signals, one corresponding to the vertically polarized portion of the transmitted wave, and the other, to the horizontally polarized portion, must now be used (although in the special cases of vertically or horizontally polarized transmission one of them may be zero).* These signals will be in phase if linear polarization is used, but they will be out of phase if elliptical or circular polarization is used. It is therefore necessary to use in-phase and quadrature components with a separate envelope function for each. Each component of the signal is then operated on by the scattering matrix; the amplitude and phase of each component are thus modified. The signal at the receiving antenna is the sum of the signals from all of the scatterers; the summation procedure and the computation of envelopes, etc., are the same as were described previously, except for the need to include in-phase and quadrature components (which were, in fact, required in some cases even when polarization effects were neglected) and the need for separate horizontal- and vertical-polarization components.

The principal difficulty associated with the polarization-inclusive clutter model is the assignment of appropriate elements to the scattering matrices. Obviously these quantities cannot be computed from basic scattering theory for any but the simplest of scatterers. Measurements of scattering matrices of all of the individual scatterers of the myriad varieties that can produce ground clutter are also not feasible. A more practical approach to the problem is to measure scattering matrices of some typical clutter-producing objects, to use the parameters so obtained as a guide in assigning coefficients to the scatterers as a group in the simulation, and then to compare the results obtained from the simulation with actual clutter measurements. In this way it might be possible to obtain realistic clutter simulation, including the polarization properties of the clutter, without an excessive number of measurements being required.

---

*In this discussion, vertical and horizontal polarization have been adopted as reference polarizations. Any orthogonal pair of polarizations might be chosen; right- and left-circular polarizations are sometimes a more convenient choice. The choice of a particular pair to simplify the discussion is not intended to preclude other choices.

7.5 MASKING EFFECTS

In the discussion so far, it has been tacitly assumed that the radar directly observes the clutter elements (and the target, if any) at all points along the scattering surface. Although this condition is frequently fulfilled for an airborne radar (though by no means always, especially in mountainous terrain) it is seldom fulfilled for a ground-based radar. Masking of clutter and targets by clutter can be produced by a wide variety of objects. In rough terrain, valleys may be masked by hills, as illustrated in Figure 7-1. The shaded regions are not observed by the radar. Clutter sources on the ground in these regions do not affect the radar because they are not observed by it; (it is generally assumed that significant diffraction into such regions is unlikely). A radar target is equally unobservable in these regions except for multipath and diffraction effects. Masking can also be produced by vegetation or buildings between the radar and more remote clutter sources.

Figure 7-1 TERRAIN MASKING

Thus it is quite possible that the radar will receive clutter returns from some range/azimuth cells and not from others; in Figure 7-1 no clutter returns would be received from those ranges corresponding to the shaded regions. The clutter simulation techniques discussed above would produce clutter returns at all ranges. To permit inclusion of terrain masking effects (not vegetation or man-made masking), it is necessary only to compute, from topographic information, which scatterers are masked and to assign zero scattering amplitude to them. Therefore, no change in the clutter model or calculations employed in the simulation is required. Computation of shadowed regions from contour information (from a topographic map) is feasible, and has been included in

digital-computer simulations at CAL[22] to evaluate gross masking effects (deep shadows). Note that such computations are based on geometry of the region involved and for a ground-based radar this set of geometrical parameters could be computed once at the start of the computations and the results stored for use in a number of situations involving the same basic terrain. The discussion in Appendix D illustrates a method for evaluating the gross effects of masking and clutter.

When masking is produced locally by trees or manmade objects that are not included in the topographic map, inclusion of these masking effects is more difficult, especially if masking is by a thin stand of trees that only partially masks the region beyond. In the latter case, reasonable approximations based on selected measurements should permit realistic simulation of the masked clutter although accurate data would probably require optical measurements performed in the field. If target-scattered signals are to be included in the simulation, the same masking information found for clutter can be used to indicate when the target is being masked.

7.6 MULTIPATH-PROPAGATION EFFECTS

In the previous discussion it has been assumed that target and clutter sources are independent. This assumption implies that signals received from clutter sources are unchanged by the presence of a target, and that the signal from the target is not affected by the rough terrain between radar and target. These independently scattered and received signals are added at the radar receiver.

Situations in which there is interaction between terrain and target can also arise, as shown, for example, in Figure 7-2. Note that the target in Figure 7-2 can also represent a clutter scatterer for which multipath effects on the clutter return would be evaluated. Several possible propagation paths are shown here: 1) along the paths RT-TR, 2) over the paths RG-GT-TR wherein the radar wave is reflected from the ground to the target and back to the radar, 3) the reciprocal path RT-TG-GR, 4) the doubly reflected path RG-GT-TG-GR, and 5) over the path RT-TS-ST-TR where the bistatically scattered energy from the aircraft (path TS) is reflected at near normal incidence from the ground

Figure 7-2 MULTIPATH EFFECTS

back to the aircraft, again suffers bistatic scattering and then proceeds to the receiver. For a low-flying aircraft (T), the differential time delays will frequently not be sufficient to permit separation in range of the echoes over these different paths. The changing interference resulting from the changes in path length cause the target signal to fluctuate rapidly even if the target would produce a steady signal in the absence of ground reflections. Multipath interference also perturbs angle tracking: since part of the signal now appears to arise from point G, the apparent angle of arrival can fluctuate over a much wider range than it would if the target were in free space. Note that multipath via the route RT-TS-ST-TR arrives at the receiver <u>from the target</u>, so that this path by itself does not produce large angle-of-arrival errors. It does, however, cause large amplitude fluctuations through interference with the direct path, RT-TR, which may then allow the TG-GR path to cause an increased angle of arrival error. If the simulation is to be capable of including angle of arrival effects, it will be necessary to include angle information with the signal components at the receiving antenna and to gather this data when performing experimental programs. For example, it might be necessary, in simulating a monopulse system, to retain sum and difference channels in the receiver. Angle-of-arrival effects would also be important for CON scan, TWS, and other angle-of-arrival measurement techniques -- the simulation of angle-of-arrival (i.e., amplitude and phase fronts) should properly be part of the "clutter" simulation.

For specular scattering from relatively smooth terrain, there is only one point G, easily found from geometrical considerations, that is especially important. It is the point at which the ray to the (inverted) image T' from

the radar intersects the ground. For the path RT-TS-ST-TR, it is the point S directly under the target that is important.

For angles near grazing over smooth terrain, the reflection coefficient is very nearly -1; at larger angles, analytical expressions depending upon wavelength, polarization, angle of incidence, and physical properties of the material in region G are available. It is thus possible to include the effect of ground reflection by including an extra simulated clutter or target-returned signal in the direction RG and with amplitude and phase determined by the reflection coefficient of the terrain near G and the radar cross section of the target.*

If the ground is gently rolling, two or more specular-reflection points analogous to G may occur. In this case the reflection coefficient of the terrain may have to be modified to take into account the spreading of the beam produced by curvature of the reflecting surface near the scattering region. The simulated target signal now must include additional components, such as are described above, for each of the specularly reflecting points. Inclusion of such effects will increase computation time and complexity, especially if several targets, rather than one, are involved, but no serious difficulties should be introduced.

So far in this section the discussion has been limited to relatively smooth terrain that produces specular reflections in the direction of the target. It is very possible that the terrain may be rough enough to produce significant amounts of diffuse scattering and only negligible specular scattering; there can also be an intermediate range of roughnesses for which

---

* For propagation path RG-GT-TG-GR, the target radar cross section is needed at a slightly different angle from that used for the RT-TR propagation path. For propagation paths RT-TG-GR and RG-GT-TR, the bistatic target cross section is required. For small bistatic angles, which will usually be required for low-flying aircraft (for which clutter problems are most serious), the bistatic cross section can be related to the monostatic cross section (Reference 23). The special case RT-TS-ST-TR entails cross section for a 90-degree or larger bistatic angle, which is frequently much greater than for the monostatic case.

significant amounts of both specular and diffuse scattering occur. A general discussion of specular and diffuse scattering is available in Reference 24; for a discussion of closely related effects, see also Reference 23. Increasing the roughness in the vicinity of a specular-reflection point reduces the reflection coefficient in the specular direction. As a rough estimate, specular reflection can be considered important when the effective roughness parameter $\frac{4\pi \Delta h \sin\gamma}{\lambda}$ is less than unity, where Δh is the standard deviation of the distribution of heights, γ is the grazing angle, and λ is the radar wavelength (Reference 24, p. 246). In a simulation, it is probably reasonable to include a factor related to the roughness parameter to reduce the reflection coefficient as roughness increases; such factors depend upon the statistical distribution of heights, but are of the same order of magnitude for several, quite different distributions (Reference 24, Figure 12.1). Slight roughness can therefore be treated in much the same manner as was smooth terrain.

As terrain roughness increases, the specularly reflected wave becomes less and less important in its effect on the radar return from the target (or targets), whereas diffuse scattering becomes more important. Inclusion of diffuse scattering is much less straightforward than was specular scattering, because propagation here occurs along many different paths with random phasings because of the many scatterers that now contribute to the signal at the target, and, on the return path, to the signal at the receiver. Diffuse scattering normally arises in a region (the "glistening surface") that is centered on the specular-reflection point and increases in size as the surface roughness increases. For small surface roughness, most of the diffuse scattering arises near the center of this region, whereas for large surface roughness most of the diffuse scattering arises near the ends of this region (Reference 24, pp. 249-277).

The basic clutter model described in earlier sections of this report can be used to include multipath-propagation effects. The ground-clutter elements that contribute to diffusely scattered target illumination can be represented by bistatic scattering coefficients analogous to the monostatic scattering coefficient a_k used to describe backscattering from clutter elements.

The scatterer location relative to the radar can still be given by τ, provided care is used to reinterpret this 2-way time delay when one-way situations are being considered. Initially, the phase associated with the scatterer can be assigned by a random process. Once the location and bistatic scattering properties of the scattering element have been chosen, the calculation of the received signal along each of the paths associated with that scattering element is possible, provided the bistatic cross section of the target is known or can be approximated. Since the bistatic angle at the scattering element changes as the target location changes, the scatterer properties must be known (or approximated) over the range of bistatic angles that can occur. The summation of received signals along all of the paths associated with many (simulated) scatterers can now be used to represent the effect of target-clutter interaction (multipath effect). Direct target return and clutter backscatter are simulated as before and those signals added to the signal arising from interaction. Also to be added are the specularly reflected interaction signals discussed at the beginning of this section.

By using a large number (of the order of the number used for simulation of clutter backscatter) of simulated clutter-interaction-producing scatterers, one can probably achieve quite realistic signal characteristics even though highly accurate bistatic information on clutter scatterers is not available. Inclusion of masking effects follows from the technique discussed in Section 7.4. Comparison of interaction-induced effects on the received signal as measured in the field (see Section 8 for a discussion of measurement techniques) and as simulated using the procedure described here would be required before good estimates of required accuracies (and number of scatterers required in the simulation) could be made.

If polarization properties of the scattering process are to be included in the simulation, scattering matrices must replace scattering coefficients, as indicated in Section 7.3. There is some doubt as to whether the bistatic scattering matrix is symmetric: it is symmetric for perfectly conducting targets, but may not be for targets of other materials (References 20 and 22). For the present application the only effect would be to raise

the number of parameters in the scattering matrix from five to seven. In any event, it is obvious that a great deal of information must be stored and that forward scattering measurements (see Section 7) are required for generating realistic values for the scatterer parameters.

7.7 BISTATIC SYSTEM CONSIDERATIONS

It is also possible that a simulator would be given the requirement to include a bistatic system simulation, that is, to be able to produce a realistic clutter (and target) signal at a receiving antenna when the transmitting antenna is elsewhere. The principal modification required in the clutter simulation is the need for bistatic scattering coefficients (or matrices) in place of the monostatic scattering coefficients (or matrices) that were used above. Similarly, of course, bistatic target information would have to be used.

Inclusion of masking effects is slightly more complicated in this situation, because masking can occur on the transmitter-to-scatterer path or on the scatterer-to-receiver path. A program capable of including masking for the bistatic radar is suitable for use with monostatic radars, of course, although the converse is not necessarily true. As the bistatic-radar program must be more complicated, however, and will require more computer time, separate monostatic and bistatic programs might well be desirable.

Extension of the target-clutter-interaction signal simulation discussed in Section 7.5 to include bistatic radar is straightforward, since bistatic scattering coefficients are needed to compute the interaction effects anyway. Programming of interaction effects should therefore probably be done directly for the bistatic situation, if bistatic systems are ever to be investigated using the simulation.

7.8 CONCLUSIONS - CLUTTER SIMULATION TECHNIQUES AND PROBLEMS

Several basic forms of clutter-signal simulators have been discussed. The most flexible general type appears to be the closed-loop form using digital computation. This type of simulation can include polarization effects, masking, clutter-target interactions, and bistatic-radar effects. Inclusion of all of these would however require a complicated computer program. Such a program can probably best be developed in stages rather than as a single effort. The necessary input data for such a computer program must be obtained from clutter measurements as described in Section 10.

Other simulations, including direct-generation digital and analog-computer simulations, have also been considered (Appendix E). These forms have various advantages and disadvantages but in general seem considerably less satisfactory than indirect-generation digital simulation. An exception occurs if a very simple simulation, embodying few refinements, is to be used for evaluation of a basic radar: here either analog or digital computation of a direct-generation simulator may permit adequate operation at lower cost.

Section 8
RADAR CLUTTER MEASUREMENTS TECHNIQUES AND PROBLEMS

8.1 GENERAL

The goal of a clutter measurements program should be to provide the systems designer with inputs which will guide radar design and allow meaningful and quantitative simulation of the effects of clutter on radar systems. The following sections will discuss some of the important elements related to the clutter measurements program.

Observables

The primary electromagnetic clutter observables are as follows:

1. amplitude
2. phase
   a. spatial
   b. temporal
3. polarization

These observables, as measured by a radar sensor system are dependent on the parameters of the radar (resolution cell size, frequency and polarization), on the terrain characteristics, and on the position of the radar relative to the terrain (aspect angle). Most measurement programs in the past have collected data on 1, 2b and 3 separately, or 1 and 2b in combination. Rarely have all three been collected simultaneously to allow correlations to be made among the variables. Additionally, the instrumentation systems used did not provide a significant parametric variation of pulse packet size to determine its influence on the measurement. As a result, the clutter measurements are tied to a particular set of sensor parameters (i.e., pulsewidth, beamwidth, and so on). A table of sources of clutter measurement data including type of data is included in Appendix F, along with a reference list.

Many of the past limitations have, of course, been brought on by the limitations of the data acquisition system. On the other hand, at this point it should be realized that a comprehensive measurements program will require a complex data collection and data analysis and must be accompanied by a correspondingly complex environmental (physical) sensing and describing system. The latter system which is meant to relate the measurements to the environment will require sensors other than the measuring radar to obtain the necessary data. Although it may be unnecessary to employ this comprehensive system in all future measurements, it is of pressing importance to gather some pilot quantities of data in this comprehensive and well-correlated manner in order to guide subsequent measurements efforts. To attempt to skimp on measurement parameters at this stage would be false economy indeed.

Figure 8-1 is a very simplified flow diagram of a possible overall approach to the problem. The various elements include the data sensing and collection system, the environmental describing functions, the various processing systems which reduce the data to levels suitable for the given task and the correlation system which relates the essential data elements (amplitude, phase and polarization) to the functions which describe the environment. Finally, the correlation system produces a series of graphs which as a function of the parameters indicated (in the box labeled "parameter variation") produce a probability of obtaining a given value of reflectivity, spectral bandwidth, clutter angle-of-arrival variation (related to spatial phase) and correlation functions among the variables as a function of the terrain area in question.

The following paragraphs will discuss the various elements indicated in Figure 8-1.

8.2 ENVIRONMENT AND ITS DESCRIPTION

Typically, one of the least defined factors in past clutter measurements programs has been an accurate quantitative description of the environment being measured. Since both natural and cultural targets may be included, a good knowledge of the distribution of various types of scatterers should be obtained.

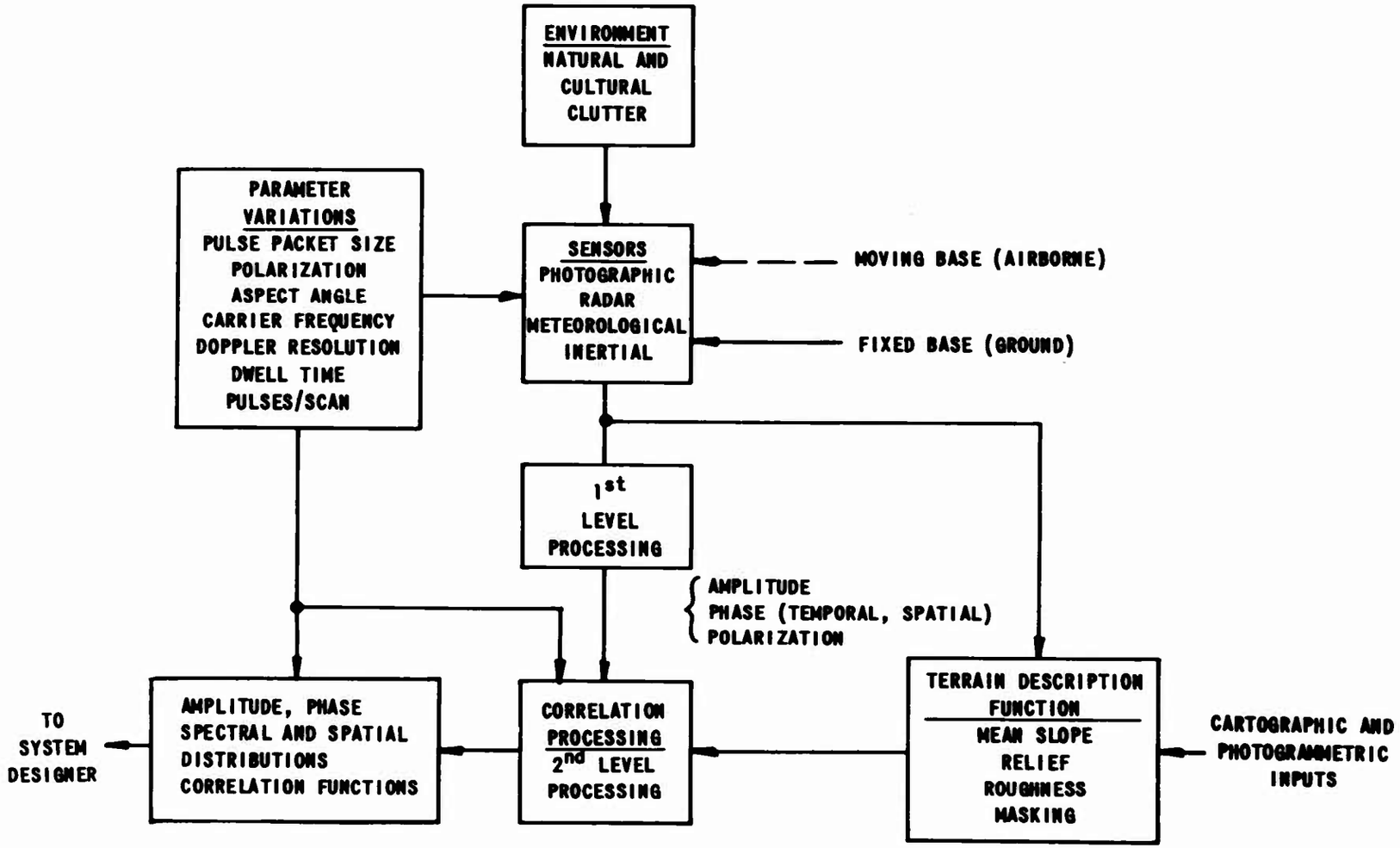

Figure 8-1 CLUTTER MEASUREMENTS PROCESSING CYCLE

Thus, accurate maps and photographic (stereo) data are needed to locate accurately potential major scatterers or low return areas within the area to be measured. If a high resolution radar is used in conjunction with a map of the area (including terrain slope), then a correlation between the cartographic map and the radar map can be made in terms of the measured radar amplitude and phase data and the terrain slope, vegetation and distribution of major scatterers or non-scattering regions. The allowed coarseness of the maps depends on whether the targets are being viewed for high altitude and long range (typically low grazing angle and negative mask angle) or from ground-based positions (positive mask angle and short ranges). In the former, local masking is typically not a problem and thus the accuracy of information on vegetation and other potential obstructions is not as critical as for the ground-based system. On the other hand, for the ground-based systems, local masking which obscures both the target and potential clutter sources must be considered and included.

At present the most accurate way to obtain local masking data is optically. This procedure is very tedious and it would be better if a series of PPI photographs could be generated as a function of height above the site (e.g., by use of helicopter mounted radar) to get a measure of the true radar mask. Conceptually, the analysis of such "PPI maps" could be automated to obtain the depth of mask as a function of range and azimuth angle. This technique could speed up the preparation of near range portions of radar coverage diagrams for ground based sites, especially when data with respect to effects of radar elevation is required. Since we are more concerned here with "on-off" type data (i.e., is or is not the terrain visible?), the radar characteristics, except where diffraction effects occur, are not extremely important.

8.3 SENSORS

Because of the desire to obtain the clutter observables and their interrelationships, any sensor planned for a future clutter measurements program must be multifunctional, i.e., it must be able to collect amplitude, phase and polarization data <u>simultaneously</u>. Furthermore, radar systems of

the future will work in environments where the radar pulse packet size may vary from a size equivalent to the target dimensions to many times greater than the target size. Thus the measurements radar sensor must have inherent resolution to cover a wide range of pulse packet variations. For airborne backscatter measurements, a synthetic aperture radar may be a good candidate because of its variable-resolution potential. Elevation and azimuth monopulse or an array of receiving antennas will allow collection of spatial information (amplitude, phase and angle-of-arrival). If a multimode antenna feed is used, polarization diversity information can also be collected.

Finally, since the clutter return varies with transmitter wavelength, different carrier frequencies must be provided. Theoretically, the focussed synthetic aperture radar resolution is independent of range and frequency. Thus, such a device seems ideal to determine the effects of pulse packet size on the clutter characteristics described above.

For ground-based measurements, it may be possible to utilize a helicopter- or truck-mounted synthetic aperture which would allow very low altitude (from essentially ground level on up) data collection.

For the forward-scatter measurements, an arrangement of two aircraft (e.g., helicopters) could be provided with one of the aircraft as the transmitter illuminator and the other as a receiver. Since coherence would be desired in the receiver (relative to the transmitter), an accurate frequency standard could be used in the aircraft and a locking pulse might be transmitted via a data link to assure phase lock between the transmitter and receiver. Alternatively, stable local oscillators in conjunction with stable platforms could be used at both link terminals to provide relative phase coherency over the measurement period (see Appendix G for a discussion of this approach). With this arrangement, amplitude, phase, angle-of-arrival and polarization data including forward scatter effects could be received by the moving aircraft of the pair and processed coherently with only one synthetic aperture receiver used in a one-way ranging configuration.

Because of the large amount of data to be collected (all ranges and azimuths for a given height of radar), the data must be collected in a form readily amenable to digital computer processing. Here again, the normal use of optical and photographic techniques by synthetic aperture radars allow the storage of large quantities of data which can be subsequently read by flying spot scanners and, potentially, pattern recognition devices. Furthermore, optical analogues of various correlation schemes are normally used to provide a transform from the spatial to the frequency domain and vice versa. With these techniques, amplitude, phase, polarization and various correlation functions could be "mapped" for a given area.

8.4 DATA REDUCTION

The first level of processing indicated in Figure 6 is designed to put the data in a form suitable for computer processing and may involve an analog-to-digital conversion or analog-to-analog (such as tape outputs to optical outputs or vice-versa). At this stage of processing, all the necessary identifying data should have been incorporated to speed second level correlation processing.

If the data is collected on film which might be the case if synthetic aperture radars are used for data collection, a flying spot scanner would be used to recover the data and processing time can be traded for bandwidth. Because optical techniques can be used to perform spatial to frequency transformations, consideration should be given to using these techniques to save digital computer processing times since joint probability or correlation function generation takes large amounts of computer time.

A major problem area in performing the second-level correlation processing is that of defining a parameter or group of parameters which will categorize the terrain and allow the generation of suitable correlation functions for certain terrain-describing parameters. Accomplishing the latter would allow one to predict clutter characteristics.

As indicated in Figure 8-1, terrain masking or mask angle distributions, relief, mean slope, etc. are all potential terrain parameters which might be used. Probably two of the most critical parameters will be mask angle and mean slope. The former is important because it indicates the lack of target, clutter, or both and is one of the primary factors in the difference between an average clutter cross section and the instantaneous value obtained in practice. Because of the variability of terrain, the problem of obtaining a single or a few generalized descriptive parameters for any terrain is exceedingly difficult and is a definite item of study in future clutter research and measurements programs.

Section 9

CLUTTER PROBLEMS - INNOVATIONS IN RADAR TECHNOLOGY

9.1 ELECTRONIC STEERING

Electronically steered phased arrays have the capability of rapidly controlling the antenna aperture illumination function. This provides the ability to perform rapid scanning among beam positions through electronic control of the (usually linear) phase taper across the aperture. In this manner, the phased array can be programmed to rapidly perform search and track procedures over the extent of the array angular coverage. The format of the search and track procedures can also be varied depending on the particular detection requirements. The primary advantage of ground-based electronically steered phased arrays over mechanically steered systems is, however, the capability to perform multiple engagements against threats from different directions. Applicable detection/tracking techniques for any single engagement are similar for both a phased array and mechanically steered antenna and thus clutter problems, in this regard, would be similar for both systems.

One form of electronically steered phased array uses digital array element phase control which provides a number of possible phase settings between $\pm 180°$ phase shift. The instantaneous array bandwidth is governed by the aperture size for a maximum allowable phase error (which in turn governs the array pattern sidelobe level) across the array aperture. For example, allowing a maximum phase error of ϕ results in an instantaneous fractional bandwidth given by

$$\frac{\Delta f}{f} = \frac{\phi}{2\pi \, d/\lambda \, \sin\theta} \qquad (9\text{-}1)$$

where $\frac{d}{\lambda}$ is the aperture length normalized with respect to wavelength and θ is the angular direction of the beam from the array normal. Thus, for an aperture dimension of 25λ ($2.5°$ beamwidth) the array bandwidth would be approximately 0.7% assuming an allowable phase error of $\phi = \frac{\pi}{4}$ radians and a scan angle of $\theta = 45°$. While this bandwidth is sufficient for most processing techniques presently used for clutter rejection, consideration would have to be given to

this factor for techniques such as frequency hopping which can be used to reduce the clutter correlation and so improve target detection.

For AMTI systems the array design with respect to antenna sidelobe control is particularly important because of increases in the clutter spectrum bandwidth due to platform motion and resultant decrease in clutter suppression. The requirement of low antenna sidelobe levels places very severe requirements on array element phase and amplitude accuracy and this factor, when compounded with the operating environment, can lead to serious design problems.

It is possible to consider techniques wherein the array amplitude and phase aperture distribution are controlled in order to maximize the target (signal) to clutter ratio. These techniques require knowledge of the angular distribution of the clutter characteristics to perform the optimization. It may be possible to employ such optimizations for fixed sites where detailed clutter "maps" can be generated although the potential advantages must be evaluated with respect to the significant increases in beam control and computer complexity. Clutter measurements, such as described in Section 8, would be required to determine the clutter environment for a given location. From these measurements a clutter model for use in indirect clutter simulation, as described in Section 7, could be obtained and used to evaluate the performance of such antenna optimizations.

9.2 SIGNAL PROCESSING/DESIGN AND COMPUTER TECHNOLOGY

The design of radar signal waveforms and data processing circuits for clutter reduction purposes requires knowledge of the signal characteristics of both clutter and targets. In the absence of detailed knowledge clutter has conventionally been modeled as an additive narrow band Gaussian process with a Gaussian spectrum. Effects of platform motion, antenna pattern and range gate movement and system instabilities on the clutter spectrum can be included by well known relations.[11] In some cases clutter rejection techniques have been evaluated using a white noise representation of the clutter signal.

The assumptions described above concerning the nature of the clutter signal are usually made on the basis of mathematical tractability and are reasonable for initial technique investigations. They may, however, yield quite incorrect results even for present-day radars. In studies of future clutter rejection schemes, where increased rejection is desired, the approach outlined above will probably not be sufficient to permit a realistic evaluation of increases in clutter rejection versus increased system cost and complexity.

The increased use of integrated circuits and computer technology can be foreseen in future radar systems, especially with regard to the use of electronically steered phased arrays and multidimensional (amplitude, frequency, polarization) radar detection and tracking. The detection and tracking functions, threat assessment and allocation of priorities will probably be automated to a high degree in these systems and the detection procedure may be controlled by a clutter/masking map for the terrain in the vicinity of the radar. It is evident that the present state-of-knowledge concerning clutter is insufficient for the design of such systems. The basic problem facing the designer is that clutter cannot be represented to good accuracy in simple functional form and that, even for a fixed radar site, the clutter characteristics vary spatially and with time. Thus, to realistically evaluate clutter rejection techniques, before field tests, some form of simulation of clutter is required. Present simulators using filtered noise are, however, little better (if any) in evaluation of clutter rejection techniques than the analytical analog. In some cases recordings of clutter data may be available for simulation purposes from a radar sensor similar to that being considered; generally such data are available only after system field tests have been performed. The only solution to this aspect of the problem is to perform a well-designed clutter measurements program (see Section 8) and use the resultant data in a realistic form of simulation (see Section 7).

Section 10
PROGRAM PLAN FOR FUTURE CLUTTER RESEARCH

The need for further research to determine the characteristics of clutter (principally ground clutter) is unquestioned because the parameters which enter into the physical process of clutter signal generation are not well understood. Thus, there are many undefined relationships which exist among the physical and electromagnetic characteristics of terrain. In general, there is a need for quantifying relationships among terrain parameters (specifically terrain cover and slope) and the explicit radar variables-frequency, amplitude, phase, polarization and pulse packet size. Furthermore, there is a need to develop techniques for using clutter data in the simulation of clutter signals and clutter-target interactions. Thus, the objective of the clutter research program plan described in this section is twofold: a) to provide a better understanding of the underlying characteristics of clutter with specific application to the air defense systems problems, and b) to provide the basic clutter data and techniques for employing the data in the design of simulators and realistic evaluation of radar systems.

It should be noted that the development of new clutter suppression techniques is dependent largely on obtaining a better understanding of the nature of clutter, that is, the scattering sources which combine to produce clutter and the characteristics of their spatial and temporal variations.

There are four major areas of development which appear to require significant efforts. A general listing follows and a discussion of possible approaches follows the general listing.

1. Data Acquisition

   Develop , with associated design configuration study, a system(s) for the field collection and recording of instantaneous clutter data (both backscatter and forward scatter) from various terrains in a manner to allow its re-creation for data reduction and analysis.

2. Environmental Description

Develop techniques for relating clutter measurements data to geomorphological data (i.e., terrain type, relief, slope, etc.) to provide clutter-signal predictions based on visual inspection of the terrain for a wide variety of clutter (cultural and noncultural) to be used in the determination of defense systems requirements and performance evaluations.

3. Data Reduction

Develop relationships defining the probability functions and spectra of clutter signals and the correlation functions of the clutter signal observables as functions of electromagnetic (frequency, polarization, phase, pulse packet size) and physical (terrain geometry, number of scatterers, spatial distribution, and so on) characteristics. Perform data interpretation studies to associate clutter measurements with scattering processes.

4. Simulation

Development of techniques for realistically simulating clutter in the design and evaluation of defense systems.

10.1 DATA ACQUISITION

In future clutter measurements program, clutter data should be collected to permit the correlation among the various radar dimensions of primary interest, i.e., frequency, polarization, amplitude, phase (spatial and temporal). In addition, implicit or derived dimensions such as angle-of-arrival (which is pertinent to the target location and tracking problem) should also be determined and correlated with the above dimensions.

Because we are dealing with a multivariable problem and furthermore, because advanced radar techniques will certainly involve multivariable radar signal processing, information on the interactions among the variables is necessary to define the behavior of clutter and clutter plus target. Sufficient variation in the radar parameters must be provided to determine its influence on the interactions among variables.

One of the most complete clutter measurements facilities in present use is the four-frequency (P, L, C and X) airborne radar with dual linear polarization capabilities available at NRL.[24] The coherent system output could theoretically be used with a suitable processor, optical or otherwise, to obtain high resolution synthetic aperture data provided suitable frequency stability and motion compensation capability were available. As it is, the pulse packet, which can be varied by 4:1 (0.25μ sec to 1.0μ sec), provides a significant variable resolution capability. Clutter conditions should, however, be investigated where the available system azimuth resolution (effective) approaches the target dimensions at ranges up to 20 n.mi. (see Section 2). This could be accomplished by using the synthetic aperture approach mentioned above or by performing the clutter measurements at ranges short enough to provide the desired resolution. Although the NRL four-frequency radar is the closest existing approximation to what might be considered an ideal system for airborne clutter measurements, the system is limited in its ability to collect data which include simultaneous measurements of the variables (amplitude, phase, polarization, and angle-of-arrival or spatial phase and amplitude) as a function of frequency, polarization and pulse packet size or resolution.

The measurement of clutter characteristics at or near the ground surface would require installing the radar on a tower (perhaps mounted on a truck) or helicopter.

10.1.1 Clutter Measurements Radar Sensor

Ideally, a clutter measurements radar sensor would have the following characteristics:

a. Frequency diversity, probably UHF through Ka bands with interpulse and intrapulse diversity (e.g., 10% bandwidth) to measure frequency dependent effects.

b. Polarization diversity (on both transmission and reception).

c. Spatial amplitude and phase measurements over an aperture.

d. Capability for both coherent and non-coherent signal processing.

e. Variable resolution or pulse packet size.

It is desirable that a clutter measurements radar have a resolution capability approaching the target dimensions at ranges up to approximately 20 n.mi. This would require a pulse width of 20 nsec and a beamwidth on the order of 1 mr. The ability to decrease the resolution (longer pulse, larger beamwidth) by a factor of, say, 500 would allow collection of clutter data over a wide range of radar parameters.

The primary difference between the clutter measurements radar described here and those previously used to obtain clutter data is that several clutter observables can be measured and recorded simultaneously. In this manner the correlations among the observables can be extracted from the data.

Development of techniques, such as described in Section 8, are required to obtain basic data on the characteristics of the forward scattered or multipath signals. The basic problem here is that the surface area on the

ground, effective in forward-scattering, is generally extremely large and the categorization of the environment becomes difficult. It is probable that the same instrument as described previously in this section for backscatter measurements, can be used to perform the forward scattering measurements. A remote illuminating antenna excited with a stable transmitter would provide a system suitable to perform short duration coherent measurements (see Section 8).

One means of obtaining the high resolution described above while retaining the flexibility of variable resolution is through the use of a coherent synthetic aperture radar employing pulse compression. The radar could be mounted on a truck, or tower for measurements near the ground, or in a helicopter or aircraft for higher altitude clutter measurements. It is not believed that new techniques or state-of-art advancements are required to develop the clutter measurements radar with the suggested capabilities.

Before it can be recommended however that a radar as described above be developed for clutter measurements the specific studies, discussed in the following paragraphs, would be required.

10.1.2 Required Studies

A study should be performed on the significant differences between clutter data obtained from a variable aperture or pulse length (real resolution) radar versus that obtained from a synthetic aperture pulse compression radar. This recommendation is made because although the systems may have the same effective resolution on discrete targets, the effect of spatial and temporal clutter signal correlations may be different, especially when one considers clutter with a few predominant scatterers among many smaller ones or cases with significant multipath present in the path between the radar and clutter.

A study should also be performed on antenna techniques to determine the spatial amplitude and phase characteristics of the clutter signal. Information derived from these measurements should be capable of determining angle of arrival clutter effects on monopulse, phased array, con-scan, beam-lobing or

TWS radars. This information could possibly be obtained by using a planar array of receiving antennas, two crossed linear arrays with vertical and horizontal orientation or with a four-beam monopulse cluster. Considerations such as effects of spatial correlation and receiver noise, measurement accuracy and relative cost/complexity should be studied for various antenna configurations.

10.1.3 Recommendations for Initial Data Acquisition Radar

The radar described in Section 10.1.1 would require extensive development and consideration should be given to a radar system with somewhat more limited capability in the first phase of the measurements program to allow ground and flight tests to be performed at an earlier data. The results of the studies described in Section 10.1.2 are required before detailed specifications of the initial data acquisition radar can be made. The characteristics described below are representative of the capabilities which would probably be required.

The clutter measurements (initial) radar would be suitable for truck or tower measurements and adaptable to airborne operations with the following basic characteristics:

a. Frequency coverage L band through Ku band preferably with separate RF heads through a common IF system

b. Polarization diversity - either linear or circular (but not simultaneously) on transmit and receive

c. Aperture amplitude and phase measurement capability

d. Both coherent and non-coherent signal processing (possibly including synthetic aperture data collection)

e. Variable pulse length (possibly through pulse compression) with a 20 ns effective pulse length lower limit

f. Provisions for remote phase lock or stability between main radar data acquisition device and remote transmitter for forward scatter measurements to determine multipath effects.

10.2 ENVIRONMENTAL DESCRIPTION

An accurate quantitative description of the environment in which the clutter is measured will be required to allow correlation of the clutter data with the environmental factors. Detailed site investigations in conjunction with high resolution radar maps will facilitate the isolating of major scatterers and provide easier interpretation and correlation of clutter characteristics in terms of terrain features.

The use of averages or maxima-minima to describe primary terrain parameters such as reflectivity and spectral bandwidth will typically give either an overly optimistic or pessimistic estimate of system performance depending on the terrain, system, or target characteristics involved. For example, if the spatial breakup of clutter caused by terrain masking - line of sight - interactions is not taken into account, assignment of an average value of terrain reflectivity to be used in a given area will produce too high a value of clutter for that particular region and could predict poor performance, where in fact the target was in the clear. Therefore, it is necessary to obtain visibility data to determine spatial clutter breakup and LOS availability for use in clutter data reduction and interpretation. In the absence of accurate detailed maps, stereophotographs should be taken to obtain a reference "image" which will provide an accurate picture of the distribution and type of scatterers in the data acquisition radar field of view. In addition, because of the need for Doppler spectra of clutter and its dependence on wind conditions, wind velocity measurement should be included in the environmental sensing system.

10.2.1 Recommendation for Environmental Designation

1. For various proposed air defense sites around the country, obtain visibility (masking) data using the most appropriate method, i.e., optical or map (200 meter grid spacing) generated. The former would be used primarily to obtain local masking data where the radar cannot be readily elevated. The latter approach could be used to describe relatively flat country for an antenna elevated above the local mask.

2. Collect aerial stereophotographs during clutter measurements to allow a reference "image" to be generated indicating distribution of cultural and non-cultural targets.

3. For airborne clutter measurements, as required to evaluate missile seeker systems, collect aircraft altitude, position, velocity and heading information to obtain information on the relative aircraft to ground position.

10.3 DATA REDUCTION

The reduction of clutter and environmental data could probably be performed using a high speed digital computer facility although optical techniques, such as described in Section 8, should also be studied to determine if sufficient flexibility is achievable to perform the many types of data processing which would be desired.

The amplitude and phase imaging collected by the data acquisition system could be read out with a flying spot scanner. Pulse height (amplitude) and spectrum analysis would yield range-azimuth "maps" (for a given area). These would present probability distributions of clutter amplitudes and power spectra vs. polarization, carrier frequency, pulse packet size and elevation angle. The major problem, as discussed in Section 8, is the definition of terrain variables for the correlation of clutter data. Simple descriptions of terrain cover, such as "hardwood forest" are not sufficient. Further delineations, such as season are also not entirely sufficient; for example, a recent

rainfall can significantly affect clutter characteristics. Certainly factors such as the ones given above, and in addition, terrain masking, relief, mean slope, and the density and characteristics of major isolated scatterers will be primary variables. Further, studies must be made to determine terrain describing functions suitable for predicting clutter characteristics.

It is recommended that data interpretation studies be performed in conjunction with the clutter data reduction to associate the observed clutter signal characteristics with scattering processes. These analytical studies may include laboratory models and experiments to perform investigations, under controlled conditions, of scattering phenomenon as related to clutter characteristics.

10.4 SIMULATION

It is recommended that simulation of clutter data for future air defense system design and evaluation be along the guidelines of the closed-loop clutter model described in Section 7 . Initial investigations of the clutter simulator would be directed to comparison of simulated and actual clutter characteristics as functions of pulse packet size, and terrain type. The required clutter parameters for implementation of the model should be available from the measurements program.

10.5 PROGRAM PLAN SUMMARY

The following list is a summary of the suggested program plan for future clutter research. The appropriate section numbers are indicated for reference purposes.

1. Study effects on measured clutter data as obtained by a synthetic aperture, pulse compression radar versus a real antenna aperture short pulse radar (Section 10.1.2).

2. Investigate antenna techniques for obtaining spatial amplitude and phase clutter data (Section 10.1.2).

3. Design and fabricate an initial clutter data acquisition radar using the results of items 1 and 2, above (Section 10.1.3).

4. Examine experimentally techniques for determining line-of-sight availability and local masking effects for radar system site investigations (Sections 2,8 and 10.2) in conjunction with the performance of clutter measurements using the initial data acquisition radar (item 3, above).

5. Study means of readily associating terrain, cultural and man-made objects with radar clutter data to aid in data interpretation and to facilitate clutter prediction (Section 10.2).

6. Perform an investigation of environmental descriptors and associated sensors or measurement techniques for various types of terrain to provide environmental data during the clutter measurements program (Section 10.2).

7. Investigate data storage (magnetic tape and optical) and reduction (digital computer and optical) techniques for obtaining various probability functions, power spectra and (cross) correlation functions of the clutter and associated environment (Section 10.3).

8. Perform study and initial development of a closed-loop digital clutter simulator (Sections 7 and 10.4). Compare, simulated and measured (item 4, above) characteristics of clutter signals.

REFERENCES

1. IRE Standards on Radio Aids to Navigation: Definition of Terms, 1954, Proc. IRE, Vol. 43, p. 194, February 1955.

2. F.M. Pelton, et al. "ADLAT Terrain Avoidance Techniques Evaluation, Vol. II: Local Masking and Low Altitude Flight," Final Report, CAL Report No. 1H-1706-E-11, Contract No. AF 33(657)-9156, AFAL-TR-65-187, October 1965 (Secret Report).

3. B.R. Tripp, "Final Summary Report, Radar Guidance Experiments," Radiation, Inc. (Melbourne, Florida), Report to BRL, Contract No. DA01-009-509-ORD-885, 9 March 1961.

4. Davenport and Root, Random Signals and Noise, McGraw Hill, 1958.

5. P. Beckmann, Probability in Communication Engineering, Harcourt, Brace, World, 1967.

6. M. Nakagami, "The m-Distribution -- A General Formula of Intensity Distribution of Rapid Facing," W.C. Hoffman (ed), Statistical Methods in Radio Wave Propagation, Pergamon, 1960, pp. 3-36.

7. J.A. Greenwood and D. Durant, "The Distribution of Length and Components of the Sum of n Random Unit Vectors," Ann. Math. Stat., 26, 233-246 (1955).

8. T.F. Leney, "ADLAT III - Final Report - Terrain Following Radar Sensor Investigation," AFAL-TR-66-240, CAL Report No. IH-2096-E-4, August 1966, SECRET.

9. "Investigation of Terrain Return Scintillation," CAL Report No. IH-1530-P-4, 20 March 1962.

10. W.S. Whitbeck, Land and Precipitation Measurements at C-Band, 14th Annual Radar Symposium, 1968, Fort Monmouth, New Jersey.

11. R.C. Emerson, Some Pulsed Doppler MTI and AMTI Techniques, Rand Report No. R-274, March 1, 1954 (Confidential Report).

12. J.W. McGinn, Jr., and E.W. Pike, "A Study of Sea Clutter Spectra," in W.C. Hoffman (ed.), Statistical Methods in Radio Wave Propagation, Pergamon Press, 1960, pp. 49-92.

13. D.E. Kerr, Propagation of Short Radio Waves, Bost Tech. Pub., 1964, pp. 527-531.

14. P.R. Wallace, "Interpretation of the Fluctuating Echo From Randomly Distributed Scatterers. II," Can. Jour. Phys., 31, pp. 995-1009 (1953).

15. A. Fleisher, "The Information Contained in Weather Noise," MIT, Dept. of Meteorology, Tech. Report No. 22, Part A (AD 5841), Jan 15, 1953.

16. R.R. Rogers, "Meteorological Applications of Doppler Radar," Appendix 5, PhD Thesis, NYU, March 1964.

17. J.S. Marshall and W. Hitcshfeld, "Interpretation of the Fluctuating Echo from Randomly Distributed Scatterers. Part I," Can. Jour. Phys., 31, pp. 962-994 (1953).

18. P.L. Smith, "Interpretation of the Fluctuating Echo from Randomly Distributed Scatterers: Part 3," McGill University Stormy Weather Group Report MW-39, Dec. 1964.

19. R.S. Berkowitz (ed.), Modern Radar Analysis, Evaluation, and System Design, Wiley, 1965.

20. A. Papoulis, The Fourier Integral and Its Applications, McGraw Hill, 1962, p. 133.

21. M.E. Bechtel, "Final Report on Project ACRE," CAL Report No. UB-1405-P-1, May 1960.

22. C.J. Krebs, Terrain Avoidance ECM Study (U), Quarterly Progress Report No. 3, Contract No. DAAB07-67-C-005, 28 August 1967 (Secret Report).

23. R.E. Kell, "On the Derivation of Bistatic RCS from Monostatic Measurements," Proc. IEEE, 53, pp. 983-988 (Aug. 1965).

24. N.W. Guinard, J.T. Ransone, Jr., M.B. Laing and L.W. Hearton, "NRL Terrain Clutter Study Phase I," NRL Report 6487, May 10, 1967.

Appendix A
INVESTIGATION OF PROBABILITY DENSITY FUNCTIONS

A.1 PROBABILITY DENSITY FUNCTIONS

The clutter signal received from N scatterers can be written:

$$S = R e^{i\theta} = \sum_{j=1}^{N} A_j e^{i\phi_j} \tag{A-1}$$

where, A_j and ϕ_j are the relative amplitude and phase of the signal from the j^{th} scatterer and R is the envelope. The sum signal S can be expressed in terms of an in-phase, x, and quadrature component, y, given by:

$$x = Re(S) = R\cos\theta = \sum_{j=1}^{N} A_j \cos\phi_j \tag{A-2}$$

$$y = I_m(S) = R\sin\theta = \sum_{j=1}^{N} A_j \sin\phi_j \tag{A-3}$$

The ϕ_j values are assumed to be uniformly distributed over 2π radians and statistically independent. The A_j values are considered to be fixed constants.

Consider first the quantities x and y and their probability densities. Since the characteristic functions of x and y are identical, we find that*(1):

$$p(x) = \frac{1}{\pi}\int_0^{\infty}\left[\prod_{i=1}^{N} J_0(A_i v)\right]\cos vx\, dv \tag{A-4}$$

is the exact expression for the probability density function corresponding to x; $p(y)$ is obtained from Equation A-4 by replacing x by y. Integration to

*References for this appendix are listed on the last page of Appendix A.

obtain $p(x)$ or $p(y)$ is not easily performed. For $N=2$ and $A_1 = A_2$ the result can be written in terms of a Legendre function of the second kind of order -1/2, but this result still requires computation to obtain $p(x)$ and in addition is only one very special case. Consequently, computer programs capable of computing $p(x)$ as a function of x for fixed parameters A_i have been written for $N=2$ and for $N=4$; these programs are discussed later in this Appendix along with results of computations using these computer programs.

Equation A-4 is exact for any set of constant amplitudes A_i. If $N \gg 1$, $p(x)$ must, by Central Limit Theorem, become Gaussian. The variance for scatterers is $\sigma^2 = \frac{1}{2}\sum_{i=1}^{N} A_i^2$; hence $p(x)$ becomes the Gaussian distribution:

$$p_G(x) = \frac{1}{\sigma\sqrt{2\pi}} e^{-\frac{x^2}{2\sigma^2}} \qquad \text{(A-5)}$$

in the limit as $N \to \infty$.

Suppose $A_i = A$ for all i. In this case it is possible to write an asymptotic expression for $p(x)$ that indicates how $p(x)$ approaches $p_G(x)$ for large but finite values of N. (Actually the A_i could all be random variables having the same distribution; for the present investigation, constant, but not necessarily equal, A_i are of interest.) Following the method of Reference 1, pp. 103-104, we obtain:

$$p_{GA}(x) \sim p_G(x)\left[1 - \frac{1}{16N}\left\{\left(\frac{x}{\sigma}\right)^4 - 6\left(\frac{x}{\sigma}\right)^2 + 3\right\}\right]; \qquad \text{(A-6)}$$

it is clear that for N large, $p_{GA}(x)$ is a good approximation for values of x not too far out into the tails of the distribution. If a good approximation is needed at some $x \gg \sigma$, then it is necessary that N be very large. Because of the very rapid rate of decrease in $p_G(x)$ for large x, errors in this region of the distribution are normally of no concern. For x within 2 standard deviations of zero, the correction factor in Equation A-6 is small even for values of N as small as 4 or 5. There is, however, reason to question the validity of Equation A-6 for small N ; for $N = 2$, for example, the correct $p(x)$ and $p_{GA}(x)$ are very dissimilar (see Figure A-1).

Also of importance is the probability density function, $p(R)$, of the amplitude, R, of the received signal defined in Equation A-1. The probability density function is stated by Nakagami (Reference 2, Equation 94) to be:

$$p(R) = R\int_0^\infty v J_0(vR) \prod_{i=1}^{N} J_0(vA_i)\, dv \qquad \text{(A-7)}$$

This result is given without proof and is claimed to hold without restriction. Watson (Reference 3) proves a very similar result in a discussion of a two-dimensional random walk (a problem completely analogous to the present one). Watson proves the expression for the probability distribution function, and it is straightforward to show that the derivative of his result is exactly the probability density function given in Equation A-7.

For the special case $N = 2$, $A_1 = A_2 = A$, an exact expression for can be written in a simple form:

$$p(R) = \frac{2}{\pi\sqrt{4A^2 - R^2}}, \qquad 0 \le R < 2A \qquad \text{(A-8)}$$

$$= 0, \qquad R < 0, \quad R > 2A$$

This result is useful in checking some of the numerical integrations performed in the following analysis.

As before, the probability density function can be written in simpler form if $N \gg 1$. In this case, we obtain the Rayleigh density function:

$$p(R) = \frac{2R}{\alpha} e^{-\frac{R^2}{\alpha}}, \qquad R \ge 0 \qquad \text{(A-9)}$$

$$= 0, \qquad R < 0$$

where;

$$\alpha = \sum_{i=1}^{N} A_i^2$$

If all of the $A_i = A$, an asymptotic approximation to $p(R)$ can be written; we have: (Reference 1, pp. 133-136)

$$p_{RA}(R) \sim p_R(R)\left[1-\frac{3}{8N}\left(\frac{R^4}{2\alpha^2}-\frac{2R^2}{\alpha}+1\right)+\cdots\right] \qquad \text{(A-10)}$$

Beckmann[1] notes that a more thorough analysis given in a Russian text has a factor 1/2 instead of the factor 3/8 given in Equation A-10 and that the larger value may be more nearly correct because of the inclusion of higher-order terms in the Russian work. Derivation of the next higher order term using Beckmann's method does not change his first-order term, however, so the question remains open. It should also be noted that for a small number of scatterers, less than about fifteen, increased accuracy cannot be obtained through use of the next term in the asymptotic expansion. As is shown later in this appendix, a better form of approximation is available for the cases of interest.

One reason for questioning the use of the asymptotic formulations given by Equations A-6 and A-10 is the total failure of $p_{RA}(R)$ when $N = 2$: although one would not expect good agreement in this case, the complete difference in the resulting functions suggested that the equation might not be valid except for quite large N. In fact, it is shown later that these equations are relatively accurate for $N \geq 4$ (and probably for $N = 3$ as well) as long as $A_i = A$.

A final approximation to $p(R)$ has been evaluated as a part of the work reported here. This approximation is the Nakagami m-distribution (Reference 3); this distribution is defined by:

$$M(R, m, \Omega) = \frac{2m^m R^{2m-1}}{\Gamma(m)\,\Omega^m}\, e^{-\frac{m}{\Omega}R^2} \qquad \text{(A-11)}$$

When $m = 1$ this distribution becomes a Rayleigh distribution, when $m = 1/2$ (the smallest allowable value) this distribution becomes a one-sided Gaussian distribution. As m increases, the distribution becomes more and more sharply peaked. Nakagami states that for practical purposes $p(R)$ is approximately equal to $p_N(R)$ where:

$$p_N(R) \equiv M(R, o^m, \sum \Omega_i) \tag{A-12}$$

where;

$$o^m = \frac{\left(\sum \Omega_i\right)^2}{\sum_{i=1}^{N} \left(\frac{\Omega_i^2}{m_i}\right) + 2\sum_{i \neq j} \Omega_i \Omega_j} \tag{A-13}$$

In these expressions Ω_i represents the mean-square value of the distribution of the A_i (assumed to be a random variable having a distribution given by Equation A-11). We are interested in constant values for the A_i ; hence $m_i = \infty$ and $\Omega_i = A_i^2$. Thus we obtain:

$$o^m = \frac{\left(\sum_{i=1}^{N} A_i^2\right)^2}{2\sum_{i \neq j} A_i^2 A_j^2} \tag{A-14}$$

and;

$$\sum \Omega_i = \sum_{1}^{N} A_i^2 \tag{A-15}$$

For $N = 2$ (a case for which one would assume that the Nakagami m-distribution is a poor approximation to $p(R)$) we have:

$$o^m = \frac{(A_1^2 + A_2^2)^2}{2A_1^2 A_2^2} \tag{A-16}$$

$$\sum \Omega_i = A_1^2 + A_2^2 \tag{A-17}$$

For larger values of N the required parameters are found from Equations A-14 and A-15. As will be shown, this approximation is very good for many situations, even when N is as small as 4; it is especially useful when one amplitude is much larger than the others, a situation in which the Rayleigh distribution fails because the Central Limit Theorem is not satisfied.

A.2 NUMERICAL CALCULATION OF PROBABILITY DENSITIES

As noted in Section A.1, the exact expressions for the probability densities (Equations A-4 and A-7) cannot in general be written in closed form. Examination of the integrands indicates relatively slow convergence; furthermore, the integrands are very oscillatory, so that small increments must be used in a straightforward numerical integration procedure. These two considerations indicate that numerical integration alone is not practical. Instead, it is possible to make use of asymptotic expansions of some of the Bessel functions to obtain integrable functions in the large-argument region for which the approximation is good. Numerical integration then need only be used over a limited range of argument values. In this way useful accuracy can be obtained with a minimum of computational effort.

Inherent in all of the CAL-developed computer programs is the approximation:

$$J_0(z) \sim \sqrt{\frac{2}{\pi z}} \cos\left(z - \frac{\pi}{4}\right) \qquad \text{(A-18)}$$

For z greater than 10 or 20 this approximation is excellent, as can be seen from Table A-1.

Table A-1
BESSEL FUNCTION APPROXIMATION

z	$J_0(z)$	$\sqrt{\frac{2}{\pi z}} \cos\left(z-\frac{\pi}{4}\right)$
10.2	-0.249617	-0.250016
11.8	+0.001967	+0.00442
19.6	+0.1800407	+0.180112
21.2	+0.002017	+0.00212

At peaks of $J_0(z)$ such as at z = 10.2 and z = 19.6, the approximation is excellent. Agreement is much poorer near zeros, such as at z = 11.8 and z = 21.2, but contributions to the integral are less important in these regions.

First, consider the computation of $p(x)$ using Equation A-4 when N = 2. The integration can be performed in two parts, viz:

$$\rho(x) = I_1 + I_2 \tag{A-19}$$

where;

$$I_1 = \frac{1}{\pi}\int_0^{v_1} J_0(vA_1)\, J_0(vA_2)\cos(vx)\,dv \tag{A-20}$$

$$I_2 = \frac{1}{\pi}\int_{v_1}^{\infty} J_0(vA_1)\, J_0(vA_2)\cos(vx)\,dv \tag{A-21}$$

I_1 was found using numerical integration; the program uses 10-point Gaussian quadratures over an externally specified number of subintervals of v_1. The limit v_1 must be chosen such that v_1A_1 and v_1A_2 are both greater than 10 or 20 so that the asymptotic approximations to the Bessel functions can be used to find I_2. If A_1 or A_2 is small, a large value of v_1 is thus required. In finding I_1, it is then necessary to break v_1 up into enough subintervals so that the 10-point quadrature is sufficiently accurate within each subinterval. This consideration is important because of the large number of oscillations the integrand can experience before v has reached v_1. This effect is especially important if A_1 and A_2 are quite different in value.

I_2 can be approximated closely by:

$$I_2 \approx I_{2a} = \int_{v_1}^{\infty} \frac{1}{\pi^2 v A_1 A_2}\left[\cos(v(A_1 - A_2)) + \sin(v(A_1 + A_2))\right]\cos(vx)\,dv \tag{A-22}$$

This integration was performed exactly in terms of sine and cosine integrals. The result is:

$$I_{2a} = \frac{-1}{2\pi\sqrt{A_1 A_2}}\left\{si\left[v_1(A_1 + A_2 + x)\right] + si\left[v_1(A_1 + A_2 - x)\right] + \right.$$
$$\left. + Ci\left[v_1\left|A_1 - A_2 + x\right|\right] + Ci\left[v_1\left|A_1 - A_2 - x\right|\right]\right\} \tag{A-23}$$

where;

$$si(z) \triangleq -\int_z^{\infty} \frac{\sin t}{t}\,dt \qquad Ci(z) \triangleq -\int_z^{\infty} \frac{\cos t}{t}\,dt$$

Note the use of $si(z) = Si(z) - \pi/2$ in place of the more common $Si(z)$; this form is used because it simplifies Equation A-23 and also because $si(z)$ is obtained, along with $Ci(z)$, from a standard computer subroutine.

The CAL computer program (PROB1) computes I_1, I_{2a} ($\approx I_2$), and $p(x)$ using numerical integration of Equation A-20 and direct numerical evaluation of Equation A-23 along with Equation A-19. In addition, the Gaussian probability density is computed from Equation A-5; although not expected to be accurate, the Gaussian density function is useful for comparison purposes.

A second computer program, PROB2, was written to permit integration of Equation 4 when $N = 4$. Again the range of integration was broken up into two parts analogous to Equations A-20 and A-21, numerical integration was used over the range 0 to v_1, and an exact analytic expression for the integral from v_1 to infinity of the asymptotic approximation to the integrand was evaluated. Thus the integral was written in the form of Equation A-19 with:

$$I_1 = \frac{1}{\pi}\int_0^{v_1} J_0(vA_1)\,J_0(vA_2)\,J_0(vA_3)\,J_0(vA_4)\cos(vx)\,dv \qquad \text{(A-24)}$$

$$I_2 = \frac{1}{\pi}\int_{v_1}^{\infty} J_0(vA_1)\,J_0(vA_2)\,J_0(vA_3)\,J_0(vA_4)\cos(vx)\,dv \qquad \text{(A-25)}$$

Provided v_1 is chosen large enough, all four Bessel functions in Equation A-25 can be replaced by their asymptotic values (Equation A-18) to form a new integral $I_{2a} \approx I_2$. This integral can be evaluated analytically, yielding:

$$I_{2a} = \frac{1}{4\pi^3\sqrt{A_1A_2A_3A_4}}\left\{\sum_{j=1}^{6}\left[\frac{\cos(B_j v_1)}{v_1} + B_j\, si(B_j v_1)\right] + \right.$$
$$\left. -\sum_{j=7}^{8}\left[\frac{\cos(B_j v_1)}{v_1} + B_j\, si(B_j v_1)\right] + \sum_{j=9}^{16}\left[\frac{\sin(B_j v_1)}{v_1} - B_j\, Ci|B_j v_1|\right]\right\} \qquad \text{(A-26)}$$

where;

$$B_1 = A_1 - A_2 + A_3 - A_4 + x$$
$$B_3 = A_1 - A_2 - A_3 + A_4 + x$$
$$B_5 = A_1 + A_2 - A_3 - A_4 + x$$

$$B_7 = A_1 + A_2 + A_3 + A_4 + x$$

$$B_9 = A_1 + A_2 + A_3 - A_4 + x$$

$$B_{11} = A_1 + A_2 - A_3 + A_4 + x$$

$$B_{13} = A_1 - A_2 + A_3 + A_4 + x$$

$$B_{15} = -A_1 + A_2 + A_3 + A_4 + x$$

$$B_{n+1} = B_n - 2x, \qquad n = 1, 3, 5, 7, 9, 11, 13, 15.$$

This computer program also computes the Gaussian probability density that should approximate $p(x)$, at least when the A_i are nearly equal, and, in addition, the asymptotically corrected Gaussian probability density which is expected to be valid only when $A_i = A$ for all four i.

Computer programs PROB1 and PROB2 thus permit computation of $p(x)$ when there are 2 or 4 scatterers. Extension to 6- or 8-scatterer cases would be straightforward but quite complicated because of the very large number of terms that would appear in the expression for I_{2a}: note the increase from 4 terms in Equation A-23 to A-32 terms in Equation A-26. Computation of $p(x)$ when N is odd is not practical because I_{2a} then is irrational and cannot be integrated in closed form.

Also of interest is the probability density function of the envelope (amplitude) of the received signal, $p(R)$. First, consider $p(R)$ when there are 2 scatterers ($N = 2$ in Equation A-7). The required integral is:

$$p(R) = R \int_0^\infty J_0(Rv)\, J_0(A_1 v)\, J_0(A_2 v)\, v\, dv \qquad \text{(A-27)}$$

Again, asymptotic expansions of Bessel functions for v between some v_1 and infinity will be used. However, since $p(R)$ may be desired for quite small R, $J_0(Rv)$ is retained in both integrals; asymptotic expansions are used only for $J_0(A_1 v)$ and $J_0(A_2 v)$. An additional change over the method of integration used above was required here: to permit analytic integration of I_2, the range must be from 0 to infinity. The numerical integration, I_1, from 0 to v_1 thus must

be modified to compensate for the inaccuracy of the asymptotic approximations for small v. We thus have:

$$I_1 = R\int_0^{v_1}\left\{vJ_0(vA_1)J_0(vA_2) - \frac{1}{\pi\sqrt{A_1A_2}}\left[\sin((A_1+A_2)v) + \cos(|A_1-A_2|v)\right]\right\}J_0(Rv)\,dv \qquad \text{(A-28)}$$

$$I_2 = \frac{R}{\pi\sqrt{A_1A_2}}(QS+QC) \qquad \text{(A-29)}$$

where;

$$QS = \int_0^\infty J_0(Rv)\sin((A_1+A_2)v)\,dv = \begin{cases} 0 & , \quad R > A_1+A_2 \\ \infty & , \quad R = A_1+A_2 \\ \dfrac{1}{\sqrt{(A_1+A_2)^2-R^2}} & , \quad 0 < R < A_1+A_2 \end{cases}$$

$$QC = \int_0^\infty J_0(Rv)\cos(|A_1+A_2|v)\,dv = \begin{cases} \dfrac{1}{\sqrt{R^2-|A_1-A_2|^2}} & , \quad R > |A_1-A_2| \\ \infty & , \quad R = |A_1-A_2| \\ 0 & , \quad R < |A_1-A_2| \end{cases}$$

Thus I_2 would give $p(R)$ if the asymptotic approximations to the Bessel functions were exact. The numerical integration of I_1 provides a correction based upon the difference between the actual integrand and its approximation used in I_2. The derived probability density is then given by:

$$p(R) \approx I_1 + I_2 \qquad \text{(A-30)}$$

As in the programs discussed above, it is necessary to do the numerical integration of I_1 in a sufficient number of subintervals to provide the required accuracy.

In addition to the computation of $p(R)$ discussed above, the PROB3 program computes the Rayleigh probability density (using Equation A-9 for $p_R(R)$).*

*PROB3 and PROB4 (to be discussed next) also compute $p_{RA}(R)$, but in their present form they produce a correct result for $p_{RA}(R)$ only if all $A_i = 1$.

When $N = 4$, integration of Equation A-7 is considerably more difficult because of the appearance of a pole at $v = 0$ in the asymptotic form of the integrand. This difficulty is circumvented through some manipulations of various terms and the use of three, rather than two, subintegrals. We have:

$$p(R) = I_1 + I_2 + I_3 \tag{A-31}$$

$$I_1 = R\int_0^{v_1} J_0(Rv)\Big\{ vJ_0(A_1v)\,J_0(A_2v)\,J_0(A_3v)\,J_0(A_4v) +$$

$$+\frac{T}{v}\Big[1-(\sin((A_1+A_2)v)+\cos(|A_1-A_2|v))\cdot(\sin((A_3+A_4)v)+\cos(|A_3-A_4|v))\Big]\Big\}\,dv \tag{A-32}$$

$$I_2 = \frac{RT}{2}\int_0^{\infty} \frac{J_0(Rv)}{v}\Big\{-(1-\cos(B_1v))+(1-\cos(B_2v)) + \sin(B_3v)+\sin(B_4v)$$

$$+\sin(B_5v)+\sin(B_6v)-(1-\cos(B_7v))-(1-\cos(B_8v))\Big\}\,dv \tag{A-33}$$

$$I_3 = RT\int_{Rv_1}^{\infty} \frac{J_0(t)}{t}\,dt \tag{A-34}$$

where;

$$T = \frac{1}{\pi^2\sqrt{A_1A_2A_3A_4}}$$

$$B_1 = |A_1 + A_2 - A_3 - A_4|$$

$$B_2 = A_1 + A_2 + A_3 + A_4$$

$$B_3 = |A_1 - A_2| + A_3 + A_4$$

$$B_4 = A_3 + A_4 - |A_1 - A_2|$$

$$B_5 = A_1 + A_2 + |A_3 - A_4|$$

$$B_6 = A_1 + A_2 - |A_3 - A_4|$$

$$B_7 = |A_1 - A_2| + |A_3 - A_4|$$

$$B_8 = |(|A_1 - A_2| - |A_3 - A_4|)|$$

Integration to obtain I_1 again was performed numerically, using 10-point Gaussian quadratures over sufficient subintervals to obtain the required accuracy. Since integrand values are not computed at the endpoints of an interval, the division by 0 in the integrand at $v = 0$ causes no problem. If a numerical integration technique requiring computation of the integrand at $v = 0$ were used, care would have to be taken to include the appropriate expression for use at $v = 0$.

Integration to obtain I_3 was performed in one or two parts, depending upon Rv_1. For Rv_1 less than 10, the expression was integrated numerically, using 10-point Gaussian quadrature, from Rv_1 to 10. Integration from 10 to infinity, or from Rv_1 to infinity when $Rv_1 \geq 10$, was performed using an asymptotic expression, equation 11.1.29 on page 482 of Reference 4. (For all of the cases so far computed, I_3 has been negligible; if I_3 were to be computed for very small, but nonzero, values of R, significant values of I_3 would result.)

Integration to obtain I_2 requires two basic integrals:

$$\int_0^\infty \frac{1}{v} J_0(Rv)\sin(Bv)\,dv = \begin{cases} \frac{\pi}{2}\,\mathrm{sgn}(B), & 0 < \left|\frac{R}{B}\right| < 1 \\ \sin^{-1}\frac{B}{R}, & 1 < \left|\frac{R}{B}\right| \end{cases} \qquad \text{(A-35)}$$

$$\int_0^\infty \frac{1}{v} J_0(Rv)\left[1-\cos(Bv)\right]dv = \begin{cases} \cosh^{-1}\left(\frac{|B|}{R}\right), & 0 < \left|\frac{R}{B}\right| < 1 \\ 0, & 1 < \left|\frac{R}{B}\right| \end{cases} \qquad \text{(A-36)}$$

There are four integrals of each type in I_2. Because of the discontinuous behavior of these integrals, considerable logic was required in the computation. Computation is simplified through use of the expression:

$$\cosh^{-1}x = \ln\left[x + \sqrt{x^2-1}\right] \quad (x \geq 1) \qquad \text{(A-37}$$

The Rayleigh density distribution, $p_R(R)$, from Equation A-9, and the asymptotically corrected Rayleigh density distribution, $p_{RA}(R)$ are also computed by the PROB4 program. In addition, the Nakagami m-distribution was computed using Equations A-11 through A-17. Thus it is possible to compare the various approximations with a relatively accurate computation of $p(R)$.

A.3 COMPARISON OF PROBABILITY FUNCTIONS

The discussion will be broken into two parts to reduce confusion. First, the behavior of $p(x)$, the probability density of either the in-phase or the quadrature components of the received signal, is discussed for both 2-scatterer and 4-scatterer cases. Then the behavior of $p(R)$, the probability density of the envelope of the received signal, is discussed for both cases.

Although the discussion in this section is centered on radar scattering from randomly located, constant-magnitude scatterers, it should be remembered that the results are much more general. The applicability of the Central Limit Theorem when there are only 2 or 4 random variables can thus be estimated from the results given here. Similarly, any problem that can be made analogous to a two-dimensional random walk can be examined using these results.

First, let us consider $p(x)$ for $N = 2$. When $A_1 = A_2 = 1$, $p(x)$ is shown in Figure A-1. Note the very rapid drop in $p(x)$ for x near 2: at $x = 1.99$, $p(x) = 0.1601$; at $x = 2$, $p(x) = 0.0808$; at $x = 2.01$, $p(x) = 0.0010$. Since $p(x) = 0$, $x \geq 2$, the value 0.0010 found at $x = 2.01$ can be considered a result of the numerical approximations used. Also shown are the Gaussian density function, $p_G(x)$, and the asymptotically modified Gaussian density function, $p_{GA}(x)$. Note that even for $N = 2$ the asymptotic correction is quite small; it is obviously insufficient to give a reasonable approximation to $p(x)$. In all of the figures for $p(x)$ it must be remembered that $p(x)$, $p_G(x)$, and $p_{GA}(x)$ are even functions of x for all values of A_1 and A_2; only the positive-x parts of the probability densities are plotted.

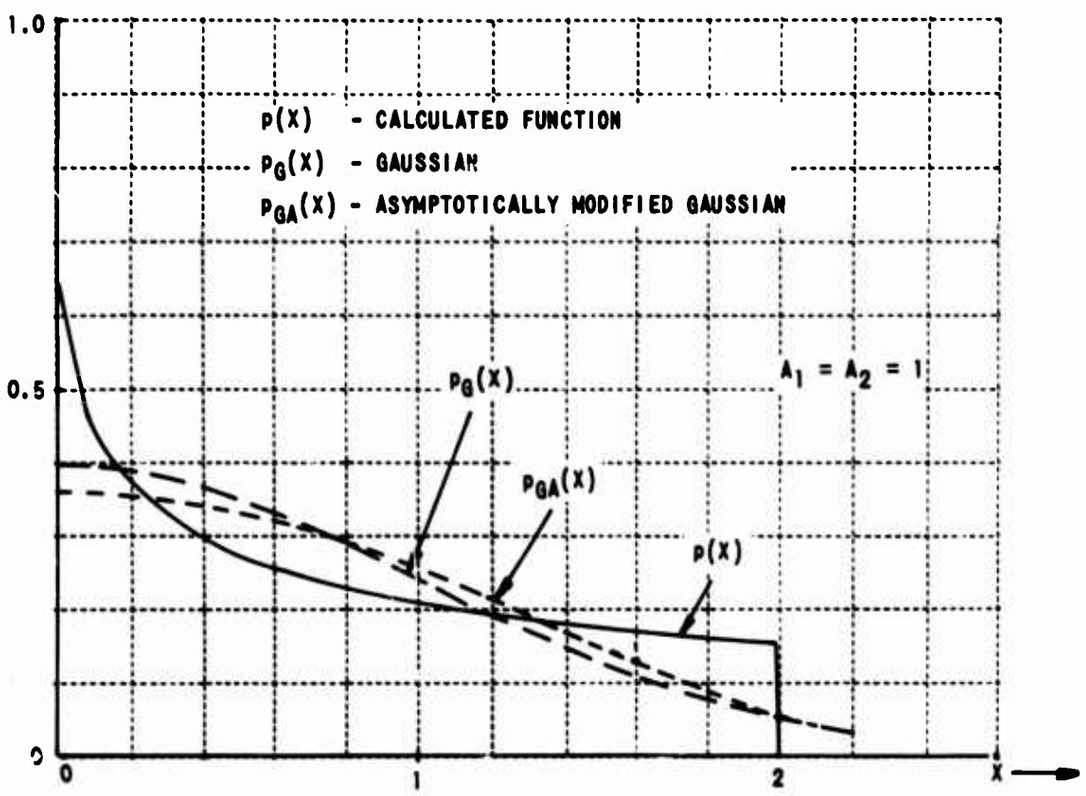

Figure A-1 QUADRATURE PHASE COMPONENT PROBABILITY DENSITY FUNCTIONS FOR TWO EQUAL AMPLITUDE RANDOM (UNIFORM) PHASE SCATTERERS

When A_1 and A_2 are unequal, the pole in $p(x)$ that occurred at $x = 0$ for $A_1 = A_2$ (see Figure A-1) moves to $x = |A_1 - A_2|$; because of the symmetry of $p(x)$, a pole now appears at $x = -|A_1 - A_2|$ as well. Several $p(x)$ curves have been plotted for unequal values of A_1 and A_2; in each case, $\sigma = \frac{1}{2}(A_1^2 + A_2^2)$ has been kept equal to unity to permit easier comparison of the results. In Figure A-2a, $A_1 = 1.36$, $A_2 = 0.40$, while in Figure A-2b, $A_1 = 1.41$, $A_2 = 0.10$. The curves shown in Figure A-2 are obviously non-Gaussian in shape, as would be expected. Also shown in Figure A-2b is the probability density for $A_1 = \sqrt{2}$, $A_2 = 0$. This limiting case occurs when the second scatterer drops to zero amplitude, leaving only one randomly phased contributor. When $A_2 = 0$, we have:

$$p_1(x) = \frac{1}{\pi\sqrt{A_1^2 - x^2}} \quad , \quad x^2 \le A_1^2$$
$$= 0 \quad , \quad x^2 > A_1^2 \qquad \text{(A-38)}$$

as the exact probability density function. Note that for $A_1 = \sqrt{2}$, $A_2 = 0$ the $p_1(x)$ curve is nearly the same as the $p(x)$ curve except for the shift in pole location. Thus, for values of A_2 between 0.1 and 0 it should be easy to estimate quite accurately the shape of $p(x)$.

We have seen that when there are only two, randomly phased components $p(x)$ bears little resemblance to a Gaussian probability density function. Consider next the situation in which there are 4 randomly phased contributors. In Figure A-3 are shown $p(x)$, $p_G(x)$, and $p_{GA}(x)$ for $x \ge 0$ (as noted before, the probability densities are even functions of x). It can be seen that the probability density function $p(x)$ is now very nearly Gaussian. Also, although the asymptotically corrected Gaussian distribution is evidently a closer approximation to $p(x)$ than is the Gaussian distribution, not that $p_{GA}(x)$ does not give a perfect representation of $p(x)$.

Consider some cases of unequal amplitude scatterers. When $A_1 = A_2 = 0.8$, $A_3 = 1$, and $A_4 = 1.3115$, $p(x)$ is still nearly Gaussian, as shown in Figure A-4. If two scatterers are large and two are small, the $p(x)$ curve departs more radically from the Gaussian in shape; for example, in Figure A-5 are compared $p(x)$ and $p_G(x)$ for $A_1 = A_2 = 0.20$, $A_3 = A_4 = 1.40$. When one scatterer

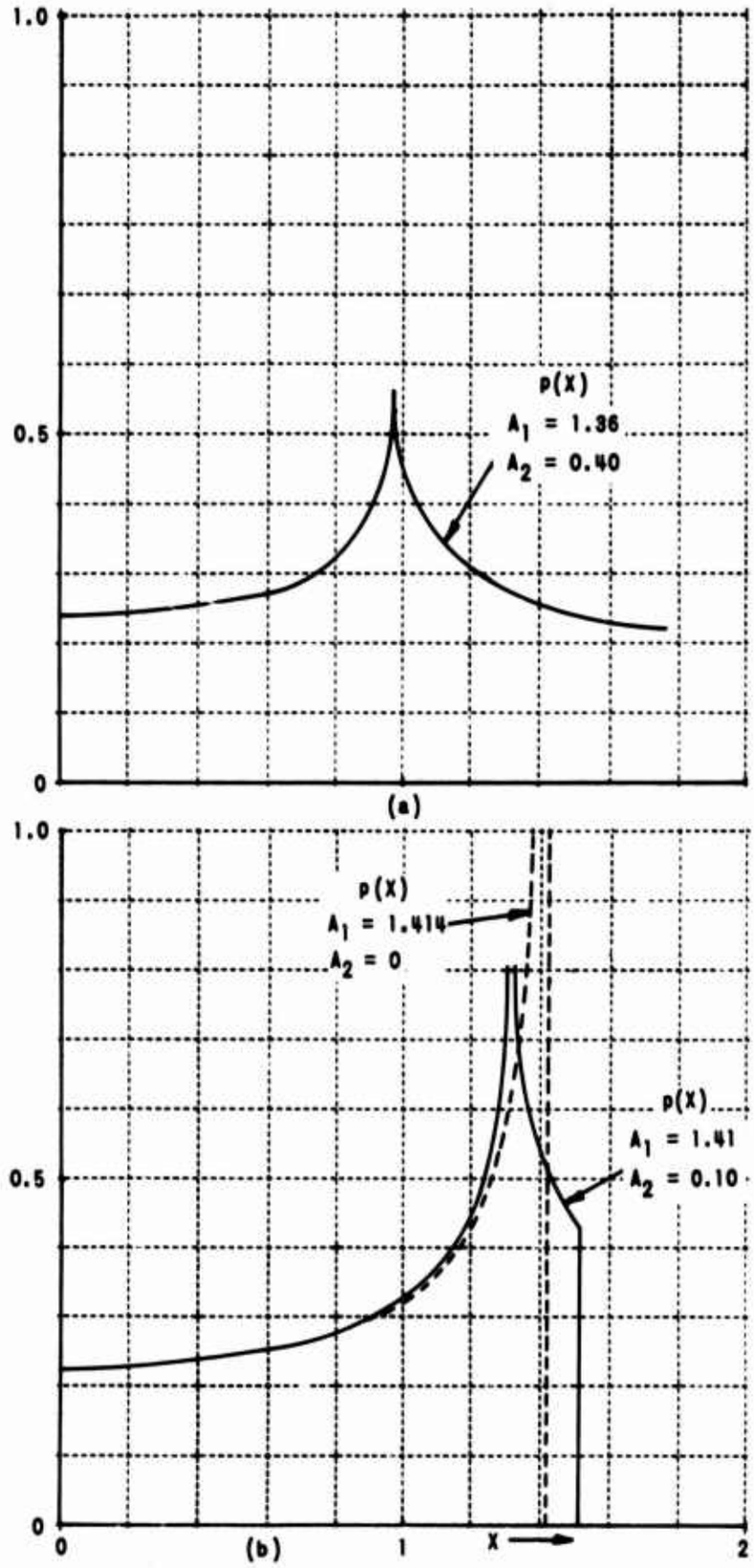

Figure A-2 QUADRATURE PHASE PROBABILITY DENSITY FUNCTIONS FOR TWO RANDOM (UNIFORM) PHASE SCATTERERS

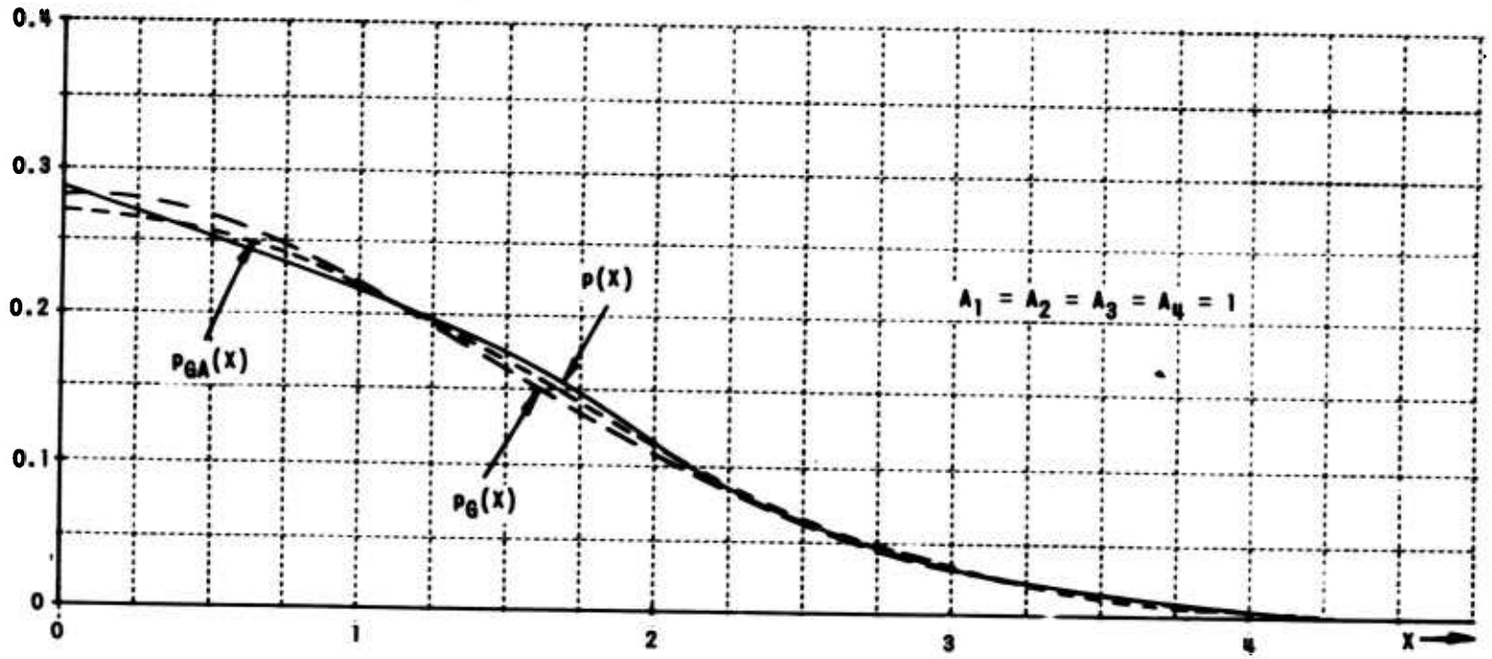

Figure A-3 QUADRATURE PHASE PROBABILITY DENSITY FUNCTIONS FOR FOUR EQUAL AMPLITUDE RANDOM (UNIFORM) PHASE SCATTERERS

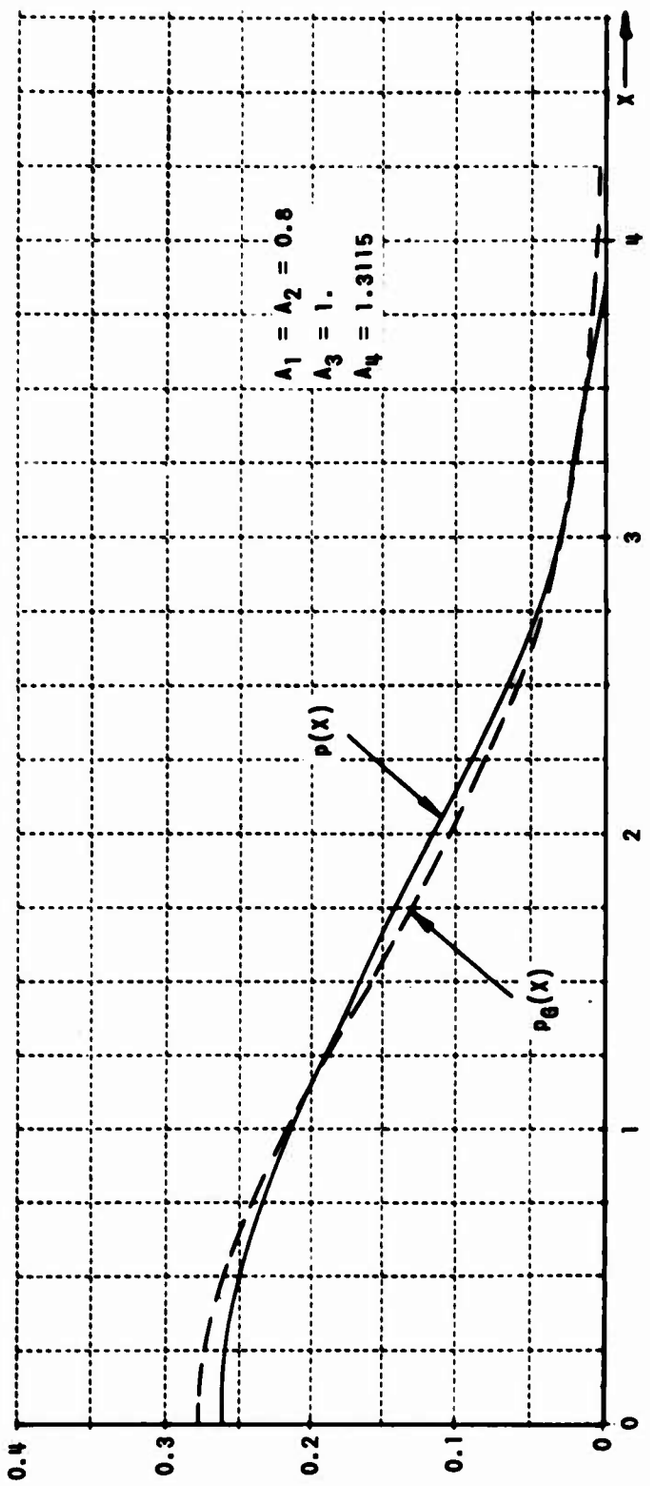

Figure A-4 QUADRATURE PHASE PROBABILITY DENSITY FUNCTIONS - FOUR SCATTERERS

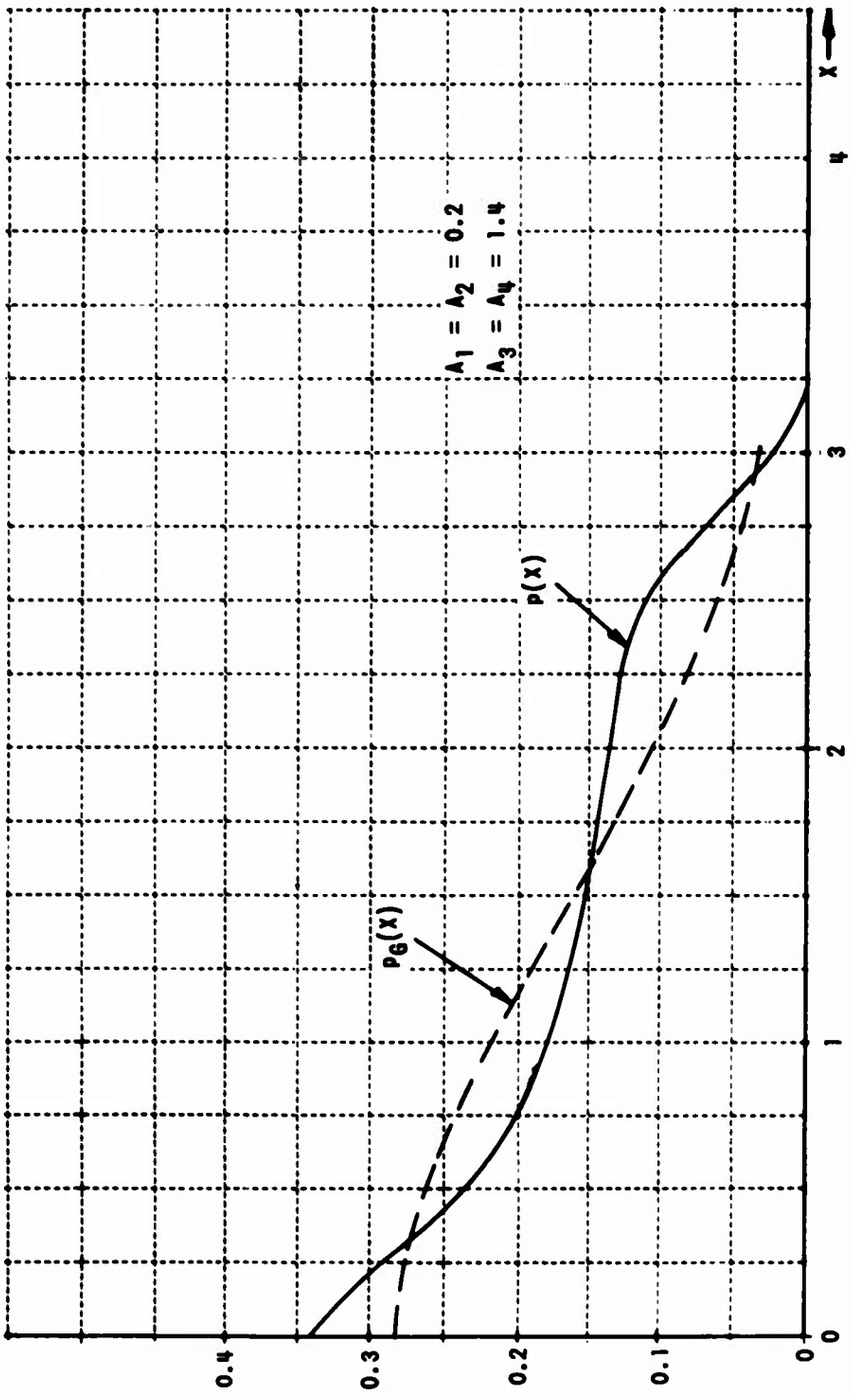

Figure A-5 QUADRATURE PHASE PROBABILITY DENSITY FUNCTIONS - FOUR SCATTERERS

Table A-2
CALCULATED ENVELOPE PROBABILITY DENSITY FUNCTION, p(R)

R	p(R) (EQ.8)	p(R) $v_1 = 10$, m = 5	p(R) $v_1 = 10$, m = 10	p(R) $v_1 = 20$, m = 20	p(R) $v_1 = 20$, m = 10	p(R) $v_1 = 20$, m = 5
0.2	0.31991	0.31972	--	--	--	--
0.4	0.32487	0.32537	0.32537	--	--	--
0.6	0.33368	0.33333	--	--	--	--
0.8	0.34730	0.34691	--	--	--	--
1.0	0.36755	0.36865	0.36865	0.36715	0.36715	0.36715
1.2	0.39789	0.39708	--	--	--	--
1.4	0.44572	0.44492	--	--	--	--
1.6	0.53051	0.53337	--	--	--	--
1.8	0.73023	0.72653	--	--	--	--

v_1 - LIMIT OF NUMERICAL INTEGRATION

m - NUMBER OF SUBINTERVALS USED IN NUMERIC INTEGRATION

strongly dominates over the other three, a distinct peaking of the $p(x)$ curve occurs. Figures A-6 through A-9 demonstrate this behavior. In Figure A-8 and A-9 there is obviously no point in comparing the probability density function with that of a Gaussian process. Instead, the curves for probability density if $A_1 = A_2 = A_3 = 0$ and A_4 remains at its original value are given; these curves are found using Equation A-38 with A_4 replacing A_1 . We see that, as for the 2-scatterer case, the actual probability density closely approximates that of a single, randomly phased scatterer when the other scatterer(s) becomes small in magnitude.

In Figures A-1 through A-3 and A-4 through A-9 it has been shown that $p(x)$ is nearly Gaussian if there are four equal, or nearly equal, scatterers but that when there are two scatterers, $p(x)$ is non-Gaussian for all sets of scatterer amplitudes tried so far. It appears probable that $p(x)$ will never be even approximately Gaussian in the two-scatterer case. If there are four scatterers and one or two dominate the others, a non-Gaussian probability density results.

Also of interest in clutter analysis is the envelope probability density, $p(R)$, that corresponds to the probability densities $p(x)$ discussed above. The situation is as shown in Figure A-10. The phasors A_1 , A_2 , A_3 , A_4 have uniformly distributed phase angles; x represents the horizontal (or, equivalently, the vertical) projection of the sum of the phasors, while R is the magnitude of the phasor sum. R thus must be greater than (or equal to) zero, where as x can be positive or negative. If $p(x)$ and $p(y)$ are Gaussian and uncorrelated, then $p(R)$ is Rayleigh. Thus it would be expected, on the basis of the results discussed above, that, for $N = 2$, $p(R)$ will not be Rayleigh, but, for $N = 4$ and scatterers of approximately equal magnitude, $p(R)$ will be approximately Rayleigh. This expectation is correct, as will be shown in the following discussion and figures.

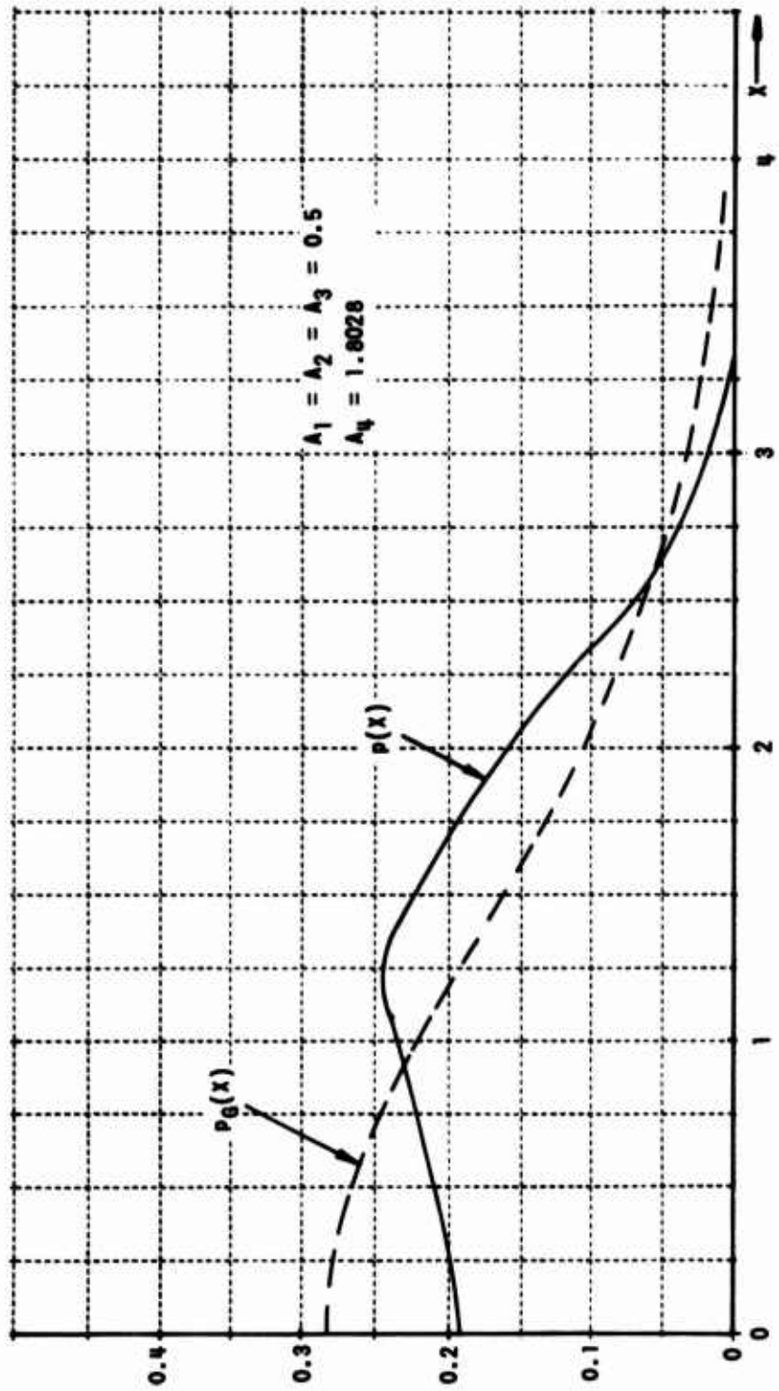

Figure A-6 QUADRATURE PHASE PROBABILITY DENSITY FUNCTIONS - FOUR SCATTERERS

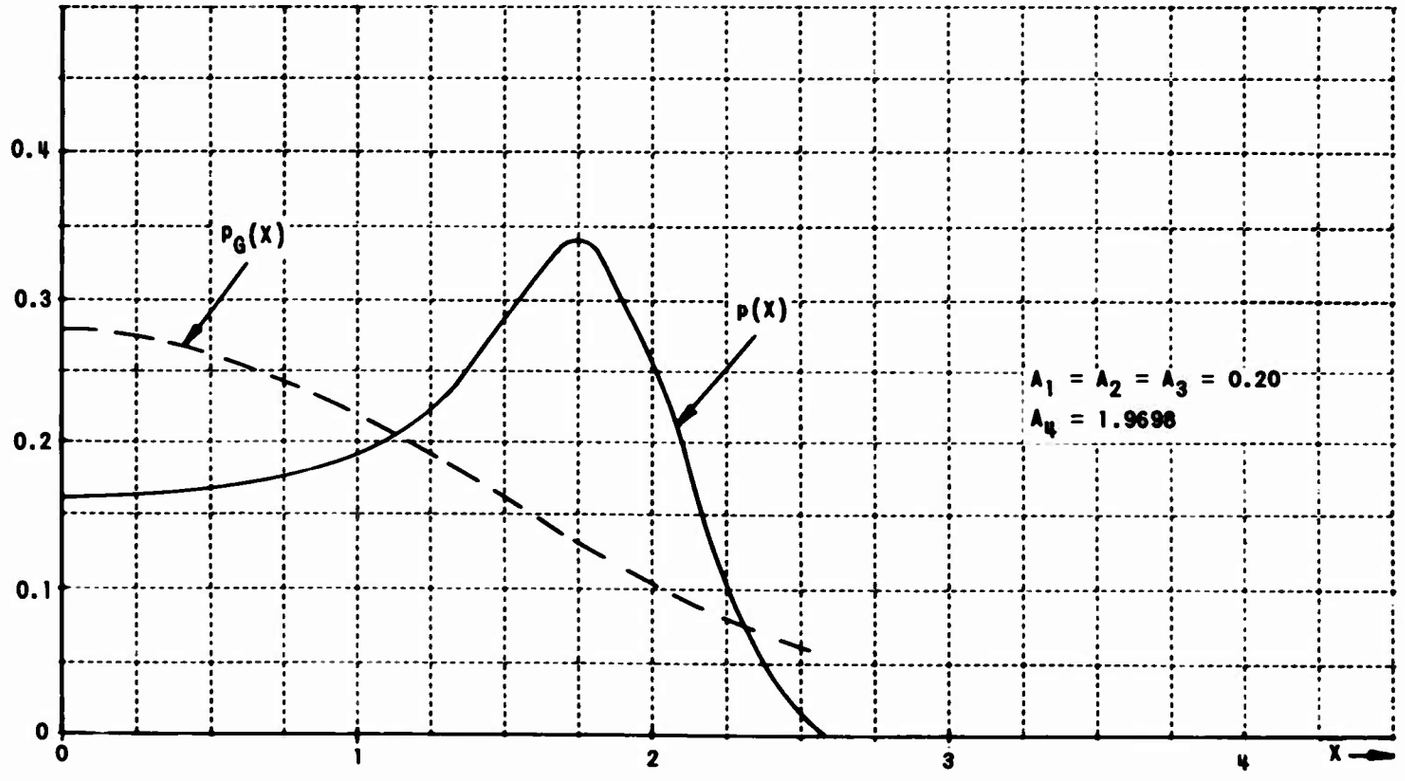

Figure A-7 QUADRATURE PHASE PROBABILITY DENSITY FUNCTIONS - FOUR SCATTERERS

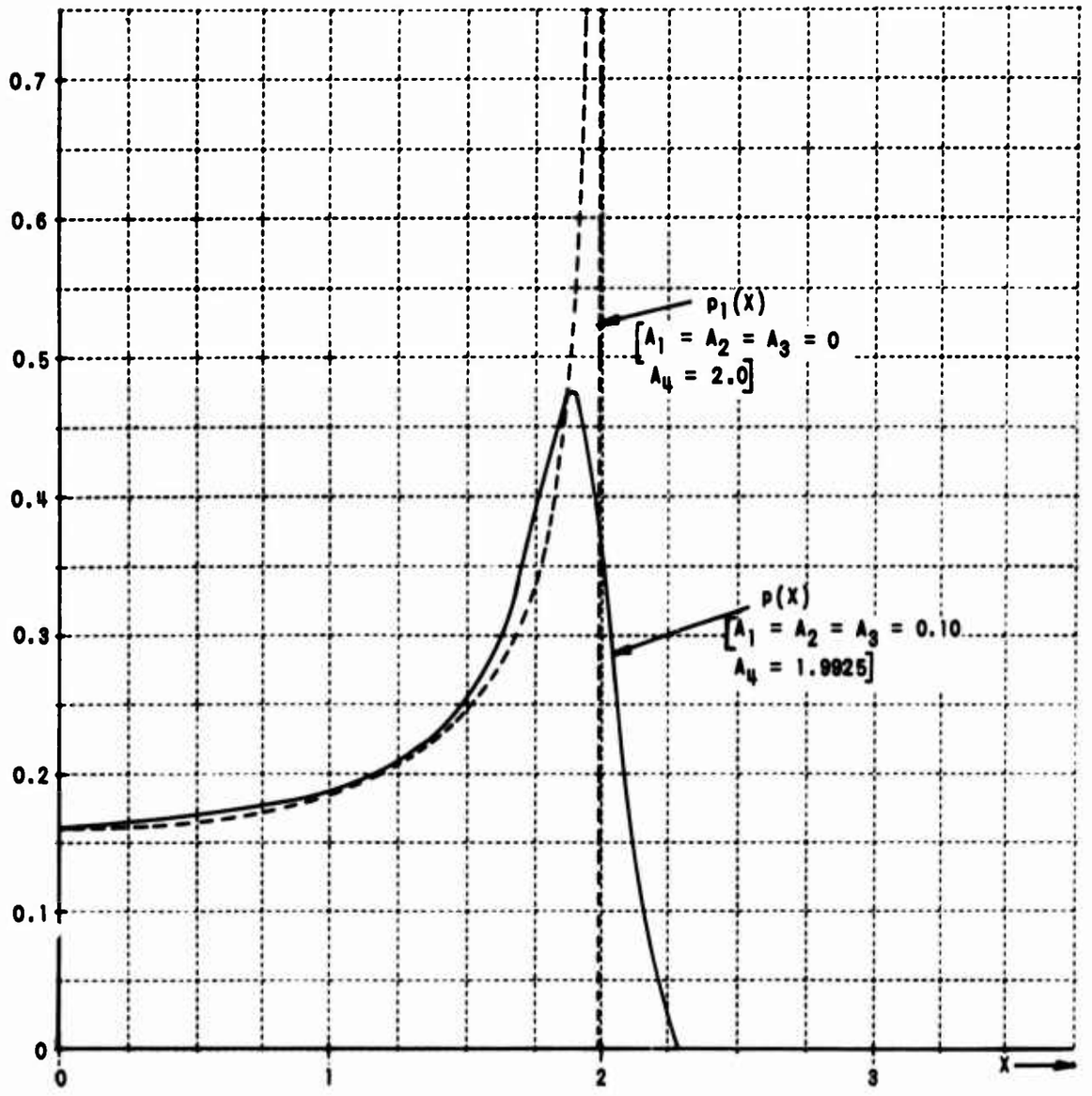

Figure A-8 QUADRATURE PHASE PROBABILITY DENSITY FUNCTIONS - FOUR SCATTERERS

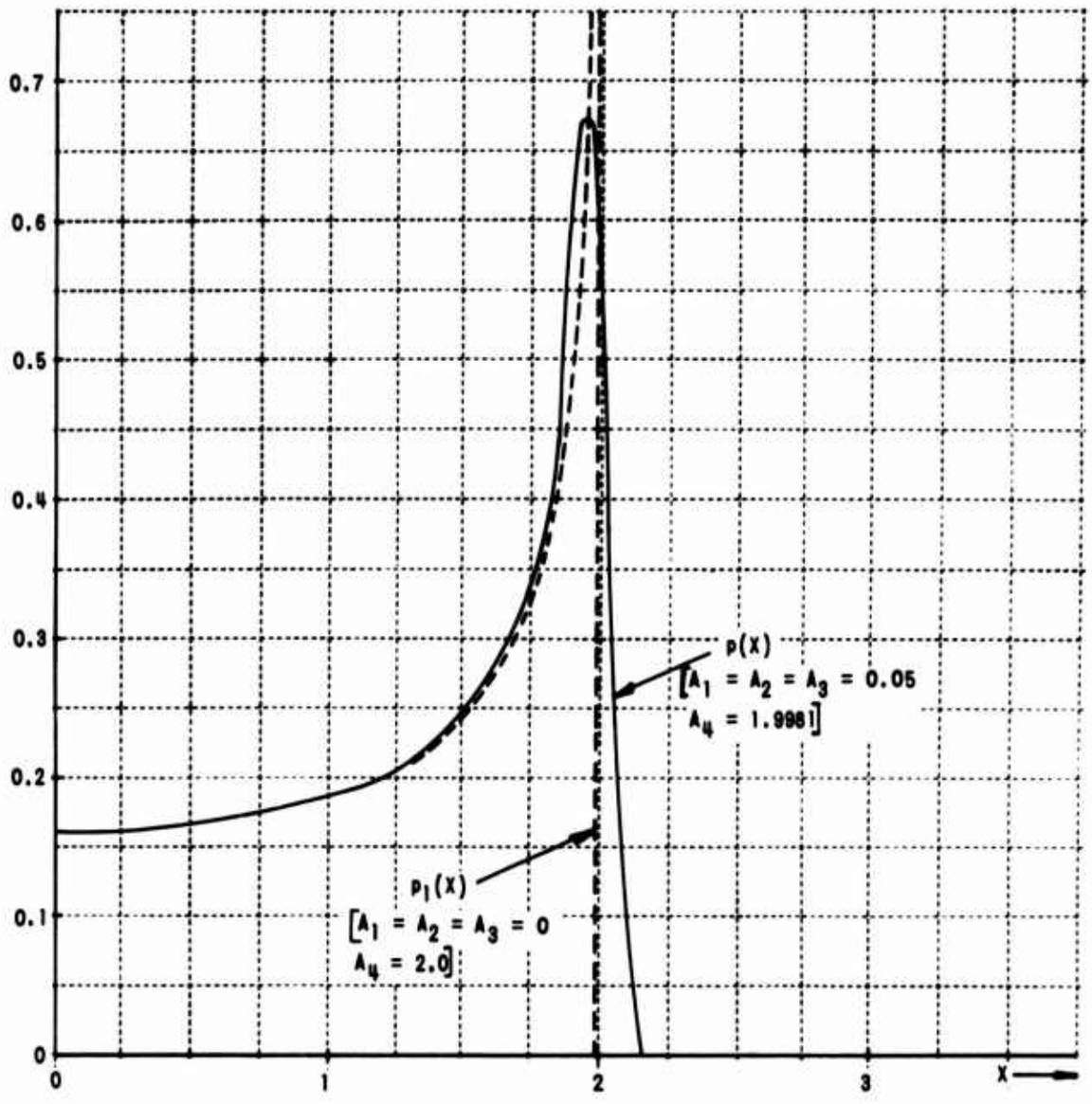

Figure A-9 QUADRATURE PHASE PROBABILITY DENSITY FUNCTIONS - FOUR SCATTERERS

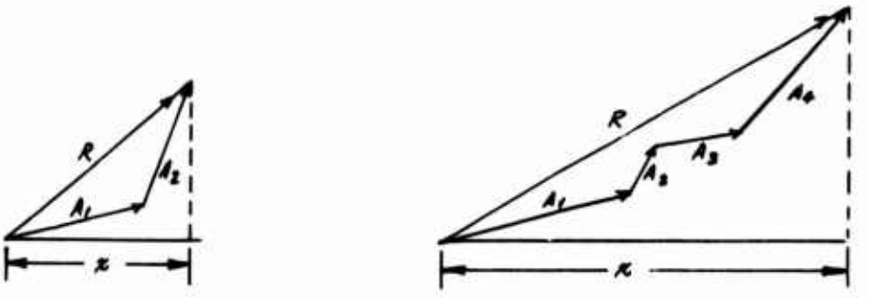

Figure A-10 ADDITION OF PHASORS

First, suppose $N = 2$ and $A_1 = A_2 = 1$. For this case, Equation A-8 was used to find $p(R)$ exactly. This equation is useful for checking the numerically computed values of $p(R)$ using the PROB3 program (see Section A.2). In Table A-2 the exact $p(R)$ is compared with the numerical solution for several choices of v_1 (v_1 is the upper limit in the numerical integration of I_1) and m (m is the number of subintervals used for the numerical integration I_1: increasing m, within bounds, increases accuracy but also increases cost of computations).

We see that $v_1 = 10$ leads to small errors, less than 0.5 percent (entirely negligible as far as a plot is concerned), and that $v_1 = 20$ leads to very small errors; $m = 0.25\ v_1$ or $0.5\ v_1$ seems to be satisfactory. A graph of the results shown in the first two columns of Table A-2 is given in Figure A-11. Also shown, for comparison, are $p_R(R)$, the Rayleigh density distribution, and $p_{RA}(R)$, the asymptotically corrected Rayleigh density. The actual $p(R)$ obviously bears no resemblance to either approximation, as was expected from the non-Gaussian character of $p(x)$. Note that in this and the remaining figures $p(R) = 0$ for $R < 0$: $p(R)$ is not symmetric, although $p(x)$ is. It is also obvious from Figure A-9 that $p(R) = 0$ for $R > \sum_{i=1}^{N} A_i$.

Next, consider the case of $A_1 \neq A_2$. From Figure A-10 we see that $p(R) = 0$ for $R < |A_1 - A_2|$. Suppose $A_1 = 1.26$ and $A_2 = 0.63$. Then $p(R)$ is non-zero only for $0.63 < R < 1.89$, as can be seen in Figure A-12. For $R < 0.63$, the PROB3 computer program produces outputs of the order of 10^{-3} or 10^{-4}; these values are a result of the numerical approximations used and indicate

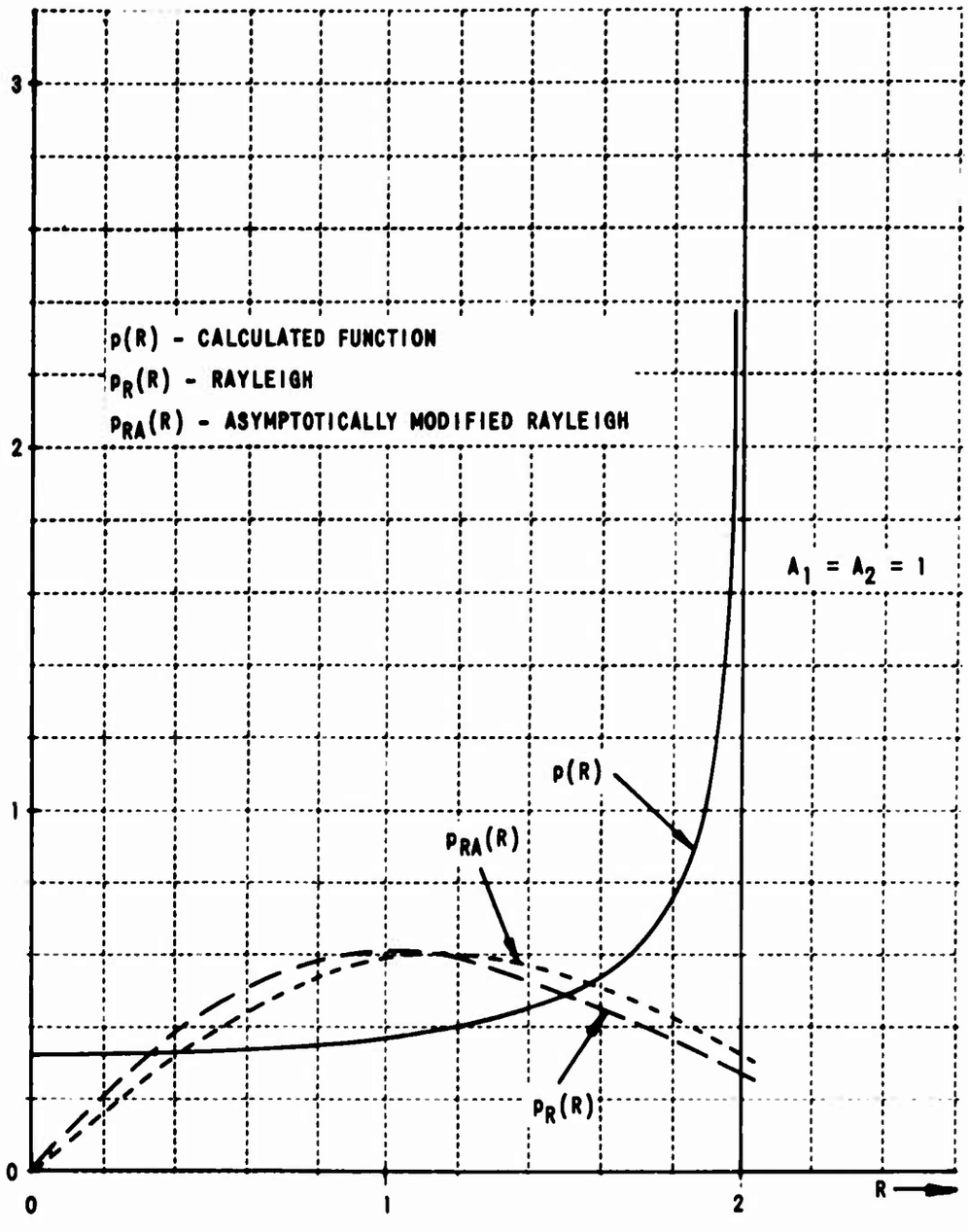

Figure A-11 ENVELOPE PROBABILITY DENSITY FUNCTION FOR TWO EQUAL AMPLITUDE RANDOM (UNIFORM) PHASE SCATTERERS

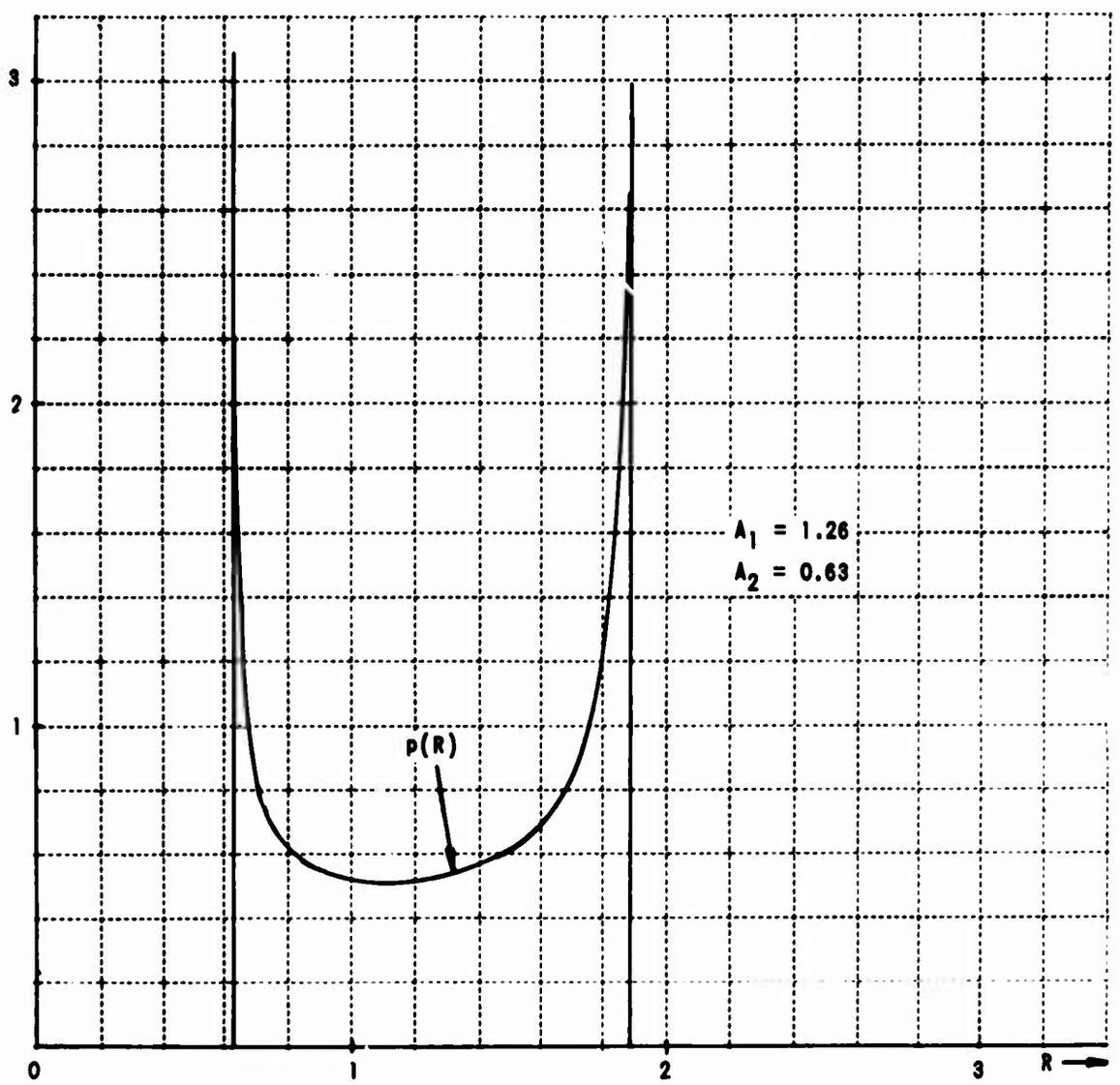

Figure A-12 ENVELOPE PROBABILITY DENSITY FUNCTION FOR TWO SCATTERERS

relatively accurate computations. For $R > A_1 + A_2$ the program always returns zero. The probability density is obviously non-Rayleigh. In Figure A-13 is shown $p(R)$ for $A_1 = 1.36$, $A_2 = 0.40$; here $p(R)$ is nonzero only for $0.9 < R < 1.76$. Hand computations of the appropriate Nakagami m-distribution were made and the resulting $p_N(R)$ shown on Figure A-13. The shape of $p_N(R)$ distribution is wrong, but it at least peaks in the region of $p(R) \neq 0$ and thus indicates where finite $p(R)$ values exist. $p_N(R)$ thus could be used as a first-order approximation to $p(R)$ if the shape of the curve were not critical. In Figurea A-14 and A-15 are shown $p(R)$ for $A_1 = 1.40$, $A_2 = 0.20$, and for $A_1 = 1.4.$, $A_2 = 0.10$. The trend noted before continues, because the range of possible R values continues to diminish.

From the results given in Figures A-11 through A-15 we see that for two scatters the probability density of is non-Rayleigh even when $A_1 = A_2$. From the one case for which the m-distribution approximation ($p_N(R)$) was computed it appears that $p(R)$ is better (although poorly) approximated by the Nakagami m-distribution $p_N(R)$ than by the Rayleigh $p_R(R)$ or asymptatically corrected Rayleigh $p_{RA}(R)$ distributions.

Finally, consider $p(R)$ when $N = 4$. In Figure A-16 $p(R)$, $p_R(R)$, $p_{RA}(R)$, and $p_N(R)$ for $A_1 = A_2 = A_3 = A_4 = 1$ are compared. The asymptotically corrected Rayleigh probability density function, $p_{RA}(R)$, is nearly the same as the Rayleigh probability density function, $p_R(R)$; both functions give a reasonable approximation to $p(R)$. The Nakagami m-distribution curve, also provides a reasonably good approximation to $p(R)$. The discontinuity in shape of $p(R)$ at $R = 2$ is characteristic of $p(R)$, as will be seen shortly. Such discontinuities in shape result from the discontinuous behavior of the integrals given in equations A-35 and A-36; consequently, the locations of discontinuities in shape can be predicted from knowledge of these integrals and the values of B_j, $j = 1, \ldots, 8$ given after equation A-34, and numerical integration can be performed at more closely spaced values of R in the region of a discontinuity to permit the shape of the $p(R)$ function to be accurately found. This technique was used for Figures A-16 through A-22.

In Figure A-17 are shown $p(R)$, $p_R(R)$, and $p_N(R)$ when $A_1 = A_2 = 0.8$,

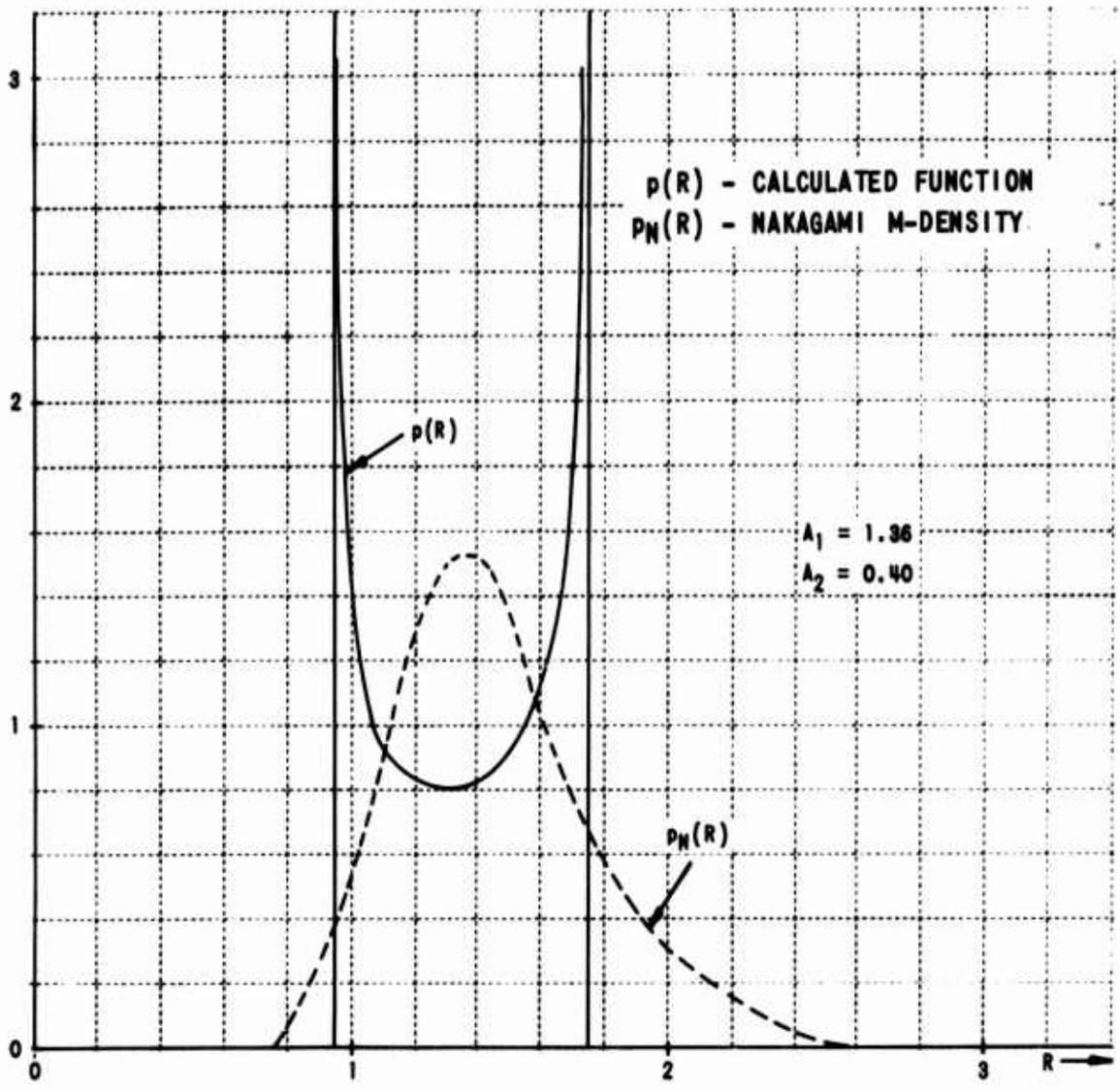

Figure A-13 ENVELOPE PROBABILITY DENSITY FUNCTION FOR TWO SCATTERERS

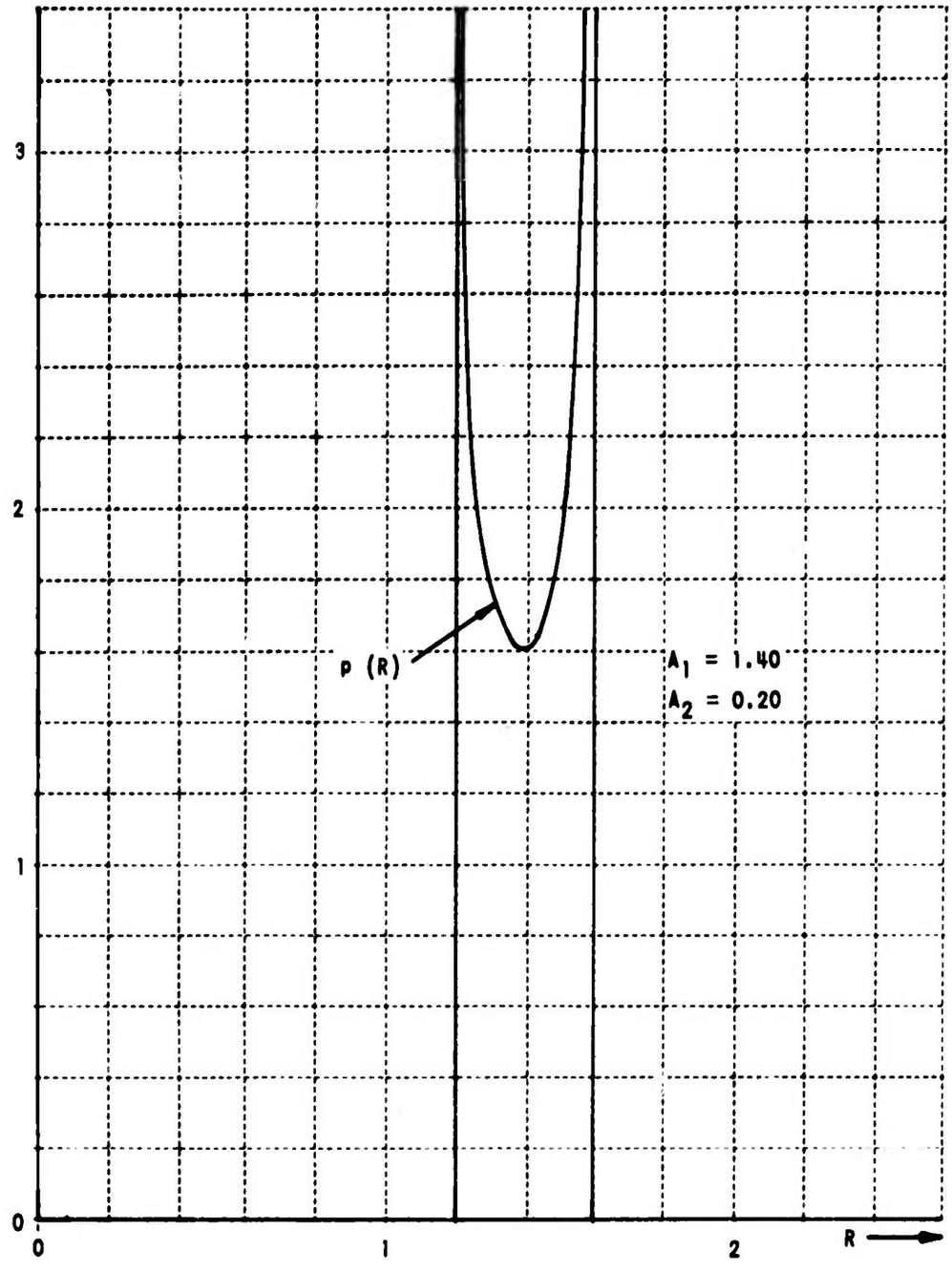

Figure A-14 ENVELOPE PROBABILITY DENSITY FUNCTION FOR TWO SCATTERERS

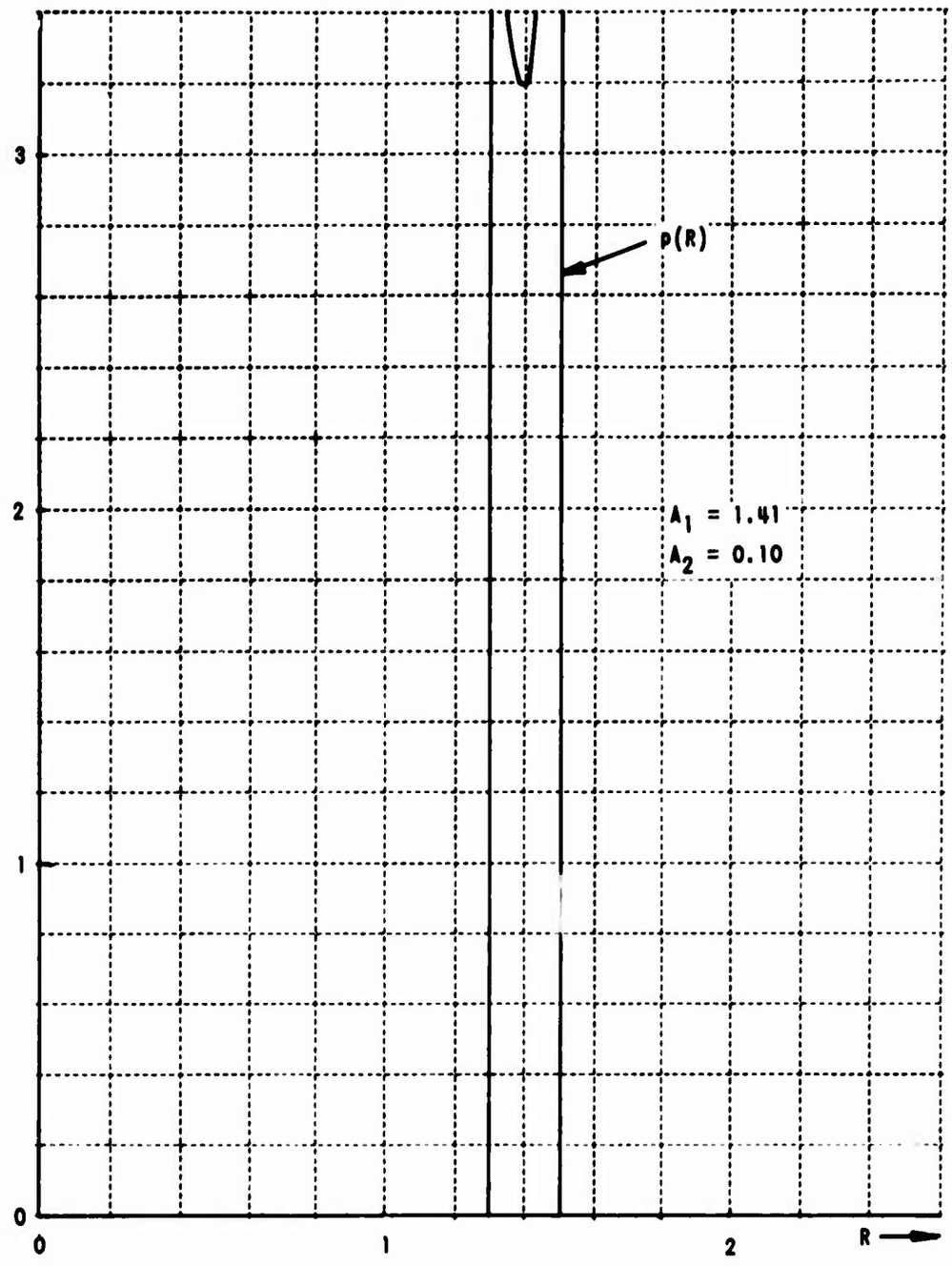

Figure A-15 ENVELOPE PROBABILITY DENSITY FUNCTION FOR TWO SCATTERERS

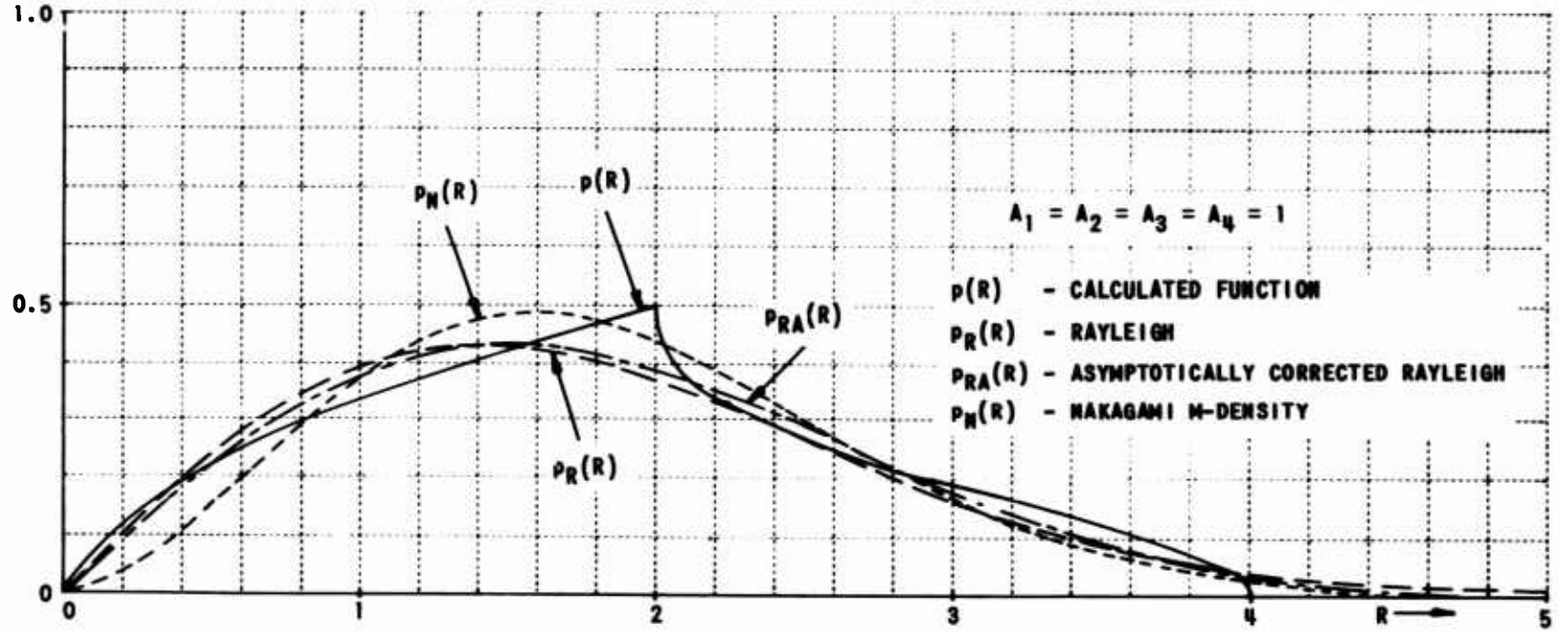

Figure A-16 ENVELOPE PROBABILITY DENSITY FUNCTION FOR FOUR SCATTERERS

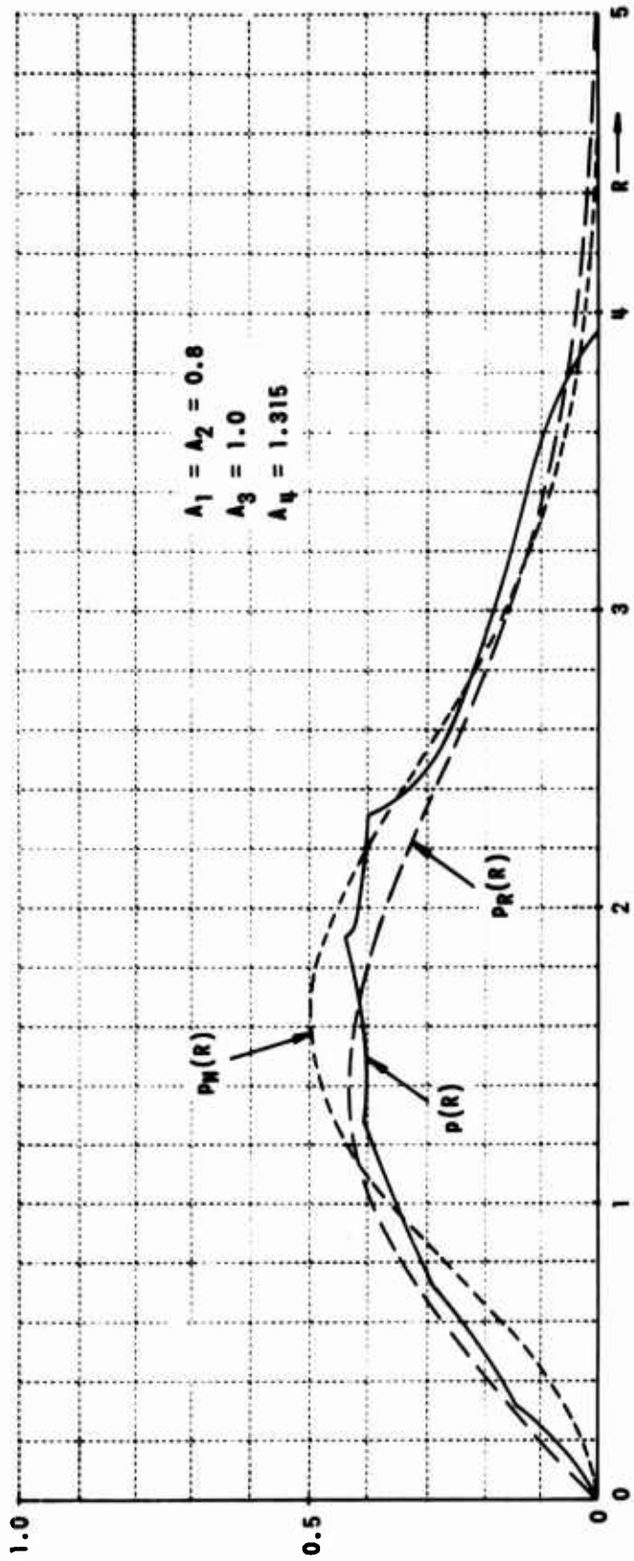

Figure A-17 ENVELOPE PROBABILITY DENSITY FUNCTION FOR FOUR SCATTERERS

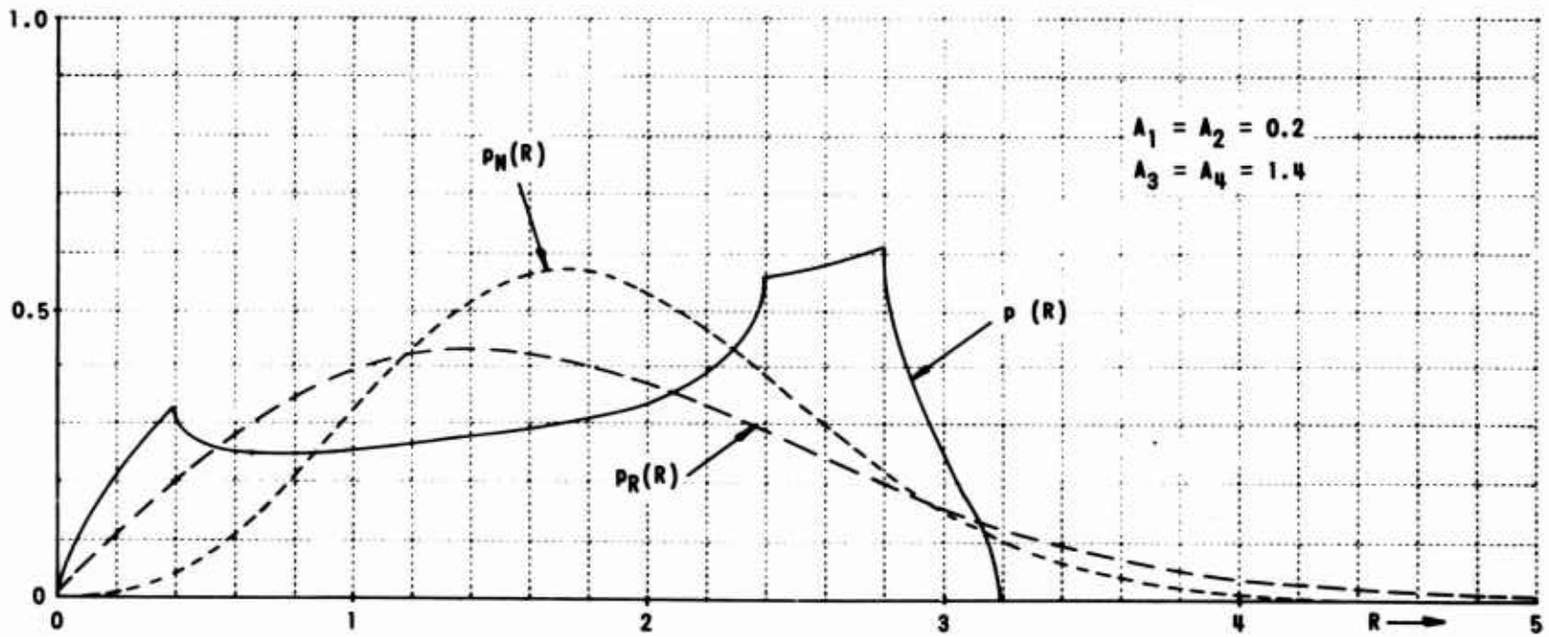

Figure A-18 ENVELOPE PROBABILITY DENSITY FUNCTION FOR FOUR SCATTERERS

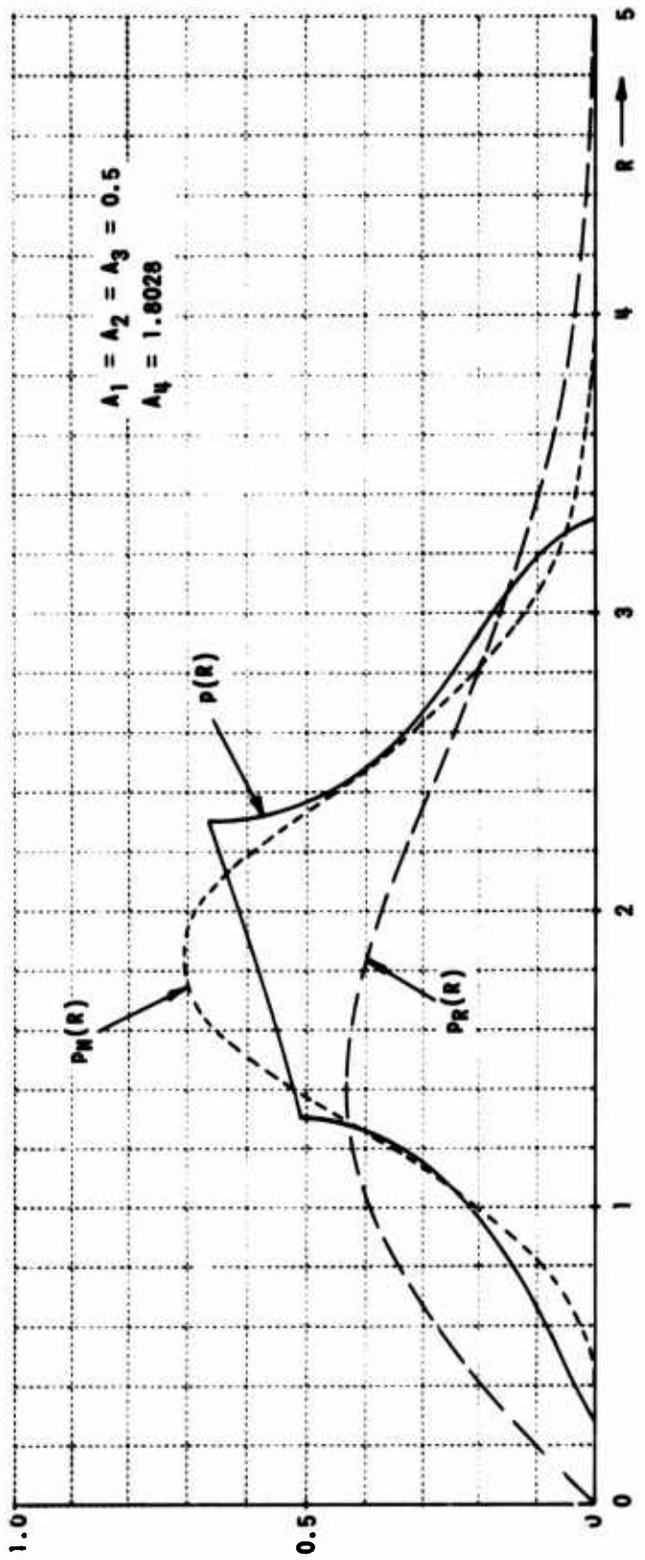

Figure A-19 ENVELOPE PROBABILITY DENSITY FUNCTION FOR FOUR SCATTERERS

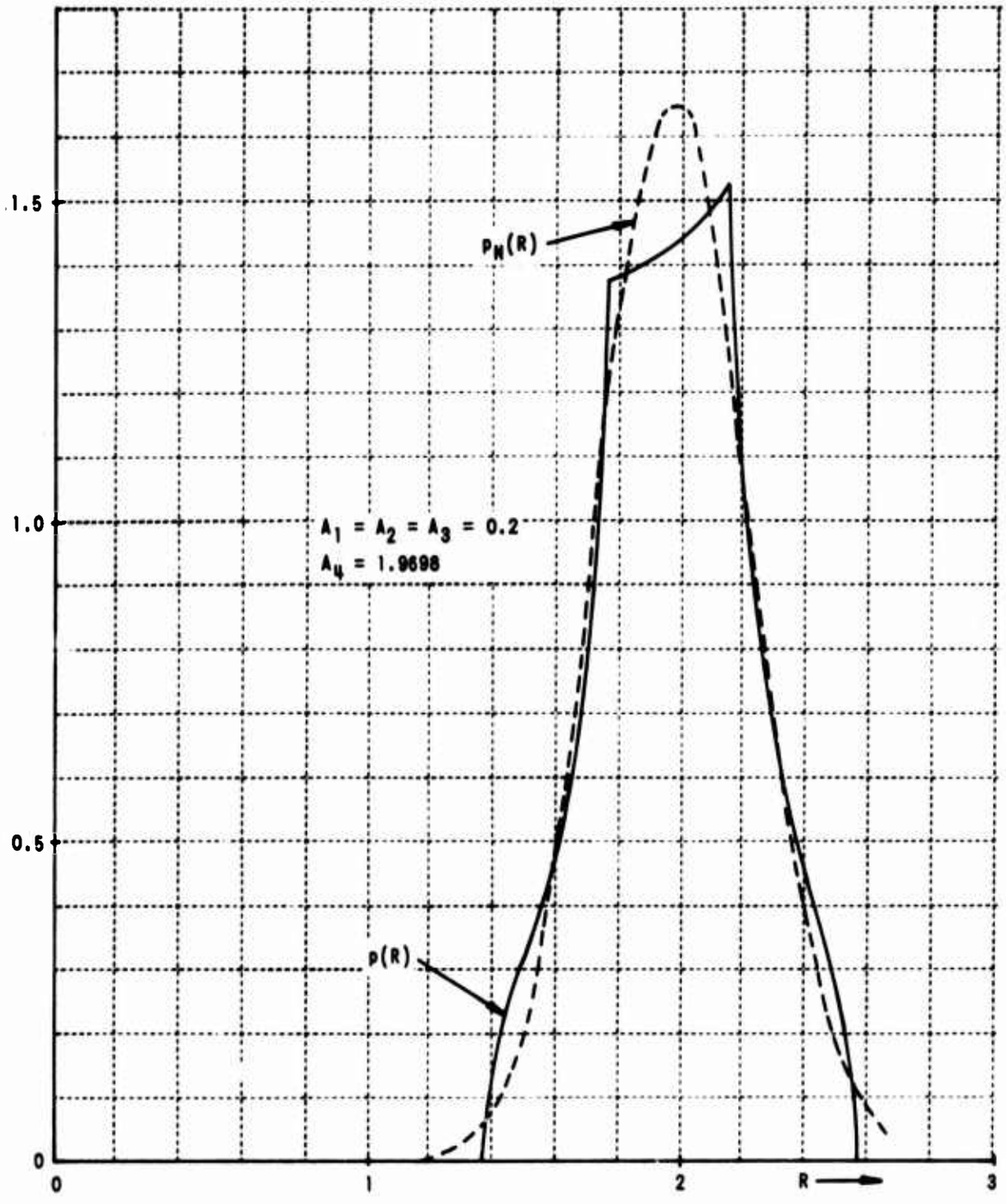

Figure A-20 ENVELOPE PROBABILITY DENSITY FUNCTION FOR FOUR SCATTERERS

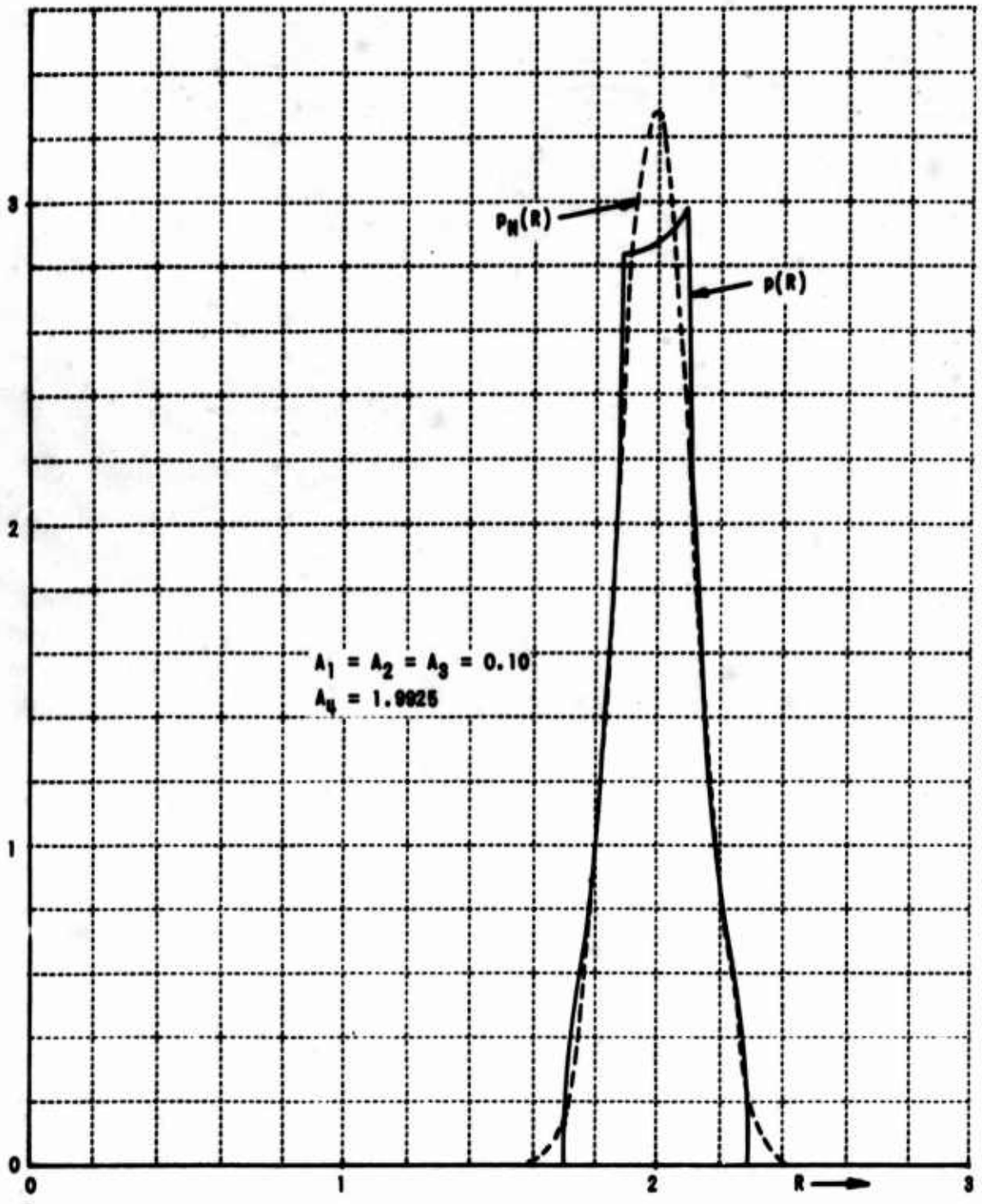

Figure A-21 ENVELOPE PROBABILITY DENSITY FUNCTION FOR FOUR SCATTERERS

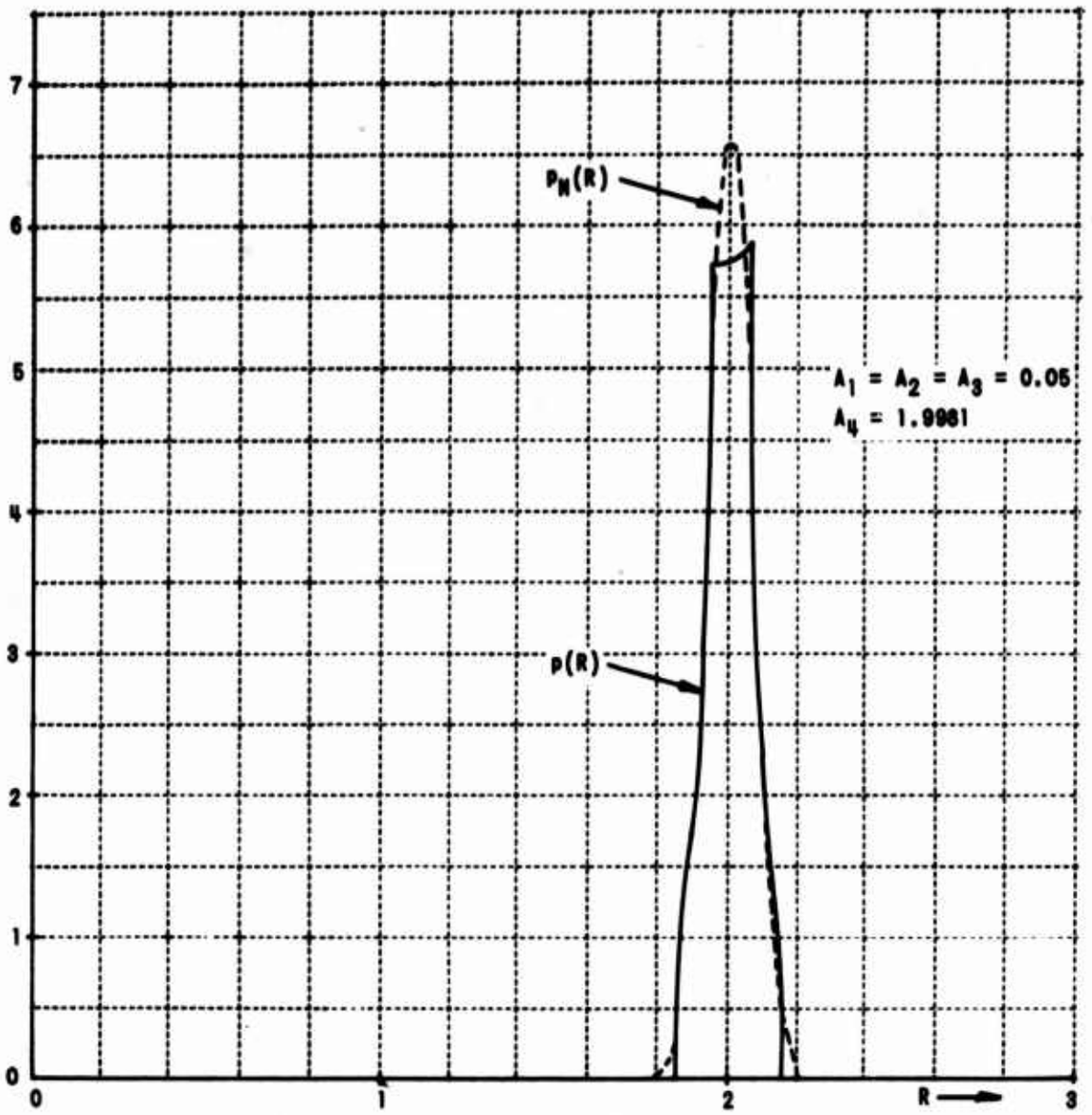

Figure A-22 ENVELOPE PROBABILITY DENSITY FUNCTION FOR FOUR SCATTERERS

$A_3 = 1$, and $A_4 = 1.3115$. We see that $p(R)$ departs more from the Rayleigh approximation, $p_R(R)$, than would be expected on the basis of the quite close agreement of $p(z)$ and the Gaussian probability density function (Figure A-10). On the basis of this result it would appear that $p(z)$ must be very nearly Gaussian if $p(R)$ is to be well approximated by a Rayleigh distribution. For this set of parameters, with all scattering amplitudes of the same order of magnitude, the Nakagami and the Rayleigh distributions are different, but either one is a reasonably accurate approximation to $p(R)$.

In Figure A-18 is given $p(R)$ for $A_1 = A_2 = 0.2$, $A_3 = A_4 = 1.4$; $p(z)$ for the same scattering amplitudes as given in Figure A-4. A tendency towards the two-spiked $p(R)$ found earlier for $N = 2$ can be noted here. For this situation neither $p_R(R)$ nor $p_N(R)$ is a very good approximation to $p(R)$.

Finally, consider the situation in which one scatterer strongly dominates three equal scatterers. In Figure A-19 it can be seen that for this situation $p_N(R)$ is a very good approximation to $p(R)$, but $p_R(R)$ is a relatively poor approximation. The Nakagami m-distribution ($p_N(R)$) much more accurately indicates the finite width of $p(R)$. In Figure A-20 are shown $p(R)$ and $p_N(R)$ for a more strongly dominant scatterer. The Rayleigh density is a very poor approximation to $p(R)$ for the cases shown in Figures A-20 through A-22 (the computed Rayleigh approximation would be the same in each of these figures as shown in Figure A-19). The Nakagami m-distribution becomes better as the strong scatterer becomes more dominant.

The curves of Figure A-22 shows typical behavior of the Nakagami m-distribution for a case of a single very strong scatterer in which $p(R)$ is nonzero over only a small part of the range of R (and for which the Rayleigh distribution is an extremely poor approximation). The Nakagami m-distribution follows the true distribution closely (except for a small discrepancy near the central peak) and drops rapidly outside the range of nonzero $p(R)$. In this case, $p(R)$ is zero for $R \geq 2.1481$ and for $R \leq 1.8481$. For $R = 2.2$ and $R = 1.5$, values closely neighboring these limits, $p_N(R)$ has already dropped to 0.0335 and 0.9×10^{-15}, respectively. The drop above the upper, and below the lower, limit is in each case monotonic; by the time R has reached 2.5 in the upper regime, $p_N(R)$ has dropped to 0.528×10^{-50}.

A.4 PROBABILITY DENSITY FUNCTIONS FOR $N > 4$

In the foregoing results were presented of computations for two and for four scatterers of like or different scattering amplitude. As noted in this Appendix, extension of the calcualtions to more than four scatterers would be highly complicated, although straightforward. The probability distribution function has already been tabulated for $6 \leq N \leq 24$ unit-amplitude scatterers by Freenwood and Durand (Reference 5). They used numerical quadrature on the integrands which, for $N \geq 6$ and $A_i = 1$, converges fast enough to obviate the necessity for analytic integration of remainders.

Their results for the probability distribution $P(R)$ can be translated into our probability density form $p(R)$ by using finite difference differentiation. In Figure 23 is shown $p(R)$ for $N = 6$; $p(R)$ has been taken from Table I of Reference 5, using $p(R + 0.25) \approx \frac{P(R+0.5) - P(R)}{0.5}$ to approximate the derivative. Also shown in Figure A-23 are $p_R(R)$, $p_{RA}(R)$, and $p_N(R)$. It is seen that $p_R(R)$ is a very good approximation to $p(R)$ in this case. $p_{RA}(R)$ is an even closer approximation at most values of R; the curve for $p_{RA}(R)$ cannot be shown, but circles indicate some of the points that lie on it. The Nakagami m-distribution approximation, $p_N(R)$, is a poorer approximation but is still quite accurate.

One important factor should be noted: $p(R)$ in Figure A-23 lacks any sharp breaks such as that at $R = 2$ in Figure A-16. Greenwood and Durand indicate that Rayleigh showed that the derivatives of the distribution function $P(R)$ of order $\frac{1}{2}(N-2)$ for N even and $\frac{1}{2}(N-3)$ for N odd are discontinuous at the points $N - 2k$, $k = 0,1,2,3,111$ Thus for $N = 4$, the density function $p(R) = P'(R)$ has discontinuities at $R = 2$ and at $R = 4$. Returning to Figure A-16, it is seen that the plot of $p(R)$ is continuous but has a discontinuity in slope; actually, there should be discontinuities at $R = 2,4$ but these do not appear because of slight inaccuracies resulting from the numerical integration. Using Rayleigh's result, we see that for $N = 6$ or 7, $p(R)$ is continuous but has discontinuities in slope. None appear in Figure A-23, but this lack may simply be a result of the lack of sufficient tabulated values of $P(R)$ to permit a sufficiently fine-increment plot of $p(R)$. For $N > 7$, $p(R)$ and its slope are continuous.

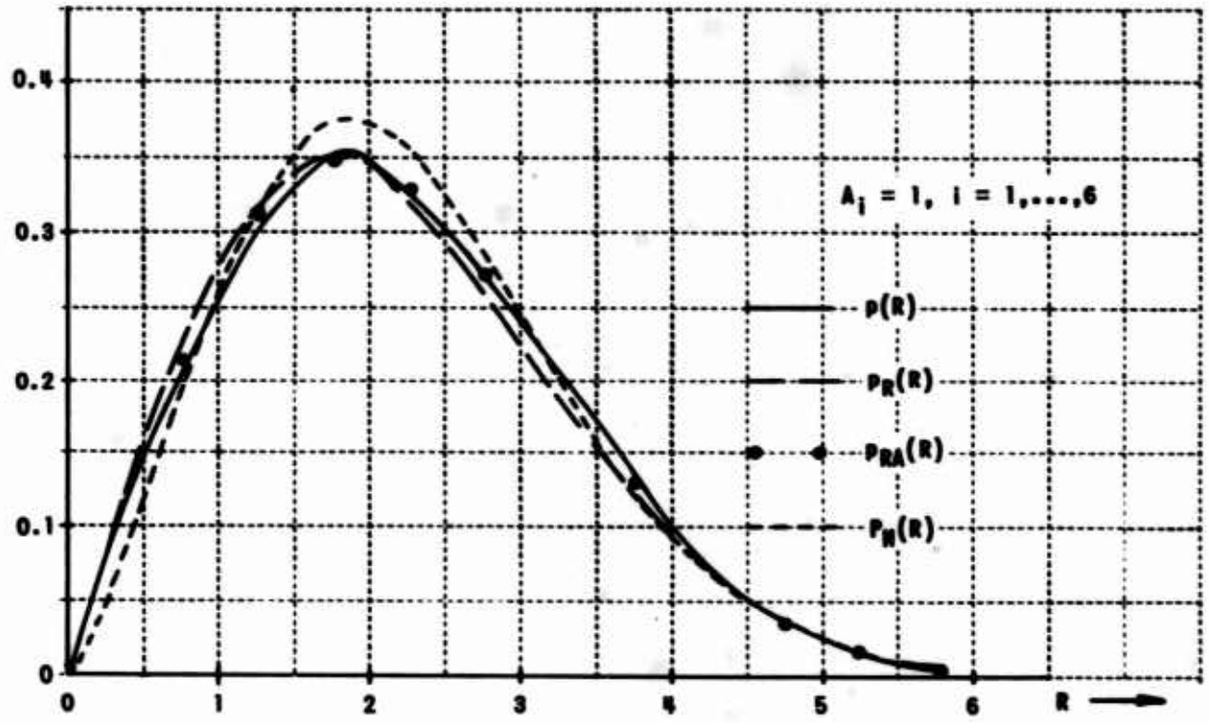

Figure A-23 ENVELOPE PROBABILITY DENSITY FUNCTION FOR SIX EQUAL AMPLITUDE SCATTERERS

References:

1. P. Beckmann, Probability in Communication Engineering, Harcourt, Brace, World, 1967.

2. M. Nakagami, "The m-Distribution -- A General Formula of Intensity Distribution of Rapid Fading," W.C. Hoffman (ed), Statistical Methods in Radio Wave Propagation, Pergamon, 1960, pp. 3-36.

3. G.N. Watson, Theory of Bessel Functions, Cambridge, 1944.

4. M. Abramowitz and I. Stegun, Handbook of Mathematical Functions, NBS Table 55, Gov't Printing Office.

5. J.A. Greenwood and D. Durant, "The Distribution of Length and Components of the Sum of n Random Unit Vectors," Ann. Math. Stat., 26, 233-246 (1955).

Appendix B
DERIVATION OF CORRELATION FUNCTION

Many situations involving stationary or moving radar, stationary or moving scatterers, stationary or moving (scanning) range bin, etc., can occur in radar system analysis. Rather than analyzing several special cases, a fairly general case was studied and the special cases arising from it are discussed later.

At time $t = 0$ the radar signal arises from N_1 scatterers having scattering amplitudes $c_1, c_2, \ldots, c_{N_1}$. The received signal is thus a voltage:

$$R_1 e^{j\theta_1} = \sum_{j=1}^{N} c_j e^{i\phi_j} \qquad \text{(B-1)}$$

where ϕ_j is the phase associated with the j^{th} scatterer. The coefficient c_j is proportional to the square root of the radar cross section of the j^{th} scatterers. Note that independence of the scatterers (single scattering) is assumed. For most clutter situations this assumption should be reasonable. R_1 is the envelope of the received signal; in Section 4 the probability density function associated with R_1, and with the real and imaginary parts of the summation, were computed and discussed. We are now interested in comparing the signal at $t=0$ with the signal at $t = \tau$. Correlation functions relating R_1 and R_2 are therefore of interest here. However, as will be seen shortly, such correlation functions cannot be obtained in any convenient form, in general, and a slightly different approach is required.

First, consider the signal received at $t=0$. From Equation B-1 we have:

$$R_1 = \left\{ A_1 + 2 \sum_{m>n}^{N_1} \sum_{n=1} c_m c_n \cos(\phi_m - \phi_n) \right\}^{\frac{1}{2}} \qquad \text{(B-2)}$$

where;

$$A_1 \triangleq \sum_{m=1}^{N_1} c_m^2$$

Phase differences affect the signal envelope R_1. Equation B-2 can be written as:

$$R_1 = \left\{ A_1 + 2 \sum_{m>n} \sum_{n=1}^{N_1} c_m c_n \cos\left[\frac{4\pi}{\lambda} (r_m - r_n) \right] \right\}^{\frac{1}{2}} \qquad \text{(B-3)}$$

where;

λ = radar wavelength

r_m = range of m^{th} scatterer (from any arbitrary reference plane)

At some later time $t + \tau$, a new envelope, R_2, will exist. Suppose the scatterers do not change their scattering coefficients c_m and that each of them has maintained a velocity component u_m along the radar line of sight during time τ. Then we have:

$$R_2 = \left\{ A_1 + 2 \sum_{m>n} \sum_{n=1}^{N_1} c_m c_n \cos\left[\frac{4\pi}{\lambda} (r_m - r_n) + \frac{4\pi}{\lambda} (u_m - u_n) \tau \right] \right\}^{\frac{1}{2}} \qquad \text{(B-4)}$$

if it is assumed that none of the scatterers has moved out of the space observed by the radar.

To obtain the correlation function relating R_1 and R_2, it is necessary to find the ensemble average (over scatterer locations) of R_1 and R_2. Because of the irrational (square root) nature of R_1 and R_2, such an average cannot be found very easily for general N_1; for large N_1 and a Rayleigh-distributed envelope, the averages can be found using the properties of multivariate Gaussian distributions. An alternative approach can also be used: investigate the correlation of intensities (power levels) rather than the correlations of envelopes (voltage levels). Thus we consider $I_1 \triangleq R_1^2$, which

is a rational function rather than R_1 itself. The intensity is a reasonable quantity to consider, because it can be thought of as the voltage obtained from a square-law detector.

The probability of density functions obtained in Section 3 were for $p(R)$, not $p(I)$. Because of the simple functional relationship between I and R it is relatively straightforward to find $p(I)$ given $p(R)$, although graphical methods (or digital computation) might be required. For the limiting case of N_1 large, and a resultant Rayleigh distribution, given by:

$$p(R) = \frac{2R}{\alpha} e^{-\frac{R^2}{\alpha}} \quad , \qquad R \geq 0 \tag{B-5}$$

the probability density, $p(I)$ where $I = R^2$, is obtained as:

$$p(I) = \frac{1}{\alpha} e^{-\frac{I}{\alpha}} \quad , \qquad I \geq 0 \tag{B-6}$$

and the Rayleigh distribution is transformed into an exponential distribution.

Before finding correlation functions of I, the squared envelope of the received signal, the expressions for R_1 and R_2 (Equations B-3 and B-4 are generalized) and the notation modified slightly. Defining:

$$\frac{4\pi}{\lambda} r_m = \omega \left(\frac{2r_m}{c}\right) \triangleq \omega \tau_m \tag{B-7}$$

so that τ_m, the equivalent two-way time delay, can now be used to specify the location of the m^{th} scatterer. It is also assumed that the radar operates at (radian) frequency ω_1 when I_1, is measured and at frequency $\omega_2 \triangleq \omega_1 + \Delta\omega$ when I_2 is measured. It is assumed that $\Delta\omega$ is small enough so that c_m can be considered constant. Also, it is possible that the radar observes a (partially) different set of scatterers when I_2 is measured. This effect, which arises from the scanning of the radar in range, requires care in the use of indices in the summations. The situation as shown in Figure B-1 is assumed. The summation for I_1 now runs from 1 to $N_1 = N_a + N_b$, and the summantion for I_2

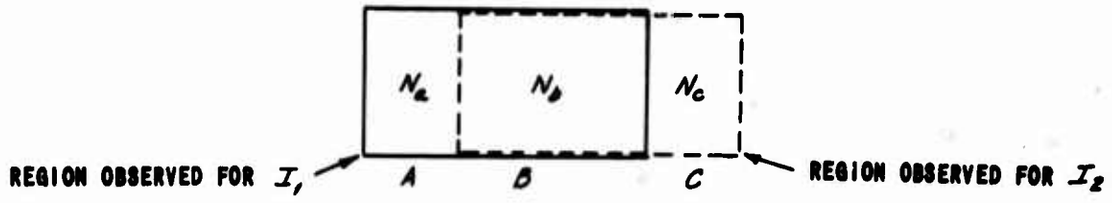

Figure B-1 OBSERVED REGIONS

runs from $N_a + 1$ to $N_a + N_2 = N_a + N_b + N_c$; thus N_1 and N_2 are the total numbers of scatterers observed at times 0 and τ . We thus have:

$$I_1 = A_1 + 2\sum_{m>n}^{N_a+N_b}\sum_{n=1} c_m c_n \cos\left[\omega_1(\tau_m - \tau_n)\right] \tag{B-8}$$

$$I_2 = A_2 + 2\sum_{r>s}^{N_a+N_b+N_c}\sum_{s=N_a+1} c_r c_s \cos\left[\omega_2(\tau_r - \tau_s) + \frac{2\omega_2}{c}\tau(u_r - u_s)\right] \tag{B-9}$$

where;

$$A_1 \triangleq \sum_{m=1}^{N_a+N_b} c_m^2$$

$$A_2 \triangleq \sum_{m=N_a+1}^{N_a+N_b+N_c} cm^2$$

From these expressions we can find correlation functions describing effects of scatterer motion, frequency shifting, and change in position of range bin. It is assumed that scatterers remain in regions A, B, C (of Figure B-1) during the times involved; dimensions of these regions thus are large relative to $u_m \tau$, in general.

First, it is necessary to find the covariance of I_1 and I_2:

$$cov(I_1, I_2) = \langle I_1 I_2 \rangle - \langle I_1 \rangle \langle I_2 \rangle \tag{B-10}$$

where $\langle\ \rangle$ indicates ensemble averages over τ_m and u_m. Since it is assumed that scatterer locations are independent of one another, many terms in the expanded form of Equation B-10 drop out, leaving:

$$cov(I_1, I_2) = 4\left[\sum_{m>n}^{N_a+N_b+N_c}\sum_{n=N_a+1}^{N_a+N_b+N_c} c_m^2 c_n^2\right]\left\{\left\langle\cos\left[\omega_1(\tau_m-\tau_n)\right]\cos\left[\frac{2\omega_2\tau}{c}(u_m-u_n)+\omega_2(\tau_m-\tau_n)\right]\right\rangle\right.$$

$$\left.-\left\langle\cos\left[\omega_1(\tau_m-\tau_n)\right]\right\rangle\left\langle\cos\left[\frac{2\omega_2\tau}{c}(u_m-u_n)+\omega_2(\tau_m-\tau_n)\right]\right\rangle\right\} \qquad \text{(B-11)}$$

Note that this summation is only over the scatterers in the common region B. If there are no scatterers in this common region, or if the range bins do not overlap, the covariance (and, hence, the correlation) is zero. This result is simply a consequence of the assumed independence of scatterer locations; if the scatterers had a high degree of spatial correlation, nonzero values of $cor(I_1, I_2)$ would occur, but this situation is not of interest here. To obtain the correlation function, the covariance must be normalized; the normalization factor is the square root of the product of the variances of I_1 and I_2, viz:

$$D(I_1, I_2) = 2\left[\sum_{m>n}^{N_a+N_b}\sum_{n=1} c_m^2 c_n^2\right]^{\frac{1}{2}}\left[\sum_{r>s}^{N_a+N_b+N_c}\sum_{s=N_a+1} c_r^2 c_s^2\right]^{\frac{1}{2}}\left\{\left\langle\cos^2\left[\omega_1(\tau_m-\tau_n)\right]\right\rangle\right.$$

$$\left.-\left\langle\cos\left[\omega_1(\tau_m-\tau_n)\right]\right\rangle^2\right\}^{\frac{1}{2}}\cdot\left\{\left\langle\cos^2\left[\frac{2\omega_2\tau}{c}(u_r-u_s)+\omega_2(\tau_r-\tau_s)\right]\right\rangle\right. \qquad \text{(B-12)}$$

$$\left.-\left\langle\cos\left[\frac{2\omega_2\tau}{c}(u_r-u_s)+\omega_2(\tau_r-\tau_s)\right]\right\rangle^2\right\}^{\frac{1}{2}}$$

so the correlation function is :

$$G(\tau, \Delta\omega, N) = \frac{cov(I_1, I_2)}{D(I_1, I_2)} \triangleq G(N)G(\tau, \Delta\omega) \qquad \text{(B-13)}$$

The correlation function indicated here gives the effect of receiving pulses a time τ apart, of changing frequency (even for the case of τ negligibly small), and of changes in observed sets of scatterers.

Note that $G(N)$, given by:

$$G(N) = \frac{\sum_{m>n}^{N_a+N_b} \sum_{n=N_a+1} c_m^2 c_n^2}{\left\{\sum_{m>n}^{N_a+N_b} \sum_{n=1} c_m^2 c_n^2\right\}^{1/2} \left\{\sum_{r>s}^{N_a+N_b+N_c} \sum_{s=N_a+1} c_r^2 c_s^2\right\}^{1/2}} \qquad \text{(B-14)}$$

expresses the effect of radar scanning which changes the observed set of scatterers. If $N_b = 0$, that is, if there are no common scatterers, $G(N) = 0$. If $N_a = N_c = 0$ and $N_b = N$ (same set of scatterers contributing to I, and I_2), $G(N) = 1$. Further discussion of $G(N)$ will be given later in this appendix.

The expressions given in Equations B-11 and B-12 are quite general and can be applied for any distributions of τ_m and u_m. To obtain manageable expressions, and, from them, a useful form for $G(\tau, \Delta\omega)$, let us make some reasonable assumptions. First, assume that scatterers are uniformly distributed within their regions (A, B, and C) and that velocities and positions (u_m and τ_m) are independent.*. We thus have a probability density:

$$p(\tau_m) = \frac{1}{\Delta\tau} \quad , \qquad -\frac{\Delta\tau}{2} < \tau_m < \frac{\Delta\tau}{2}$$

$$= 0 \quad , \qquad |\tau_m| > \frac{\Delta\tau}{2} \qquad \text{(B-15)}$$

*But note that τ_m and u_m can be statistically dependent in Equations B-11 and B-12: it is only in the following analysis that the assumption of independence is made.

It must be remembered, however, that the appropriate $\Delta\tau$ may be different in regions A,B, and C, because we are not assuming a homogeneous distribution of scatterers. We therefore will describe the $p(\tau_m)$ in Equation B-15 with the $\Delta\tau$ parameter distinguished by a subscript. Each of the ensemble averages over $\tau_m - \tau_n$ must use the $\Delta\tau$ parameter appropriate for the region involved. For the averages required for the covariance, $\Delta\tau_\beta$ will be used, this being appropriate for region B in Figure B-1. For the averages in the terms of Equation B-12 involving $\tau_m - \tau_n$, the $\Delta\tau$ parameter must be $\Delta\tau_1$, corresponding to regions B and C. For identically distributed and independent τ_m and τ_n and for $p(\tau_m)$ given by Equation B-15 we have:

$$\begin{aligned} p(\tau_m - \tau_n) &= \frac{1}{\Delta\tau} - \frac{\tau_m - \tau_n}{(\Delta\tau)^2} \quad , \quad 0 \le \tau_m - \tau_n \le \Delta\tau \\ &= \frac{1}{\Delta\tau} + \frac{\tau_m - \tau_n}{(\Delta\tau)^2} \quad , \quad -\Delta\tau \le \tau_m - \tau_n < 0 \\ &= 0 \qquad\qquad\qquad , \text{elsewhere} \end{aligned} \tag{B-16}$$

where in each case the appropriate (subscripted) value of $\Delta\tau$ must be used. Since only $\tau_m - \tau_n$ is involved, it is obviously unimportant what τ value is used as a reference; it is also clear that the reference can be chosen differently for each region, so that $p(\tau_m)$ can be made symmetrical about zero for each region of interest.

We now can use Equation B-16 to simplify the averages in Equations B-11 and B-12. The ensemble averages over scatterer locations will thus be achieved, and it will only be necessary to average over the velocity distribution to obtain the desired answer. We can show that:

$$\left\langle \cos\left[\omega_1(\tau_m - \tau_n)\right] \cos\left[\frac{2\omega_2\tau}{c}(u_m - u_n) + (\omega_1 + \Delta\omega)(\tau_m - \tau_n)\right] \right\rangle = \tag{B-17}$$

$$= \frac{1}{2}\left\langle \cos\left[\frac{2\omega_2\tau}{c}(u_m - u_n)\right] \right\rangle \left\{ \frac{\sin^2\left(\frac{\Delta\omega\Delta\tau_\beta}{2}\right)}{\left(\frac{\Delta\omega\Delta\tau}{2}\right)} + \frac{\sin^2\left(\frac{(2\omega_1 + \Delta\omega)\Delta\tau_\beta}{2}\right)}{\left(\frac{(2\omega_1 + \Delta\omega)\Delta\tau}{2}\right)} \right\};$$

as before, the value of $\Delta\tau$ appropriate to the region of interest must be used. Equation B-11 now can be written:

$$cov(I_1, I_2) = 2\left[\sum_{m=n}^{N_a+N_b}\sum_{n=N_a+1} c_m^2 c_n^2\right]\left\{\frac{\sin^2\left(\frac{\Delta\omega\Delta\tau_\theta}{2}\right)}{\left(\frac{\Delta\omega\Delta\tau_\theta}{2}\right)} + \frac{\sin^2\left(\frac{(2\omega_1+\Delta\omega)\Delta\tau_\theta}{2}\right)}{\left(\frac{(2\omega_1+\Delta\omega)\Delta\tau_\theta}{2}\right)} + \right. \tag{B-18}$$

$$\left. -2\,\frac{\sin^2\left(\frac{\omega_1\Delta\tau_\theta}{2}\right)\sin^2\left(\frac{(\omega_1+\Delta\omega)\Delta\tau_\theta}{2}\right)}{\left(\frac{\omega_1\Delta\tau_\theta}{2}\right)^2\left(\frac{(\omega_1+\Delta\omega)\Delta\tau_\theta}{2}\right)^2}\right\} < \cos\left[\frac{2\omega_2\tau}{c}(u_m-u_n)\right] >$$

Note that effects of frequency shift are now separated from scatterer-velocity effects. If region B is at least several wavelengths long, or if $\Delta\omega >> \omega_1$, as will nearly always be the case, the second and third terms of the factor in curly brackets can be ignored relative to the first; this approximation will be made in the following discussion. A similar approximation can be made in the evaluation of Equation B-12; in this case, dependence on the velocity difference drops out altogether, giving:

$$D(I_1, I_2) \approx \left[\sum_{m=n}^{N_a+N_b}\sum_{n=1} c_m^2 c_n^2\right]^{\frac{1}{2}}\left[\sum_{r=s}^{N_a+N_b}\sum_{s=N_a+1}^{N_a+N_b} c_r^2 c_s^2\right]^{\frac{1}{2}}\left\{\frac{1}{2}\right\} \tag{B-19}$$

We thus have:

$$G(\tau,\Delta\omega) \approx \frac{\sin^2\left(\frac{\Delta\omega\Delta\tau_\theta}{2}\right)}{\left(\frac{\Delta\omega\Delta\tau_\theta}{2}\right)^2} < \cos\left[\frac{2\omega_2\tau}{c}(u_m-u_n)\right] > \tag{B-20}$$

If the u_m are assumed to be uniformly distributed over the range $u_0 - \frac{\Delta u}{2}$ to $u_0 + \frac{\Delta u}{2}$, we obtain:

$$G(\tau,\Delta\omega) = \frac{\sin^2\left(\frac{\Delta\omega\Delta\tau_\theta}{2}\right)}{\left(\frac{\Delta\omega\Delta\tau_\theta}{2}\right)^2}\cdot\frac{\sin^2\left(\frac{\omega_2\tau\Delta u}{c}\right)}{\left(\frac{\omega_2\tau\Delta u}{c}\right)^2} \tag{B-21}$$

If the u_m are assumed to be normally distributed with mean u_o and standard deviation σ_u, we obtain:

$$G(\tau,\Delta\omega) = \frac{\sin^2\left(\frac{\Delta\omega\Delta\tau_\theta}{2}\right)}{\left(\frac{\Delta\omega\Delta\tau_\theta}{2}\right)^2} e^{-\frac{4\omega_o^2\tau^2\sigma_u^2}{c^2}} \qquad \text{(B-22)}$$

We have thus shown that $G(\tau,\Delta\omega) \approx G(\tau)G(\Delta\omega)$, very nearly, so long as the observed region is several wavelengths long. Thus, the correlation functions for time (scatterer velocity effect), frequency shift, and change in observed region are simply separate factors (under the conditions assumed) and can be considered separately. Of central importance here is the fact that nowhere in our derivation was it necessary to assume a large number of scatterers or a set of equal-amplitude scatterers: the results derived here are valid for situations involving only a few scatterers or strongly dominant scatterers.

Appendix C

PHASE RELATIONSHIPS OF ISOLATED, FREQUENCY INDEPENDENT SCATTERERS

The analysis performed shows that so long as the scattering amplitudes and phases associated with individual scattering centers are frequency independent, only the relative scattering phases associated with the carrier frequency are significant, regardless of the bandwidth of the pulse. Only if the scatterers have scattering coefficients that vary over the bandwidth of the pulse will the straightforward approach of adding weighted time-delayed images of the radar pulse give incorrect results. There are no new results in this appendix, but it seems appropriate to give these results in the context of the present study.

Assume the radar transmits a waveform:

$$e_t(t) \triangleq e_1(t) \cos \omega_0 t \tag{C-1}$$

where ω_0 is an RF carrier frequency and $e_1(t)$ is an envelope function which is real and finite but is in no way restricted as to length. The envelope function has a Fourier transform:

$$e_1(t) \leftrightarrow E_1(\omega) \triangleq \int_{-\infty}^{\infty} e_1(t) e^{i\omega t} dt \tag{C-2}$$

The Fourier transform of the transmitted waveform is then:

$$E_t(\omega) = \frac{1}{2} \int_{-\infty}^{\infty} e_1(t) \left\{ e^{i\omega_0 t} + e^{-i\omega_0 t} \right\} e^{i\omega t} dt \tag{C-3}$$

or, using Equation C-2:

$$E_t(\omega) = \frac{1}{2} E_1(\omega + \omega_0) + \frac{1}{2} E_1(\omega - \omega_0) , \tag{C-4}$$

a well-known result.

Next, consider a set of N scatterers, each at a distance producing a delay τ_k for propagation from radar to target and back and each having a scattering amplitude a_k that is independent of frequency. Note that a_k can be complex and thus can include any phase shift inherent in the scattering process; this phase shift is assumed here to be frequency independent.* Suppose the transmitted signal were $e^{-i\omega t}$, then the received signal would be:

$$\sum_{k=1}^{N} a_k e^{-i\omega(t-\tau_k)} \tag{C-5}$$

from which we have, for the transfer function,

$$G(\omega) = \sum_{k=1}^{N} a_k e^{i\omega\tau_k} \tag{C-6}$$

We can now use this transfer function to obtain the received spectrum; we have:

$$E_r(\omega) = \frac{1}{2}\sum_{k=1}^{N} a_k \left\{ E_1(\omega+\omega_0)\, e^{i\omega\tau_k} + E_1(\omega-\omega_0)\, e^{i\omega\tau_k} \right\} \tag{C-7}$$

so that received waveforms can now be found using the inverse Fourier transform.

$$e_r(t) = \frac{1}{2}\sum_{k=1}^{N} a_k \frac{1}{2\pi} \left\{ \int_{-\infty}^{\infty} E_1(\omega+\omega_0) e^{i\omega\tau_k} e^{-i\omega t}\, d\omega + \int_{-\infty}^{\infty} E_1(\omega-\omega_0) e^{i\omega\tau_k} e^{-i\omega t}\, d\omega \right\} \tag{C-8}$$

---

*If the phase shift were linearly dependent on frequency the following results would still hold; τ_k would, in that case, be increased to include the phase shift.

which can also be written as:

$$e_r(t) = \frac{1}{2}\sum_{k=1}^{N} a_k \frac{1}{2\pi}\left\{\int_{-\infty}^{\infty} E_1(\omega+\omega_o)e^{-i(\omega+\omega_o)(t-\tau_k)}e^{i\omega_o(t-\tau_k)}e^{i\omega_o(t-\tau_k)}d(\omega+\omega_o) + \right.$$

$$\left. + \int_{-\infty}^{\infty} E_1(\omega-\omega_o)e^{-i(\omega-\omega_o)(t-\tau_k)}e^{-i\omega_o(t-\tau_k)}d(\omega-\omega_o)\right. \qquad \text{(C-9)}$$

Some rearrangement and an obvious change of variable leads to:

$$e_r(t) = \frac{1}{2}\sum_{k=1}^{N} a_k \left\{e^{i\omega_o(t-\tau_k)} \cdot \frac{1}{2\pi}\int_{-\infty}^{\infty} E_1(\omega)e^{-i\omega(t-\tau_k)}d\omega + \right.$$

$$\left. + e^{-i\omega_o(t-\tau_k)} \cdot \frac{1}{2\pi}\int_{-\infty}^{\infty} E_1(\omega)e^{-i\omega(t-\tau_k)}d\omega\right\} \qquad \text{(C-10)}$$

Both integrals are the same and are, in fact, just the Fourier inverses of Equation C-2. Thus we have:

$$e_r(t) = \sum_{k=1}^{N} a_k\, e_1(t-\tau_k)\cos\left[\omega_o(t-\tau_k)\right] \qquad \text{(C-11)}$$

The conditions on a_k are simply those that are required so that no distortion of the pulse occurs on scattering from the k^{th} scatterer. Since the phase shift produced by a fixed spacing is linearly dependent on frequency, it is not surprising that only a delay, and no distortion, occurs. If amplitude and phase properties of a scattering center vary rapidly with frequency in the band occupied by the pulse (as, for example, in the case of a resonant scatterer), then further distortion, not accounted for by Equation C-11, results. This type of scattering could occur with some types of clutter, so the possibility cannot be completely ignored. As-yet unpublished work at CAL on internally funded Project PURE indicates that moderate variation of amplitude across the radar bandwidth produces essentially no effect.

Whether $e_r(t)$ consists of a series of replicas of the transmitted pulse or is a highly complex waveform depends upon whether the various τ_k values differ by more than the pulse length; if the elemental pulses overlap, a complicated waveform can result.

Appendix D

A TECHNIQUE FOR THE EVALUATION OF THE RADAR DETECTION CAPABILITY OF AN MTI RADAR

The detection of low altitude aircraft by ground radars is significantly affected by terrain clutter and masking effects. In addition, the target characteristics (for example, cross section versus aspect angle) will affect radar system performance. During the performance of measurements to evaluate target clutter interactions or during field tests to evaluate the performance of specific radars, it is difficult to interpret resulting data unless information is available on both target and clutter characteristics and their interactions. In this appendix, some of the factors involved in interpreting field test data are described for a specific example for which target, clutter and masking effects are important.

The approach taken is to present an approach for gross evaluation of the radar detection performance of an MTI radar which includes terrain clutter and terrain masking effects. Little or no account of local masking is included, and it will be assumed that the radar can be elevated above the local mask. For the terrain that can be seen, an estimate of the terrain slopes as a function of range provides information to obtain an approximate measure of the magnitude of clutter competing with the target. The latter estimate can be obtained by utilizing available data on terrain reflectivity as a function of incidence angle. This type of information is presented in Figure D-1 for X-band. Data on tree covered terrain at X- and L-band does not differ significantly within the boundaries shown in Figures D-1a and D-1b.

Now the terrain clutter cross section (σ_T) is given by the following:[1]

$$\sigma_T = \gamma R \theta C \frac{\tau}{2} = \frac{\sigma_o}{(\delta + M)} R \theta C \frac{\tau}{2} \qquad (\delta + M) \leq 10^\circ \qquad \text{(D-1)}$$

[1] Skolnik, Introduction to Radar Systems, McGraw Hill, 1962.

where;

γ = terrain reflectivity (dimensionless) = $\sigma_o/(\delta + M)$

σ_o = normalized terrain cross section (m^2/unit area of surface)

δ = incidence angle of radar beam with local horizontal (radians)

M = slope of terrain with local horizontal (radians)

R = range to terrain patch (m)

θ = 3 dB antenna azimuth beamwidth (radians)

τ = radar pulsewidth (s)

C = velocity of light (m/s)

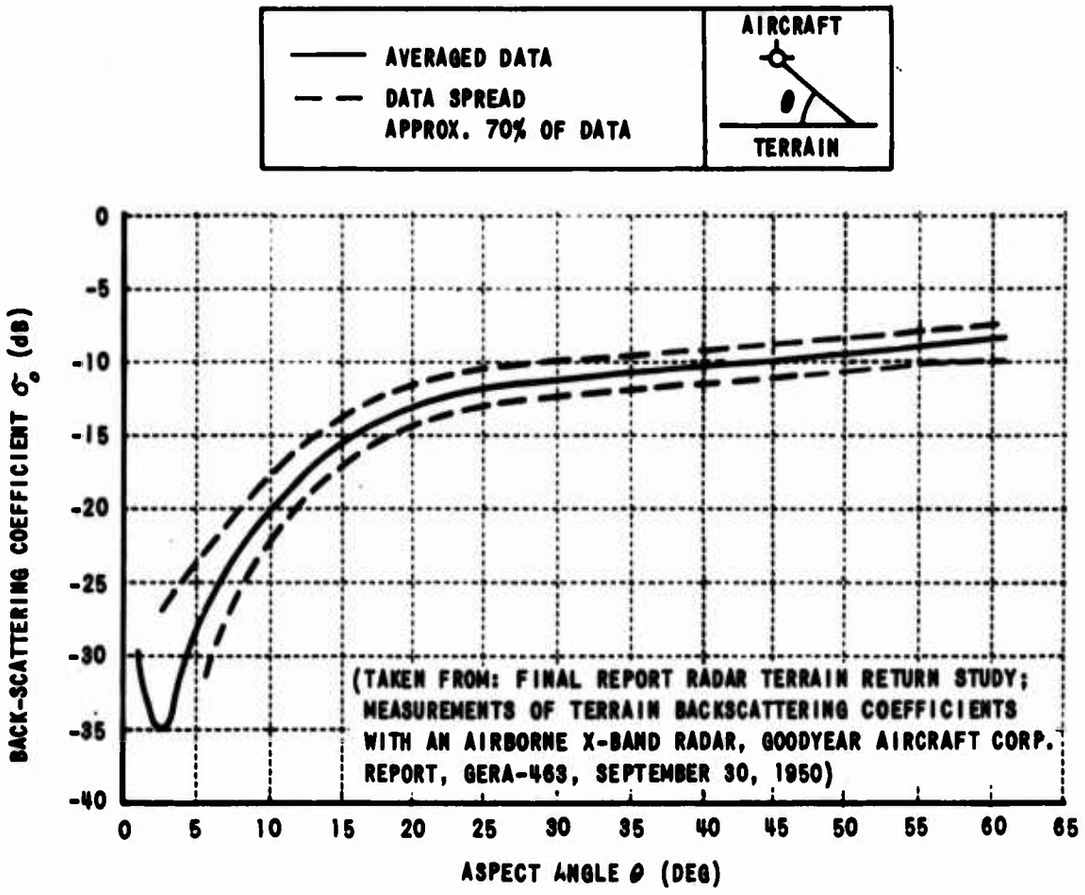

Figure D-1a BACK-SCATTERING COEFFICIENT VERSUS ASPECT ANGLE; ARIZONA COTTON SEEDLINGS

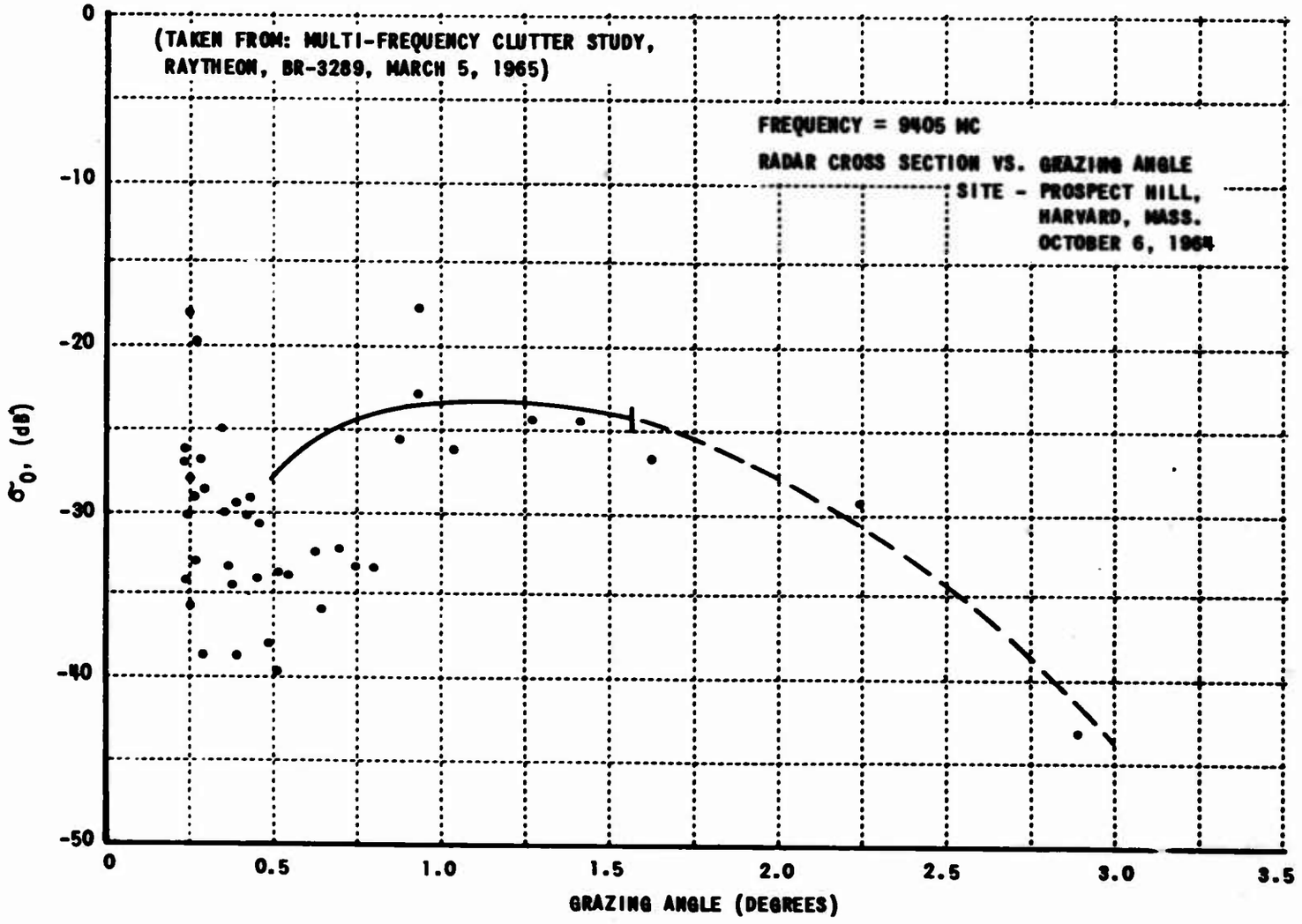

Figure D-1b NORMALIZED RADAR CROSS SECTION OF WOODED TERRAIN
(LEAVES ON THE TREES)

A composite curve of γ vs. aspect angle can be produced from the curves in Figure D-1 as shown in Figure D-2. Using this curve, an estimate of the average terrain cross section can be obtained for a given radar. If the target aircraft cross section is σ_A , then the target-to-clutter ratio (T/C) can be obtained by the relationship $T/C = \sigma_A/\sigma_T$. For the MTI radar system to be effective, the subclutter visibility (SCV) must be equal to or greater than C/T, i.e., to reduce a 1000 m^2 clutter signal to the receiver noise level requires that the SCV = 30 dB. Then depending on the other system parameters (peak power, bandwidth, receiver noise figure, losses, integration, etc.), the signal-to-noise ratio (SNR) to the target and resulting probability of detection can be estimated using the curves shown in Figure D-3*.

To evaluate this approach, a study was made of actual detection performance data obtained by the U.S. Air Force using a radar with the objective of establishing a verification of the performance predicted by the employed evaluation analysis. The specifications of the radar are shown in Table D-1.

The detection criteria suggested earlier in this appendix which is used to evaluate the performance of the search is based on a comparison of the clutter power appearing at the radar MTI filter output with that of a particular size target. When this S/C ratio fell below 0 dB in areas of high terrain reflectivity, the system was said to clutter limited. In practice, many false PPI scope indications would continuously exist in these areas because of uncancelled clutter residue power exceeding the thresholds monitoring the MTI filter outputs. It is apparent, therefore, that an assumption was necessary in the selection of the MTI filter output threshold level, viz.,

*These curves assume that the clutter residues after filtering by the MTI system have the characteristics of receiver noise (white and Gaussian) which is not always true.

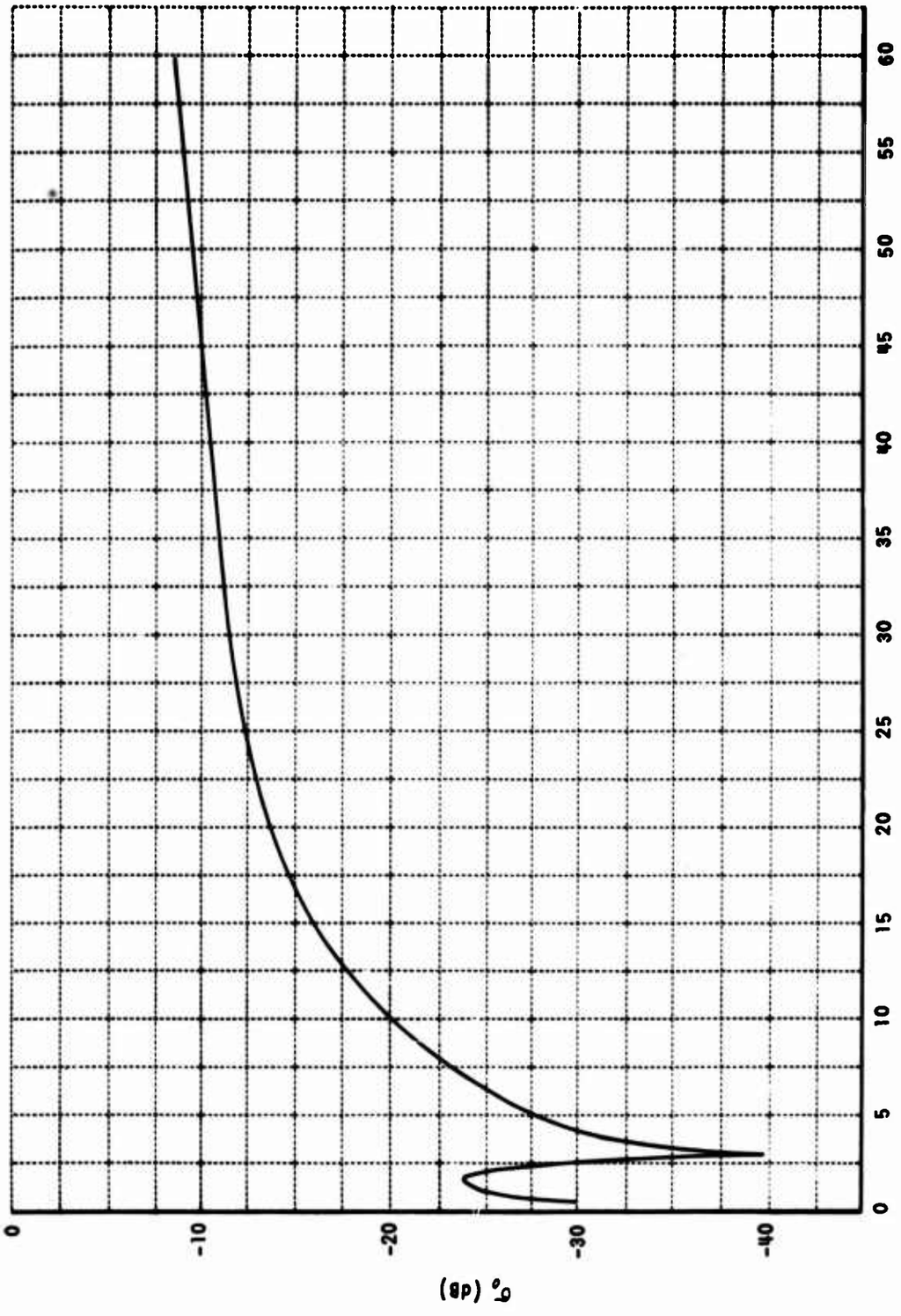

Figure D-2 COMPOSITE TERRAIN REFLECTIVITY DATA

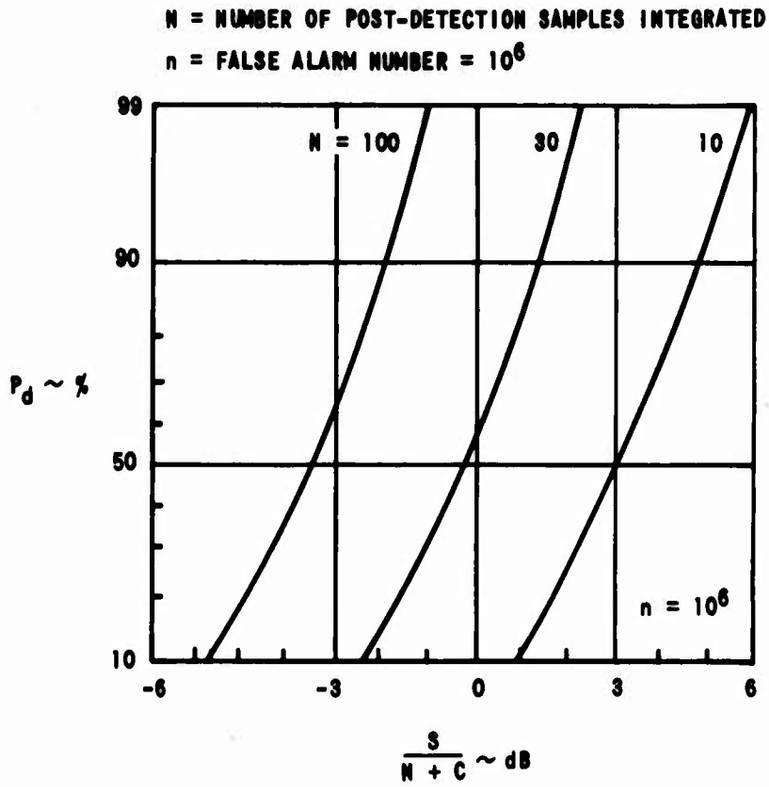

Figure D-3 PROBABILITY OF DETECTION VS. SIGNAL-TO-CLUTTER - PLUS-NOISE RATIO

Table D-1
RADAR CHARACTERISTICS

PARAMETER	
FREQUENCY	1300 MHz
PEAK POWER	25 KW
POLARIZATION	VERTICAL
PRF	340 PPS
PULSEWIDTH	6 μ SEC
SCAN RATE	4 RPM
BEAMWIDTH AZ	3.1°
BEAMWIDTH EL	$CSC^2\theta$
SUBCLUTTER VISIBILITY	> 35 dB
SYSTEM NF	3 dB
DETECTION RANGE	100 NM

level corresponding to the assumed target size. For this analysis, a minimum or threshold target size of 5 m^2 is compatible with the system sensitivities which can be determined using the data in Table D-1.

The U.S. Air Force at Rome Air Development Center conducted tests of the radar indicated in Table D-1 on a test course near Lake Oneida, N.Y., using a helicopter as the target vehicle. Test runs incorporating dive and climb maneuvers were conducted at altitudes ranging from 500 feet to 10,000 feet above the radar site. A target detection was recorded if a spot was at all detectable during a sweep of the PPI indicator. Results of these tests can be used to substantiate, to a degree, the analysis suggested above to evaluate detection capability. Figure D-4 shows a compilation of the Air Force data, with a MTI detection indicated by a short vertical mark and a loss of detection by a small open circle. Outbound runs are indicated by marks above the flight path line and inbound runs by marks below the flight path line.

In order to apply the detection criteria to the above particular terrain and target (helicopter) combination, it was necessary to obtain terrain slope as a function of range along the aircraft ground track. In addition, the radar cross section of the helicopter was estimated by comparing this aircraft to a helicopter which is very similar in size and configuration. Cross section data on this A/C is available for S-band (3.5 GHz) along with translated values at L-band (1.3 GHz). Measurements were taken on a 1/10 scale model using K_a-band.

The terrain profile over which most of the test runs were made is known on Figure D-5 (heading of 200 degrees). It consists of a relatively flat interval out to a range of approximately 5.0 n.mi. followed by a 800 foot hillside rise terminating at approximately 7.5 n.mi. A line-of-sight check from the radar site to the top of this hill indicates that terrain clutter signals cannot be received beyond 7.5 n.mi. because of masking. Discussions with AF project personnel who conducted these tests indicates that the helicopter may have strayed from the desired heading such that complete clutter

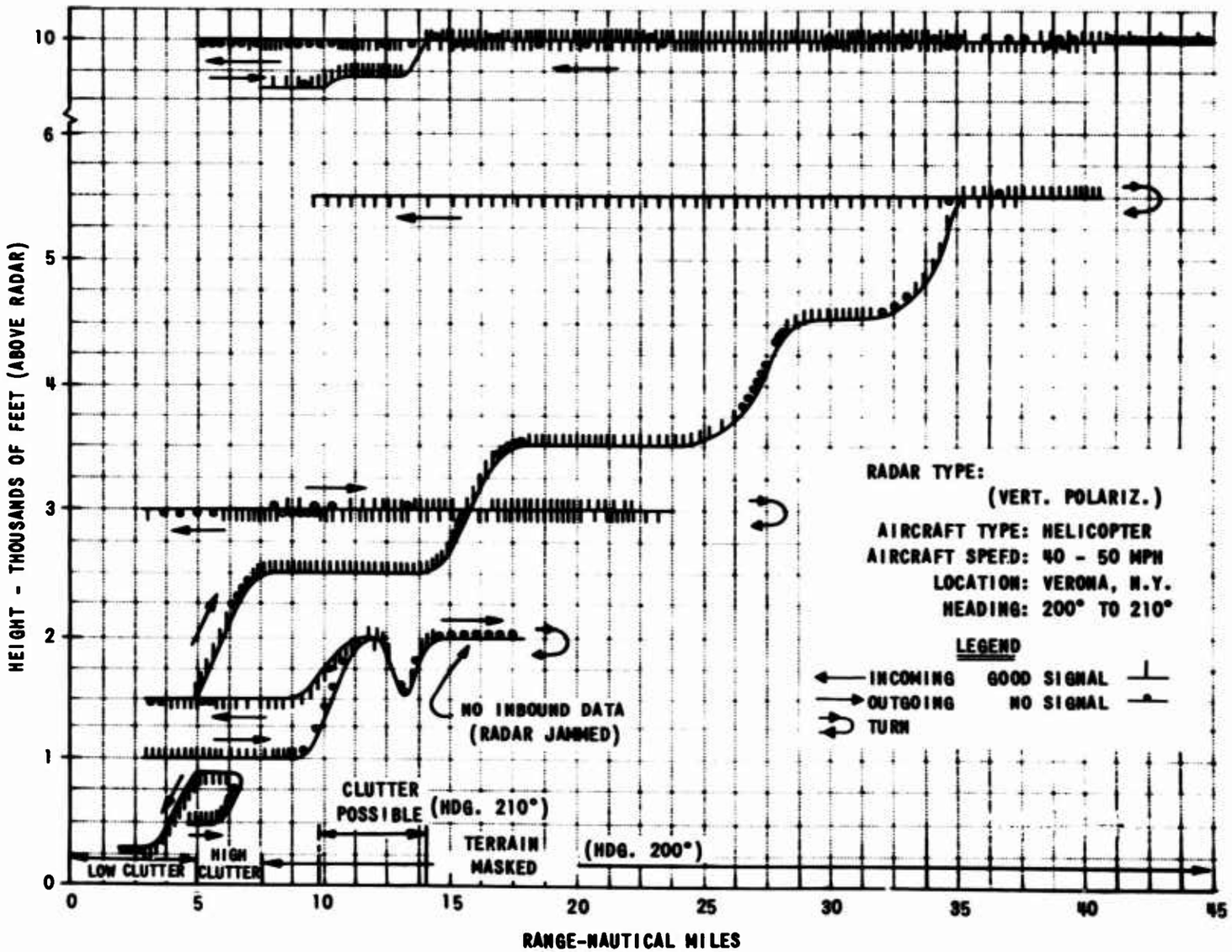

Figure D-4 RADAR DETECTION PERFORMANCE

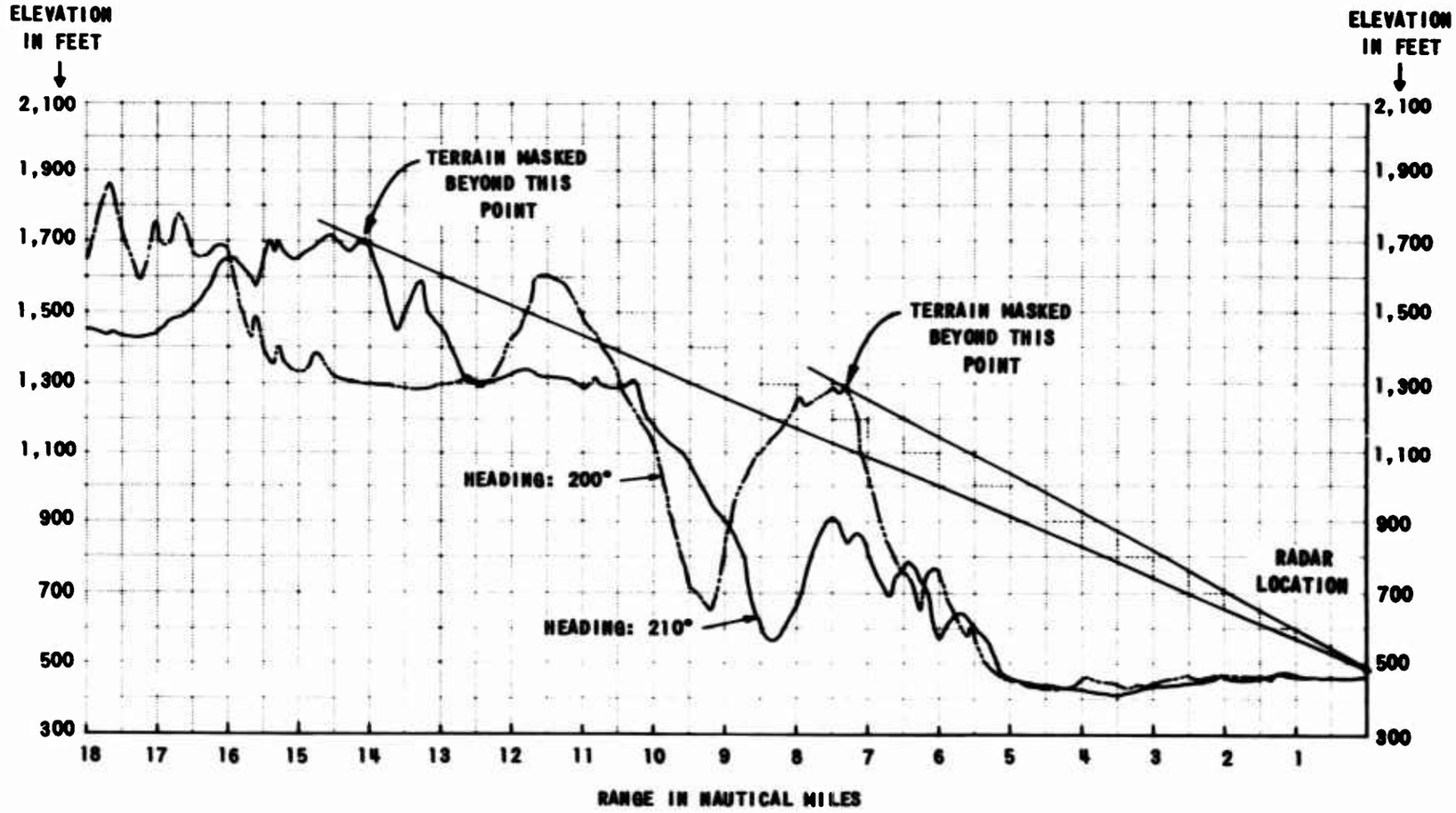

Figure D-5 RADAR PERFORMANCE TESTS TERRAIN PROFILES

masking for ranges greater than 7.5 n.mi. may not have been experienced for a small percentage of the data. Map data indicates that ten degree heading error could allow some clutter (see Figure D-5) returns out to approximately 14 n.mi. where complete masking takes place.

An examination of the data of Figure D-4 for the outbound run at 1000 feet indicates a complete detection loss during a climb maneuver from 1000 feet to 2000 feet, but not during the return run over the same terrain from 2000 feet to 1500 feet. Terrain returns are absent (masked) in this interval making MTI detection of the noncoherent radar dependent on a "beat" signal formed by the combination of returns from fixed and moving parts of the target, i.e., the fuselage return is the reference signal and the rotor return is the variable. Because of the pitch attitude of the helicopter under normal flight conditions, the aspect angle from the radar site to the aircraft on the inbound run is approximately 1.5 degrees above the fuselage centerline, and approximately 3.0 degrees above during the dive. The outbound run results in an approximate aspect angle of 4.5 degrees below tail during normal flight and 1.5 degrees below tail aspect in the climb maneuver. It will be shown below that aspect angle changes during maneuvers can explain some the detection behavior that occurred during the test.

A system sensitivity check of the radar indicates that a 4 m^2 target can be detected out to the system maximum range of 50 n.mi. with a detection probability of 90 percent and a false alarm probability of 10^{-6}. It is, therefore, assumed that the system threshold is approximately set for this size target with effective S/N improvement being accomplished by the integrating action of the PPI indicator. Clearly, target or clutter returns not exceeding this value at the MTI output will not be detected at all.

An examination of the helicopter fuselage cross section reveals a generally constant nose-on cross section of approximately 8 m^2 over the aspect angles experienced during the above mentioned 1500 foot run. The tail-on cross section is approximately 6.0 m^2 for 5 degrees below tail aspect and

about 1.0 m^2 at 0 degrees aspect. The cross section of the rotor blades appears to be somewhat uniform at L-band in that a cross section of approximately 5 m^2 has a high probability of occurance over most azimuth aspect angles. Since the maximum aircraft cross section variation resulting from the summation of the fixed and variable (changing relative phase) returns is equal to twice the amplitude of the smaller return, it becomes apparent why no detection was observed for the near 0 degree aspect tail-on case. Although the rotor return remains relatively constant for the aspect angles under consideration, the fixed fuselage return of approximately 1 m^2 theoretically results in no more than a 2 m^2 effective MTI target cross section for detection - which is below the 4 m^2 threshold level. The actual quantities used are probably in error to some extent, but the detection loss is believed to be due to this reference signal loss effect. Similar losses will be observed on Figure D-4 during a stair case type run from 1500 feet to 5500 feet while the aircraft is proceeding outbound. Aspect angles during the climb maneuvers are similar to those just examined.

A second test of the evaluation detection criteria can be made for the available data as the aircraft appears over that terrain which results in the highest clutter returns. An examination of Figure D-4 shows that reliable detection is maintained in this region (5.0 - 7.5 n.mi.) for most of the runs. The radar to terrain aspect angle is about 7.0 degrees for this hillside which amounts to a normalized terrain coefficient σ_o of -24 dB according to the data of Figure D-3. For the radar beamdwidth and pulsewidth and range a σ_o of -25.0 dB or greater will cause the radar to be clutter limited for the hillside. Although the criteria predicts marginal performance because of large clutter returns for a 5 m^2 target threshold setting, the fact that good detection was indeed observed can be explained by the fact that the helicopter cross section is generally greater than 5 m^2 (thereby allowing a higher threshold setting) and that both the fuselage and rotor returns combine with the clutter reference signals producing greater energy in the nonzero (detectable) doppler spectral regions.

Two inbound runs (10,000 feet and 3,000 feet) result in a detection loss in the region from approximately 8.5 to 10 n.mi. The clutter reference is completely absent in this region due to terrain masking but detection is evident on other inbound and outbound runs over the same terrain. Consequently, detection must be accompanied by a sufficiently strong fuselage return. A plausible explanation appears to be the presence of nulls in the fuselage cross section pattern as a function of elevation aspect angle. There is some evidence which indicates that helicopter average cross section tends to drop off for viewing angles 10 to 15 degrees below nose-on.

The detection loss evident at a range of approximately 5 n.mi. during the 10,000 feet inbound run is attributed to a decrease in sensitivity (gain) of the elevation plane CSC^2 antenna pattern. The radar used in this study is advertised as being able to detect targets at an altitude of 10,000 feet in as close as 5 n.mi. This corresponds to a maximum elevation angle of 18.4 degrees. Targets of nominal cross section (5 m^2) evidently do not result in sufficient signal amplitude to exceed the system threshold at higher elevation angles.

Although some of the flight test data is difficult to explain by means of the supplied and derived information, most of the detection performance experienced was predicted using the detection evaluation criteria used in this appendix. The data which apparently does not conform to the criteria is believed to be the result of the uncertainty associated with helicopter position (true clutter amplitude) and the differences between the actual radar cross-section of the helicopter used in tests and the data available for this analysis.

Appendix E
CLUTTER SIMULATION

E.1 DIGITAL-COMPUTER OPEN-LOOP SIMULATOR

Open-loop simulation relies upon knowledge of received signal characteristics to permit the generation of a realistic clutter signal to add to a similarly generated target-return signal. If one were willing to simulate the clutter return by random noise, without concern for time-, frequency-, and spatial-correlation effects, then digital simulation of the clutter signal would be easy. Time correlation could be approximated by appropriate (numerical) filtering of the sequence of random numbers used to simulate the noise. Frequency- and spatial-correlation effects would be much harder to include in an open-loop simulation. Artificial modification of the noise-simulated clutter signal to introduce these effects would probably involve as much complexity as is involved in the closed-loop method but with none of the advantages (primarily greatly increased flexibility) of that method. If dominant clutter scatterers existed, so that the probability density of the signal amplitude distribution was non-Rayleigh, it would be considerably harder to produce a simulated clutter signal using open-loop simulation.

Inclusion of polarization effects would require still further complexity if the directly generated signals were to have appropriate characteristics in the channels corresponding to the two orthogonally polarized radar returns. Again it appears likely that, except for a very crude modeling of the clutter characteristics, open-loop simulation will be as complicated as closed-loop simulation. Similar difficulties arise if masking, target-clutter interaction, and bistatic-radar effects are to be included in the simulation.

Open-loop simulation is recommended only for a very simple, first-order simulation that is not to be used for detailed investigation of sophisticated radars.

E.2 ANALOG OPEN-LOOP SIMULATOR

Because analog computers frequently offer advantages for some types of simulation, it is reasonable to consider briefly the possibility of using analog rather than digital simulation. Open-loop simulation is considered in this section, and closed-loop simulation in the following section.

First, consider the simulation of the return from the target. Suppose the radar is a conventional pulse radar. The received signal is a sum of weighted, possibly slightly distorted, time-delayed replicas of the transmitted pulse, one such pulse being received from each scattering center on the target. For a moving nonfluctuating target a similar waveform would result, but the frequency would be offset by the Doppler shift.

Most radar targets produce returns that are rapidly fluctuating, because of changes in relative phase of the scattering centers of the target. To a first order, one might represent the fluctuations by a random process and impose noise modulation on the waveform representing the signal received from a nonfluctuating target. This model basically assumes that there are many, randomly phased scatterers on the target and will not permit realistic simulation of correlation-function properties of the target signal. Thus, from pulse to pulse the signal amplitude (pulse level) varies randomly at a mean rate depending on target size, relative motion of scattering centers, and radar wavelength. Depending upon the instantaneous (line-of-sight) differences in scattering-center velocities, different Doppler shifts might be required for the individual pulses. Note that this form of target signal is much like a clutter signal, since it has an amplitude that is at least partially, and may be entirely, random; the rate of fluctuation will, in general, be quite different, however.

The many-scatterer and random-phasing approximations for scattering from such targets as aircraft has been criticized, largely because there are usually relatively few scatterers on an aircraft, for example, that dominate

its radar return at a particular time (or aspect angle). It is possible, for some types of target, to compute the radar return as a function of aspect angle and radar parameters. In such cases, a more accurate waveform can be generated to simulate the return from the target. However, this approach probably fits in better with closed-loop simulation than with open-loop simulation.

Another possibility for open-loop simulation of the target return lies in the recognition that for many aircraft, as stated in the preceding paragraph, significant scattering arises from a relatively few scattering centers that have random phases. A random process having appropriate statistics (other than the Rayleigh envelope obtained from many scatterers) can then be used to establish the output of the target-signal generator; statistical characteristics of such random processes have been discussed previously (see Section 4 and Appendix A).

Finally, one could use analog recordings of radar returns from real targets or, possibly, from scale models. In this way, excellent simulation of returns from targets is possible. The price paid for this accuracy is a loss in flexibility arising from the need for new recordings for each change in radar parameters and for various types of target motion.

In the above discussion, analog techniques for open-loop simulation of radar returns from a target were considered. Consider now the simulation of returns from clutter. If the clutter arises from a large number of independent scattering elements, none of which dominates the rest and which move in such a way as to produce random phasing, the clutter signal has a Rayleigh-distributed envelope. Clutter within a particular radar resolution cell could, in this case, be simulated by white noise passed through a filter to impose appropriate time-correlation properties. If there were, in addition, one, or more, larger scatterers that caused the clutter-signal envelope to be non-Rayleigh, these scatterers could be treated as additional targets and the signals from them added to the noise signal representing background clutter. The total simulated clutter signal then would be non-Rayleigh. In the limit, one could synthesize the complete clutter signal through the summation of

many randomly phased signals whose amplitudes corresponded to typical clutter-element returns. Since more than 5 or 6 equal-amplitude, randomly phased signals would result in approximately a Rayleigh envelope distribution (Section 4), a very large number of signals would not be required, in practice. This technique is analogous to that used earlier for digital-computer simulation wherein a_k and τ_k defined reflection properties of the k^{th} scatterer.

At first, the analog clutter-simulation technique appears straightforward. Several serious difficulties exist, however. First, consider the most common radar, an incoherent pulse radar. Returned pulses from clutter elements arrive at different times because of the different distances to the elements. The resultant waveform is generally quite complicated. Consider a configuration in which a signal generator or oscillator is used to form the clutter signal as shown in Figure E-1. Randomly phased signals of appropriate amplitudes (and frequencies, if Doppler-shift effects are to be included) are not alone sufficient to simulate the received waveform: each signal must be pulsed or sampled so that its output has the pulsed-sinusoid form of the signal received from a single scattering element as shown in Figure E-1. These keying pulses must be randomly set so that clutter returns occur at random times, at least initially; at later times, it might be desirable to let the (initially random) pulse times vary continuously, so as to provide realistic spatial and time correlations.

The technique discussed in the preceding paragraph would be suitable to represent the return from stationary clutter in a single, range-resolution cell for a nonscanning radar operating at a fixed frequency. But suppose the radar uses some form of signal processing (e.g., integration) that depends upon the signals received from several transmitted pulses. It is necessary in this case to account for the correlation properties of the signal. At least three types of correlation can be significant, depending on the situation, as discussed in Section 5. As stated above, appropriately filtered noise could be used in simulation of single-frequency returns from randomly moving scatterers; here the filtering operation imposes time correlation on the noise voltage to produce the correlation that usually arises from the finite time

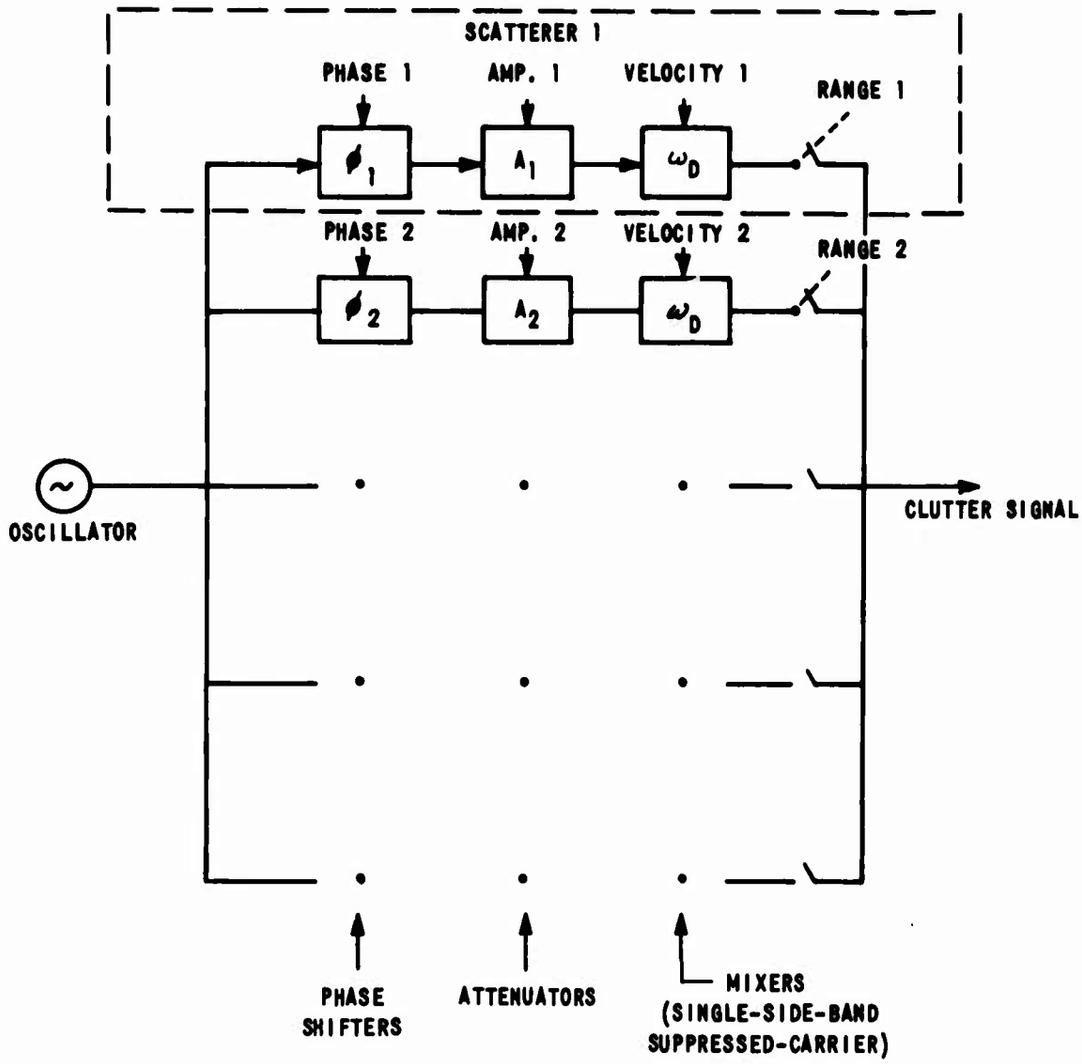

Figure E-1 ANALOG CLUTTER SIMULATION-OPEN LOOP

required for the relative phasing of the scatterers to change significantly. If the scatterers and radar were stationary, however, this form of simulation would fail to produce the same clutter signal on each pulse and thus would not simulate the actual (fixed) clutter. Next, suppose the scatterers were stationary and the radar frequency changed from pulse to pulse, or, if not pulse to pulse, at some rate producing significant changes in relative phases of scatterers during the integration time. If clutter were being simulated by band-limited noise, the effect of a shift in radar frequency on clutter return could not be simulated, because the noise signal cannot include actual relative phases of the scatterers. Before such clutter simulation could be used, it would be necessary to establish the correlation properties of the clutter signal for the actual (variable-frequency) radar and to generate a signal having similar statistical properties.

If clutter were instead being simulated by the output of a set of (separately pulsed) oscillators, effects of scatterer motion could be included by setting the oscillators to slightly different frequencies, corresponding to the Doppler-shifted frequencies of the radar returns from the separate scatterers. Effects of changes in radar frequency could be introduced by changing the frequencies of all of the oscillators by the same amount.

A third form of correlation that must be accounted for if a signal-processing (e.g., integrating) radar is used is the spatial correlation of clutter returns. Assume, for the moment, that the radar antenna is stationary but that the radar returns from successively farther away are being received (for a single transmitted pulse). Since this scan is occurring at half the velocity of propagation, scatterer motion is relatively unimportant for the single scan except for Doppler shifts that are important for a coherent radar. Spatial (in range direction) correlation now can arise from two sources. First, suppose the clutter-producing scatterers are uniformly and homogeneously distributed. Correlation in the clutter signal now arises from the fact that some of the same scatterers produce the return for a finite time; parts of the clutter signal separated by more than the radar pulse width are uncorrelated.

This form of correlation was discussed in Section 5. Correlation can also result from actual spatial correlations of the scattering elements (ground contour, vegetation, buildings, etc.). This form of correlation can produce a clutter signal that is correlated for times (ranges) much greater than a pulse width. In practice, of course, the first (pulse-width) form would also occur along with the second.

Next, consider range-scan to range-scan correlation (still assuming a stationary radar). At a particular range, from scan to scan, the clutter return will change only if the scatterers move or if the radar frequency is changed; in either of these cases the appropriate time and frequency correlation functions should be satisfied, as discussed above. Thus some means must be used to permit range-scan to range-scan correlation to be maintained while clutter returns as a function of range (during any single range scan) are much less strongly correlated. If the clutter signal were being simulated by a noise source with a bandpass filter adjusted to produce appropriate scan-to-scan correlation, the time correlation during one scan would then be much too high. If, on the other hand, the noise were filtered to produce appropriate time correlation during a single range scan, the scan-to-scan correlation would be essentially zero. To maintain correct correlation both in time during one range scan and from scan to scan thus requires a considerably more complicated implementation than a simple bandpass-filtered noise source. One way in which such correlation could be introduced is through the use of a noise source filtered to produce appropriate time correlation during a single scan feeding a tapped delay line or other delay device, as shown in Figure E-2; the (possibly weighted) sum of the outputs of the taps of the delay line then is a simulated clutter signal with both the appropriate time correlation and scan-to-scan correlation. It is necessary, of course, that the time delay between taps on the delay line be equal to the time between scans. The principal disadvantage of this technique is its lack of flexibility; for example, to change scan rates the delay-line taps must be shifted correspondingly. It is also difficult to allow for offsets of scatterer motion or radar frequency shifts from scan to scan when this technique is used. One might also use a large number of noise

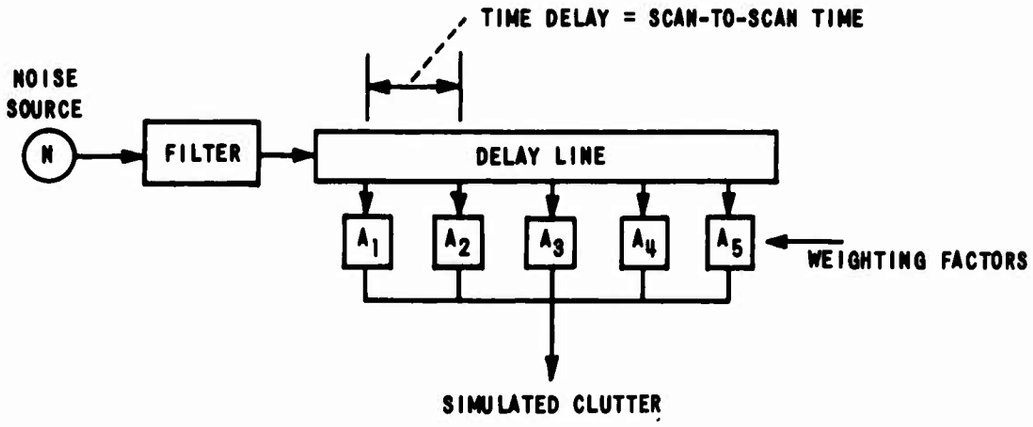

Figure E-2 NOISE SOURCE CLUTTER GENERATOR WITH RANGE AND SCAN-SCAN CORRELATION

sources, each of which represents the clutter signal from a patch of ground that is smaller than the resolution cell of the radar. Each noise source would be filtered to produce a time correlation function equivalent to that produced by scatterer motion. Effects of frequency correlation could not easily be included, however. The signal received during a range scan would now be found by adding the outputs of those noise generators representing the patches of ground within the range resolution cell of the radar; the noise generators being sampled at any instant would be changed to simulate the motion of the range gate along the ground. This method of clutter simulation offers much greater flexibility than the one using delay lines, but it requires many oscillators and filters.

If the clutter signal is to be simulated by adding the outputs of a large number of randomly phased oscillators, as discussed above for the single-range case, range scanning can be included directly by having a (possibly large) set of oscillators whose outputs are pulsed at random times (corresponding to scatterer locations) over a range equivalent to a range scan. A range gate can be used to select the signal coming from any desired range. Scan-to-scan correlation is unity if no parameters are changed between simulated scans. If radar frequency is changed, relative phasings of returns from scatterers are taken into account and the correlation correspondingly reduced. Scatterer motion can be introduced by slowly changing the times of the output pulses of appropriate oscillators and changing oscillator frequency to correspond to the Doppler shift. The multiple-oscillator simulation has the added advantage of permitting effects of dominant scatterers to be included in a realistic manner, so that one is not limited to clutter producing Rayleigh-distributed signals. The principal disadvantage is, of course, the large number of oscillators that are required.

In the discussion above, a nonscanning antenna was assumed. If the antenna scans in azimuth, some new clutter elements are observed on each range scan (or all new clutter elements if the azimuth scan rate is high relative to the PRF). To include these effects, as is necessary if appropriate spatial

correlation is to be retained in the simulation, requires still more elaboration. If filtered noise sources are to be used in the simulation, ground patches can be set up over a two-dimensional array and sums of signals from sources corresponding to appropriate elements of the array used to represent the clutter signal. The effect of the antenna pattern can also be included by appropriately weighting the sums. Similarly, if a set of randomly phased oscillators is used to produce the clutter signal, as described in the preceding paragraph, it is possible to use a larger set than was needed there and to add the outputs of appropriate members of the set. Thus, in essence, one gives each of the randomly phased oscillators in the azimuth angle and, for any particular range scan, takes a sum of the outputs of those oscillators corresponding to azimuth angles observed during that range scan. Again, outputs of various oscillators can be weighted by a coefficient depending upon the antenna patterns.

In the above discussion, no consideration was given to the frequency at which the simulator will operate. Conventional analog computation at radar RF frequencies is not feasible. What considerations are necessary for scaled-frequency operation? First, since interference between pulses of various phases and delays is important, it seems important to use pulsed oscillatory waveforms: the use of envelopes alone is not feasible. If the IF waveform, rather than the RF waveform, is used, frequencies of the order of 30 MHz are required. Scaling of time and frequency to permit operation at analog-computer frequencies is possible, of course, but very slow computation results. To permit operation at 30 Hz, time is increased by a factor of 10^6, so a 10-sec (real time) simulation would require about 4 months. If the computer could operate at 3 kHz, time would only be increased by 10^4, but the 10-sec simulation would still require 28 hours. Scaled-frequency operation is, for numbers of this size, obviously suitable only for an investigation in which a few pulse shapes are to be found. It is possible, of course, that in some situations

scaled-frequency operation may prove quite useful: the numbers given here are intended only to serve as a warning that exact frequency scaling is not necessarily an answer to all of the problems of analog-computer simulation.

Alternatively, one might use components (filtered noise sources or oscillators) actually operating at the radar RF or IF frequency. Conventional analog-computer elements might be used to compute (real-time) target location, aspect angle, and other significant parameters which could be used to adjust parameters in the RF or IF circuitry. This technique appears to be the only practical form of analog computation for general use, although in special cases it might be possible to use scaled frequencies on a conventional analog computer to obtain some information.

One significant parameter that has been omitted in this discussion is the polarization properties of the received radiation. Radar scattering properties of targets and clutter sources depend upon the polarization of the transmitted wave. The received signal also depends upon the polarization of the receiving antenna and its relationship to the polarization of the scattered wave. One way to include polarization diveristy in an open-loop analog simulation is to provide two separate channels corresponding to horizontal and vertical polarization; amplitudes of separate clutter-signal and target-signal generators would be fixed at appropriate levels for their respective polarizations. The output signal from the antenna (i.e., the input to the processor) would then be synthesized from an (appropriately phased) sum of signals from the two channels. The principal disadvantage of this technique is the need for twice as many signal-generating components plus additional complications arising from the need for an appropriate combination of signals for the processor input.

Inclusion of masking effects or of target-clutter interactions and bistatic-radar effects are probably not practical in open-loop simulation, although they might be approximately simulated in some cases. Open-loop simulation, whether digital or analog, does not appear practical for these more complicated situations.

E.3 ANALOG-COMPUTATION CLOSED-LOOP SIMULATOR

Analog generation of a signal representing the radar transmission poses no problem, aside from the question of what frequency is to be used in the simulation; as noted in the preceding section, frequency scaling must be handled with care because of the time requirement involved if large scaling factors are used. For the moment, assume the generation of a pulse at the actual radar RF.

Clutter returns can now be formed by means of delay lines of different lengths having variable transmission coefficients or adjustable attenuators. The variable attenuation permits adjustment of a_k, and the variable delay adjustment of τ_k, where a_k and τ_k are as defined in Section 5. Range scanning is automatically accounted for by time variation; spatial correlation in the range direction is likewise automatically accounted for. Spatial correlation for the scanning-antenna case is not so easily included. It appears necessary to provide sets of delay lines corresponding to targets at different angles from the radar and to switch from one set to another, gradually, as the (simulated) antenna scans in azimuth.

Simulation of the returns from the target can be effected in the same way as simulation of the clutter returns, provided the scattering from the target can be expressed in terms of amplitudes and phases of signals returned from the scattering centers on the target. To simulate target motion, the delays of the delay lines associated with the target scattering centers must be changed continuously. Obviously the main problem in simulating target and clutter signals using this method is the need for many delay lines producing low distortion, variable delay, and variable attenuation.

Inclusion of polarization effects would seem to require two sets of delay lines and their controls with provision for coupling (artificially introduced crosstalk) of outputs of these sets to correspond to polarization transformation caused by the scattering process. Inclusion of masking effects is possible through the use of an auxiliary computation of shadowed regions to

blank out the appropriate delay-line outputs. Target-clutter interaction might be treated using combinations of delay-line outputs, but the simulation would be exceedingly complex.

Another technique would involve the recording of actual terrain-clutter radar signals for a variety of situations. Quite realistic clutter signals can be obtained in this way, of course. This method, while effective for the situation involved in the recording (i.e., for the particular radar parameters and terrain characteristics used), lacks the flexibility that should be available in a general-purpose simulator.

Appendix F

CLUTTER MEASUREMENTS DATA AND ANALYSES

In this Appendix is given a list of references on clutter measurements and analyses which were used during the program. Table F-1 shows the types of data available.

Admiralty Signal and Radar Establishment Tech. Note R4/50/15, "Sea-Clutter Investigation," 7 September 1950 (SECRET).

Boeing Airplane Co., Doc. No. D-11738, "An Experimental Investigation of Radar Ground Clutter," 15 January 1952 (CONFIDENTIAL).

K. Bullington, "Reflection Coefficients of Irregular Terrain" Proc. IRE, 42, 1258-1262 (1954).

University of Illinois, Control Systems Lab. "Sea Clutter Spectrum Studies Using Airborne Coherent Radar III" by B.L. Hicks (May 1958), Report No. R-105.

R.E. McGarwin and L.J. Maloney, "A Study at 1046 MC of the Reflection Coefficient of Irregular Terrain at Small Grazing Angles" NBS Report No. 5099, 25 November 1968.

R.L. Cosgriff, W.H. Peaks, R.C. Taylor, "Electromagnetic Reflection Properties of Natural Surfaces with Applications to Design of Radars and Other Sensors (Terrain Handbook)" Ohio State Univ. Report No. 694-9, 1 February 1959.

1959 Symposium on Radar Return, Part I (Unc. papers) Univ. of New Mexico, 11-12 May 1959.

J. Atkins, H.V. Bikel, M. Weiss, "Realistic Simulation of Radar Clutter" Electronics, 25 September 1959, pp. 78-81.

Goodyear Aircraft Corp. "Radar Terrain Study Final Report: Measurements of Terrai Back-Scattering Coefficients with Airborne X-band Radar" GERA-463, 30 September 1959 (Unclassified).

M.P. Bachynski, "Microwave Propagation over Rough Surfaces," RCA Rev. 20, pp. 308-335 (1959).

1959 Symposium on Radar Return, Part 2, Confidential papers, 11-12 May 1959, (CONFIDENTIAL).

Hughes Aircraft Co. Tech. Memo 656, "A Summary of Measurement and Theories of Radar Ground Return," September 1960 (CONFIDENTIAL).

J.W. McGiven, Jr. and E.W. Pike, "A Study of Clutter Spectra," in Statistical Methods in Radio Wave Propagation, Pergamon, 1960, pp. 49-92.

S.O. Coleman, G.R. Hetrich, "Ground Clutter and the Calculation for Airborne Pulse Doppler Radar" Proceedings of 5th MIL-E-CON National Convention on Military Electronics, 26-28 June 1961, pp. 409-415.

Hughes - "Overland AEW Radar Study(U)," Final Report - Report No. OR-F 1 October 1961 (CONFIDENTIAL).

"Final Report - Generic Ranging Study," Vol. I, G.E. Report No. ASER-37-61, 15 February 1962.

"Limited War Missions Study Program - Part I - Problem Definition Requirements and System Techniques - Vol. 2 of Final Report on Radar Techniques Study, Development and Evaluation Study," 17 March 1962 (CONFIDENTIAL).

J.L. Farrell, R.L. Taylor, "Doppler Radar Clutter," Trans. IEEE, ANE-11, September 1964, pp. 162-172.

G.R. Corry, "Measurements of UHF and L-Band Radar Clutter in Central Pacific Ocean," Trans. IEEE MIL-9, January 1965, pp. 39-44.

RRE Memorandum No. 2158, "The X-Band Reflectivity of Terrain Targets at Small Angles of Incidence" by G. Crossley, February 1965.

"Mulitfrequency Clutter Study," Raytheon Report No. BR-3289, 5 March 1965.

L.F. Helgostam, B. Ronnerstam, "Ground Clutter Calibration for Airborne Doppler Radars," Trans. IEEE, MIL-9, July-October 1965, pp. 294-297.

Army Missile Command Report, RETR66-13, "Analysis of Clutter Data (U)," 9 May 1966 (SECRET)

Tech. Memorandum, "Report of Radar Clutter Signal Processing Committee, Part I, Radar Clutter Effects (U)," JHU Report TG 842-1, September 1966, (CONFIDENTIAL).

J.M. Hunter, TBA Senior "Experimental Studies of Sea-Surface Effects on Low Angle Radars," Proc. IEEE, 113, November 1966, pp. 1731-1740.

"Clutter Model for AEW Radar Design," U.S. Naval Air Development Center Report No. NADC-AE-6638, 29 November 1966.

J.R. Barnum, "High Frequency Backscatter from Terrain with Buildings," Stanford U. Report SEL-67-002, January 1967.

JHU-APL Tech. Memo No. TG-899, "Radar Precipitation Echoes: Experiments on Temporal, Spatial and Frequency Correlation," by Nathanson and Reilly, April 1967.

V.W. Pidgeon, "Radar Land Clutter for Small Grazing Angles at X-Band and L-Band," JHU-APL Tech. Note, May 1967.

V.W. Pidgeon, "Time, Frequency, and Spatial Correlation of Radar Sea Return," JHU-APL Tech. Note, May 1967.

N.W. Guinard, J.T. Ransome, Jr., M.B. Laing and L.W. Hearten," NRL Terrain Clutter Study Phase I, NRL Report 6487, May 10, 1967.

T.A. Croft, "Computation of HF Ground Backscatter Amplitude," Radio Science, VOL. 2 (New Series) July 1967, pp. 739-746.

T.R. Benedict and T.T. Soong, "The Joint Estimation of Signal and Noise from the Sum Envelope," Trans, IEEE IT-13, pp. 447-454, July 1967.

D.F. DeLone, Jr. and E.M. Hofstatter, "On the Design of Optimum Radar Waveforms for Clutter Rejection," Trans. IEEE, IT-13, pp. 454-463, July 1967.

J. Kroszezyinski, "Efficienty of Attenuation of Moving Clutter," Radio and Electronics Engineer 34, pp. 157-159, September 1967.

Reports on Masking and Clutter, Including Information on HAWK Sites:

1. Allied Air Forces Central Europe Rept. ORA/72/AMB (1964) Radar Screening Data for Hawk Missile Sites, Wurzburg (U), NATO SECRET Report.

2. Allied Air Forces Central Europe Rept. ORA/74/AMB (1964) Radar Screening Data for Hawk Missile Sites, Kitzingen (U), NATO SECRET Report.

3. AIRCENT (Allied Air Forces Central Europe) Rept. ORA/39/AIL, 19 Oct. 1962, NATO CONFIDENTIAL Report.

4. AIRCENT Rept. ORA/66/AMB, 6 June 1966, NATO SECRET Report.

5. AIRCENT Rept. ORA/80/AMB, 25 June 1965, NATO SECRET Report.

6. AIRCENT Rept. ORA/82/AMB, 17 May 1966, NATO SECRET Report.

7. AIRCENT Rept. AEV-1730/6, 29 July 1965, NATO SECRET Report.

8. Royal Armament Res. & Dev. Establishment Memo 2/64, no date (rec'd CAL Library 15 July 1964), CONFIDENTIAL Report.

9. RRE (Royal Radar Establishment) Memorandum No. 1592, 26 May 1959, NATO SECRET Report.

10. RRE Memorandum No. 1791, December 1960, NATO SECRET Report.

11. RRE Memorandum No. TIL/BR/7365, 7 June 1964, SECRET Report.

Table F-I
SOURCES AND TYPES OF CLUTTER DATA

SOURCE	ANALYTIC OR EXPERIMENTAL	$\bar{\sigma}$	$P(\sigma)$	SPECTRUM OR CORRELATION FUNCTION	POLARIZATION	ANGLE	FREQUENCY BAND	REMARKS
OHIO STATE UNIV. REPORT NO. 694-9	A & E	✓	✓	✓	H & V	10°-80°	X & Ka	GROUND CLUTTER
GOODYEAR AIRCRAFT GERA-463	A	✓	✓			10°-70°	X	SIDE LOOKING RADAR
SYMPOSIUM ON RADAR RETURN (U) PART II	A & E	✓	✓✓		VV,HH,VH,HV, RR,RL		X	
JHU, REPORT TG 842-1	A	✓	✓	✓	V & H	0.1°,0.3°,1°,3°, 10°,30°-90°,60°	500 MHz TO 95 GHz	VERY EXTENSIVE COVERAGE GIVEN
JHU-APL TECH. MEMO NO. TG-899	E	✓	✓	✓			C	
NRL REPORT 6487	E	✓	✓	✓	VV,HH,VH,HV		P,S,C,X	4-FREQUENCY AIRBORNE RADAR
ADMIRALTY SIGNAL & RADAR ESTABLISHMENT. TECH NOTE: R4/50/15	A & E							
BOEING AIRPLANE CO. DOC. NO. D-11738	E	✓						DATA FOR EACH OF MISSILE SYSTEM
UNIV. OF ILLINOIS REPORT NO. R-105	A & E	✓		✓			X-BAND	SEA CLUTTER
UNIV. OF NEW MEXICO SYMPOSIUM ON PART I RADAR RETURN	A & E	✓			VV,HH	45° & 90°	X	COMBINED RESULTS OF 3 PAPERS
PRE MEMO NO. 2158	A & E	✓		✓	✓	~ 2°-10°	X	FLAT TERRAIN
RAYTHEON REPORT NO. BR-3289	E	✓				> 1.5°	L,S,X	WOODED TERRAIN COMPARES S & X BAND
HUGHES AIRCRAFT CO. MEMO 656	A & E	✓	✓	✓	HH,VV,VH,HV	10°-90°	(425 MHz TO 35 GHz)	INCLUDES RESULTS FROM SEVERAL OTHER PAPERS
JHU-APL TECH. NOTE MAY 1967	E	✓					X,L	
JHU-APL TECH. NOTE MAY 1967	A	✓		✓	VV,HH		C	SEA CLUTTER
ARMY MISSILE COMMAND, REPORT RE TR 66-13	A & E	✓	✓					COMPARES VARIOUS TYPES OF CLUTTER

Appendix G

MEASUREMENT OF FORWARD-SCATTERING USING HIGHLY STABLE FREQUENCY SOURCES

Because of the long baselines involved, coherency measurements of a forward scattered microwave transmission using conventional single source interferometry techniques may not be feasible. An alternative approach involves the use of separate sources which have sufficient frequency stability (or spectral purity) so that phase variations between them during the period of observation are acceptably small. This technique has been successfully applied to radio-astronomical interferometry where rubidium atomic frequency sources allowed observation times of 2-1/2 minutes without loss of coherence (Reference 1). For the purpose of microwave forward scattering measurements, however, observation periods over which coherent measurements are desired will probably not exceed a few seconds. In this case high-stability quartz crystal oscillators would perform satisfactorily. Typical rms phase variation during a 1 second observation period for a filtered 5 MHz quartz crystal oscillator multiplied to 10 GHz is about 0.2 radians, from short-term frequency stability data presented in References 2 and 3. It may also be noted from these data that, although the phase stability deteriorates for observation periods greater than 1 second due to 1/f noise, it generally improves or remains constant for shorter periods.

From the spectral viewpoint, these phase instabilities may be characterized as a wide band noise spectrum surrounding the carrier frequency. This noise spectrum will limit the usable dynamic range of forward scatter spectral measurements. At 10 GHz, this limit is approximately 45 dB down from the carrier level for a 10 Hz analyzer bandwidth.

Since both phase stability and S/N ratio are inversely proportioned to the frequency multiplication factor (References 2 and 3), tests conducted at frequencies lower than 10 GHz will yield higher phase accuracy and improved spectral dynamic range. Thus, coherent forward scattering measurements are

quite feasible using independent, high-stability quartz crystal oscillators multiplied to microwave frequencies up to 10 GHz.

References

1. C. Bare, B.G. Clark, K.I. Kellermann, M.H. Cohen, D.L. Jauncey, Interferometer Experiment with Independent Local Oscillators, Science, Vol. 157, No. 3785, pp. 189-101, (1967).

2. W.J. Riley, Frequency Stability in Precision Oscillators, Electro-Technology, Vol. 79, No. 4, pp. 42-44, (1967).

3. R.J. Munn, 'Spectral Purity' Can Hide a Lot of Sins, Electronic Design, Vol. 15, No. 13, pp. 76-89, (1967).

UNCLASSIFIED

Security Classification

DOCUMENT CONTROL DATA - R & D

(Security classification of title, body of abstract and indexing annotation must be entered when the overall report is classified)

1. ORIGINATING ACTIVITY (Corporate author) Cornell Aeronautical Laboratory, Inc. of Cornell University Buffalo, New York 14221	2a. REPORT SECURITY CLASSIFICATION Unclassified 2b. GROUP N/A

3. REPORT TITLE

RADAR CLUTTER RESEARCH (U)

4. DESCRIPTIVE NOTES (Type of report and inclusive dates)

Final Report

5. AUTHOR(S) (First name, middle initial, last name)

Stephen N. Andre, Marley E. Bechtel and David A. Foster

6. REPORT DATE	7a. TOTAL NO. OF PAGES	7b. NO. OF REFS
July 1968	179	29

8a. CONTRACT OR GRANT NO.	9a. ORIGINATOR'S REPORT NUMBER(S)
DAAH01-67-C-2516 b. PROJECT NO. UB 2508-E c. d.	UB 2508-E-1 9b. OTHER REPORT NO(S) (Any other numbers that may be assigned this report) RE-TR-68-11

10. DISTRIBUTION STATEMENT

Notice 1 Distribution of this document is unlimited.

11. SUPPLEMENTARY NOTES	12. SPONSORING MILITARY ACTIVITY
	U.S. Army Missile Command Redstone Arsenal, Alabama

13. ABSTRACT

The objective of this program was to prepare a clutter research plan for Army air defense weapons that encompasses the anticipated methods of employment of these weapons, as well as the problems associated with the introduction of new radar technology in these systems. Specifically, the investigations included studies of the physics of electromagnetic scattering from rough surfaces, a definition of clutter problems as related to innovations in radar technology such as electronic beam steering, signal processing and design, computer technology, study of clutter models and simulation techniques, and a study of clutter effects in a radar defense complex.

Probability density functions, correlation functions and doppler spectra of clutter signals are derived for the configuration in which only a few major scatterers are present. Results are presented for both coherent and noncoherent detection.

Methods of simulating clutter, using both analog and digital approaches, are described. Emphasis is placed on advanced forms of simulators such as would be required for evaluation of future multi-dimensional radar systems rather than on additive filtered noise for the simulation of clutter. The simulation techniques are based on two suggested generic forms of clutter models, called open-loop and closed loop. Because of the greater flexibility of closed-loop simulation, this is presented in greater detail.

Techniques for performing radar clutter measurements are described and some of the significant problems, related primarily to terrain and cultural observables, are

DD FORM 1 NOV 68 1473

UNCLASSIFIED

Security Classification

14. KEY WORDS	LINK A		LINK B		LINK C	
	ROLE	WT	ROLE	WT	ROLE	WT
Radar Clutter Problems						
Clutter Simulation						
Clutter Probability Functions						
Clutter Correlation Functions						
Clutter Measurements						

Abstract (Cont.)

discussed. Clutter problems as related to radar systems and innovations in radar technology, such as electronically steered phase arrays, are also described.